

**REPUBLIC OF TURKEY  
YILDIZ TECHNICAL UNIVERSITY  
GRADUATE SCHOOL OF NATURAL AND APPLIED SCIENCES**

**DEVELOPING MODELING STRATEGIES TO INCREASE PPP  
ACCURACY**

**ADEM GÖKHAN HAYAL**

**Ph.D. THESIS  
DEPARTMENT OF GEOMATIC ENGINEERING  
GEOMATIC PROGRAM**

**ADVISOR  
PROF. DR. DOĞAN UĞUR ŞANLI**

**İSTANBUL, 2016**

**REPUBLIC OF TURKEY**  
**YILDIZ TECHNICAL UNIVERSITY**  
**GRADUATE SCHOOL OF NATURAL AND APPLIED SCIENCES**

**DEVELOPING MODELING STRATEGIES TO INCREASE PPP  
ACCURACY**

A thesis submitted by Adem Gökhan HAYAL in partial fulfillment of the requirements for the degree of **Doctor of Philosophy** is approved by the committee on 15.04.2016 in Department of Geomatic Engineering, Geomatics Program.

**Thesis Advisor**

Prof. Dr. Doğan Uğur ŞANLI  
Yildiz Technical University

**Approved By the Examining Committee**

Prof. Dr. Doğan Uğur ŞANLI  
Yildiz Technical University

\_\_\_\_\_

Prof. Dr. Rahmi Nurhan ÇELİK  
Istanbul Technical University

\_\_\_\_\_

Prof. Dr. Atınc PIRTI  
Yildiz Technical University

\_\_\_\_\_

Assoc. Prof. Dr. M. Tevfik ÖZLÜDEMİR  
Istanbul Technical University

\_\_\_\_\_

Assoc. Prof. Dr. Bahattin ERDOĞAN  
Yildiz Technical University

\_\_\_\_\_

## ACKNOWLEDGEMENTS

---

I would like to express my sincere gratitude to my academic advisor, Prof. Dr. D. Uğur Şanlı, for his continuous support, guidance, and encouragements throughout my thesis research. Additionally, I would like to thank my thesis advisory committee for reviewing my thesis and providing their valuable recommendations.

I am also grateful to NASA JPL for providing the license of GIPSY/OASIS II software to my advisor and IGS for doing a great service in providing various data and products. In this study I used the GPS data of the IGS using SOPAC servers, and I am grateful to SOPAC researchers as well.

This thesis would not be able to be completed without Asst. Prof. Dr. Alper Yılmaz's help in generating Linux commands. I would also like to acknowledge Assoc. Prof Dr. Bahattin Erdoğan for his kind help in determining positional outliers and Asst. Prof. Dr. Sibel Uzun for helping me with her great adjustment computation skills.

Finally, I would like to take this opportunity to thank my family for patiently supporting me during my thesis research.

April, 2016

Adem Gökhan HAYAL

## TABLE OF CONTENTS

---

	Page
LIST OF SYMBOLS .....	vii
LIST OF ABBREVIATIONS.....	viii
LIST OF FIGURES .....	x
LIST OF TABLES.....	xii
ABSTRACT.....	xiv
ÖZET .....	xvi
CHAPTER 1	
INTRODUCTION .....	18
1.1 Literature Review .....	18
1.2 Objective of the Thesis .....	21
1.3 Hypothesis .....	22
1.3.1 Thesis Outline .....	22
CHAPTER 2	
GENERAL INFORMATION .....	23
2.1 Precise Point Positioning .....	23
2.2 International GNSS Service.....	28
2.3 Jet Propulsion Laboratory .....	29
2.4 Advancements in JPL Analysis Strategy .....	30
2.5 GIPSY/OASIS II.....	31

## CHAPTER 3

METHODOLOGY .....	33
3.1 Data Set Management .....	33
3.2 GPS Data Processing .....	34
3.3 Outlier Removal Procedure .....	36
3.3.1 Traditional Method .....	36
3.3.2 Median Method .....	36
3.3.3 Outlier Detection Model Test Results .....	37
3.4 PPP Accuracy Model .....	41

## CHAPTER 4

NUMERICAL STUDY AND RESULTS .....	45
4.1 Current PPP Accuracy Model .....	45
4.2 Contributions of Ambiguity Resolution and Second Order Ionospheric Correction 51	
4.3 New Accuracy Model Trials .....	56
4.3.1 Straightforward Polynomial Accuracy Model .....	56
4.3.2 Logarithmic Accuracy Model .....	58
4.3.3 Internal Model Assessment .....	58
4.3.4 External Model Assessment .....	62
4.4 Revised PPP Accuracy Model .....	62
4.5 PPP Accuracy Model from a Densified Network .....	67
4.6 Regional PPP Accuracy Models .....	71

## CHAPTER 5

CONCLUSIONS AND SUGGESTIONS .....	73
REFERENCES .....	75

## APPENDIX-A

GPS STATION INFORMATION .....	80
APPENDIX-B	
GPS OBSERVATION SCHEDULE INFORMATION .....	85
APPENDIX-C	
PPP ACCURACY MODEL ESTIMATIONS.....	91
APPENDIX-D	
PPP ACCURACY MODEL FIT FIGURES.....	104
CURRICULUM VITAE.....	109

## LIST OF SYMBOLS

---

$A$	Design matrix
$a_n, b_n, c_n, d_n$	Accuracy model coefficients (for north)
$\alpha$	Significance level
$c$	Speed of light
$\delta_{trop}$	Tropospheric effect
$\delta_{tide}$	Tidal effect
$\delta_{rel}$	Relativistic effect
$\delta t_r$	Receiver clock errors
$\delta t_s$	Satellite clock errors
$e$	Random error vector
$\tilde{e}$	Residual vector
$\varepsilon_{pc}$	Residuals after the combination of phase
$\varepsilon_{cc}$	Residuals after the combination of code
$f_1, f_2$	GPS L1 and L2 frequencies
$\varphi$	Geographical latitude of the stations
$\phi$	Carrier phase
$I$	Identity matrix
$L_n, L_e, L_v$	Logarithmic accuracy model results for north, east and vertical
$\lambda$	Wavelength of the combination
$N_1, N_2$	Phase ambiguity terms on L1 and L2 frequencies
$P$	Weight matrix
$P_n, P_e, P_v$	Polynomial accuracy model results for north, east and vertical
$Q$	Cofactor matrix
$R$	Pseudorange
$\rho$	Geometric range between satellite and receiver
$S_n, S_e, S_v$	Accuracy model results for north, east and vertical
$\sigma$	Standard deviation
$\sigma_0^2$	Unknown variance component
$\hat{\sigma}_0^2$	Estimated variance component
$\sigma_{mad}$	Threshold value for the median method
$T$	Observing session duration
$X$	Unknown parameter vector
$\hat{X}$	Estimated parameter vector
$y$	Observation vector

## LIST OF ABBREVIATIONS

---

AC	Analysis Center
APC	Antenna Phase Center
APV	Satellite and Receiver Antenna Phase Centre Variation
APPS	Automatic Precise Positioning Service
BERNESE	GNSS Processing software by Astronomical Institute, University of Bern
BINEX	Binary Exchange Format
BKG	Bundesamt für Kartographie und Geodäsie
BNC	BKG NTRIP Client
CALTECH	California Institute of Technology
CIRES	Cooperative Institute for Research in Environmental Sciences
CORS	Continuously Operating Reference Stations
CSRS	Canadian Spatial Reference System
DGNSS	Differential GNSS Positioning
DORIS	Doppler Orbitography and Radiopositioning Integrated by Satellite
EDM	Electronic Distance Measurement
FSL	Forecast Systems Laboratory
GAMIT	GPS Analysis at MIT
GAPS	GPS Analysis and Positioning Software
gd2p.pl	GPS Data to Position
GIPSY	GNSS-Inferred Positioning System
GLOBK	Global Kalman Filter VLBI and GPS Analysis Program
GLONASS	Global Navigation Satellite System
GMV	GMV Innovating Solutions Inc.
GNSS	Global Navigation Satellite System
GPS	Global Positioning System
IAG	International Association of Geodesy
IGS	International GNSS System
ITRF	International Terrestrial Reference Frame
JPL	Jet Propulsion Laboratory
LS	Least Squares
MODEST	VLBI software package
NASA	National Aeronautics and Space Administration
NEV	North-East-Vertical Coordinate Frame
NOAA	National Oceanic and Atmospheric Administration
NRCan	Natural Resources Canada
OASIS	Orbit Analysis Simulation
OMC	Observed Minus Computed
OPUS	On-line Positioning Users Service



PAGES Program for Adjustment of GPS Ephemerides  
PPP Precise Point Positioning  
RINEX Receiver Independent Exchange Format  
RMS Root Mean Square  
RP Relative Positioning  
RTK Real Time Kinematic  
RTK-LIB An Open Source Program Package for GNSS Positioning  
SIM Site Information Manager  
SLR Satellite Laser Ranging  
SOPAC Scripps Orbit and Permanent Array Center  
SP3 NGS Standard GPS Orbit Format  
SPP Single Point Positioning  
SRIF Square Root Information Filter  
TEQC Translation, Editing, and Quality Check  
UNAVCO University NAVSTAR Consortium  
UNB University of New Brunswick  
USA, US United States of America  
VLBI Very Long Baseline Interferometry

## LIST OF FIGURES

---

	Page
Figure 2.1 Flowchart of PPP.....	27
Figure 2.2 IGS reference stations .....	28
Figure 2.3 JPL orbits versus other IGS ACs.....	30
Figure 2.4 Work flow diagram for GIPSY GNSS-based terrestrial positioning .....	32
Figure 3.1 Outlier detection model results for north .....	38
Figure 3.2 Outlier detection model results for east.....	39
Figure 3.3 Outlier detection model results for vertical.....	40
Figure 4.1 GPS stations used in Sanli and Tekic .....	46
Figure 4.2 RMS estimations of QUIN based on the four scenarios .....	53
Figure 4.3 Prediction/model fit of the accuracy models of the four scenarios to the RMS values of this study, from observing session durations of 1 through 24 h.....	54
Figure 4.4 Effects of the JPL’s new modeling and analysis strategy on positioning accuracy coefficients.....	55
Figure 4.5 Prediction/model fit of the accuracy models to the RMS values of this study, from observing session durations of 1 through 24 h.....	61
Figure 4.6 Prediction/model fit of the revised accuracy model to the RMS values, from observing session durations of 1 through 24 h .....	66
Figure 4.7 Densified GPS network .....	67
Figure 4.8 Prediction/model fit of the denser accuracy model to the RMS values of this study, from observing session durations of 1 through 24 h.....	70
Figure 4.9 Estimated coefficients for position components north ( $a_n$ ), east ( $a_e$ ), and vertical ( $a_v$ ).....	72
Figure D.1 Prediction/model fit of the regional accuracy models to the RMS values of this study, from observing session durations of 1 through 24 h (high latitude northern hemisphere) .....	104
Figure D.2 Prediction/model fit of the regional accuracy models to the RMS values of this study, from observing session durations of 1 through 24 h (middle latitude northern hemisphere) .....	105
Figure D.3 Prediction/model fit of the regional accuracy models to the RMS values of this study, from observing session durations of 1 through 24 h (equatorial).....	106
Figure D.4 Prediction/model fit of the regional accuracy models to the RMS values of this study, from observing session durations of 1 through 24 h (middle latitude southern hemisphere).....	107

Figure D.5 Prediction/model fit of the regional accuracy models to the RMS values of this study, from observing session durations of 1 through 24 h (high latitude southern hemisphere).....	108
--	-----

## LIST OF TABLES

---

	Page
Table 2.1 Web-based online PPP services.....	25
Table 2.2 IGS GPS Satellite ephemerides / satellite & station clocks.....	29
Table 3.1 Summary of options used in GIPSY processing.....	35
Table 3.2 Outlier detection model estimations .....	41
Table 4.1 Observation time schedule for the current accuracy model, X denotes that data from this day were included in the study .....	46
Table 4.2 Estimated RMS values of the current accuracy model, for north (in mm).....	47
Table 4.3 Estimated RMS values of the current accuracy model, for east (in mm).....	48
Table 4.4 Estimated RMS values of the current accuracy model, for vertical (in mm)	49
Table 4.5 Estimated coefficients, their 1-sigma uncertainties and ratio values of the current accuracy model, for position components north, east and vertical.....	50
Table 4.6 Estimated coefficients, their 1-sigma uncertainties and ratio values of the current accuracy model, for position components north, east and vertical.....	50
Table 4.7 Accuracy model estimates of the ambiguity resolution and second order ionospheric correction.....	52
Table 4.8 Significant constants and their formal 1-sigma uncertainties for the position components north, east, and up from the least squares analysis of the polynomial modeling performed as a function of observing session duration .....	57
Table 4.9 Comparison of the predicted accuracy from three different models with the actual mean RMS .....	59
Table 4.10 Comparison of the results from this study with those of the published work previously (predictions of 24 hours are compared) .....	62
Table 4.11 Observation time schedule of the revised accuracy model, X denotes that data from this day were included in the study .....	63
Table 4.12 Estimated coefficients, their 1-sigma uncertainties and ratio values of the revised accuracy model, for position components north, east and vertical .....	64
Table 4.13 Estimated coefficients, their 1-sigma uncertainties and ratio values of the revised accuracy model, for position components north, east and vertical .....	64
Table 4.14 Summarized observation time schedule for the denser accuracy model, X denotes that data from this day were included in the study .....	68
Table 4.15 Estimated coefficients, their 1-sigma uncertainties and ratio values of the denser accuracy model, for position components north, east and vertical .....	69

Table 4.16 Estimated coefficients from the denser and the regional accuracy models, for position components north, east and vertical.....	71
Table 4.17 Denser and regional accuracy model prediction values .....	71
Table A.1 GPS stations used in Sanli and Tekic .....	80
Table A.2 GPS stations from the densified GPS network .....	81
Table B.1 Quarter daily geomagnetic data for January 2008 prepared by the U.S. Dept. of Commerce, NOAA, Space Weather Prediction Center.....	85
Table B.2 Quarter daily geomagnetic data for January 2014 prepared by the U.S. Dept. of Commerce, NOAA, Space Weather Prediction Center.....	86
Table B.3 Observation time schedule of the denser accuracy model, X denotes that data from this day were included in the study.....	87
Table B.4 Quarter daily geomagnetic data for March 2013 prepared by the U.S. Dept. of Commerce, NOAA, Space Weather Prediction Center .....	90
Table C.1 Estimated RMS values of the revised accuracy model, for north (in mm)....	91
Table C.2 Estimated RMS values of the revised accuracy model, for east (in mm) .....	92
Table C.3 Estimated RMS values of the revised accuracy model, for vertical (in mm)	93
Table C.4 Estimated RMS values of the denser accuracy model, for north (in mm) .....	94
Table C.5 Estimated RMS values of the denser accuracy model, for east (in mm) .....	97
Table C.6 Estimated RMS values of the denser accuracy model, for vertical (in mm)	100
Table C.7 Estimated coefficients, their 1-sigma uncertainties and ratio values of the denser accuracy model, for position components north, east and vertical .....	103

---

**DEVELOPING MODELING STRATEGIES TO INCREASE PPP  
ACCURACY**

Adem Gökhan HAYAL

Department of Geomatic Engineering

PhD. Thesis

Adviser: Prof. Dr. D. Uğur ŞANLI

The demand for precise positioning in geodetic studies, especially in deformation monitoring studies, increases parallel to the advances in the production of geolocation instruments. Currently, the Global Positioning System (GPS) is the most commonly used positioning technique providing accurate three dimensional positioning information. However, in order to obtain reliable positions or deformation rates with a certain accuracy, the researchers need to know the accuracy of GPS when they are planning their field survey. Therefore, the prediction of GPS positioning accuracy has been an important research area for researchers for more than a decade.

Early studies mainly focused on predicting the accuracy of static GPS surveying, which is the most precise GPS surveying method. Recently, Precise Point Positioning (PPP) has emerged as an alternative method to relative positioning (RP). In contrast to commonly used RP, PPP employs only one GPS receiver which makes it more efficient and cost effective. For processing the GPS data, GIPSY/OASIS II (or GIPSY) academic software has had a leading role among its counterparts such as BERNESE and GAMIT.

Various studies have been performed investigating the parameters that affect the PPP accuracy, and the observing session duration was found to be the most significant parameter by the researchers, i.e. Sanli and Engin [1], Sanli and Tekic [2], Ozturk and Sanli [3]. Although permanent and 24 hour operating GPS stations provide the most accurate positions, we still need to take into account the campaign or episodic GPS surveys because of financial problems or various other constraints. Thus, predicting the accuracy of GPS based especially on the observing session duration will be a useful tool for pre-survey planning activities.

Former studies of GIPSY PPP accuracy by using the NASA, JPL's legacy products, and by using GIPSY v 4.0, showed coarser results compared to those of the RP accuracy. In August 2007, JPL started releasing its products using new modeling and analysis

strategies and included these developments to GIPSY starting from the version of 5.0. The main developments provided by JPL includes the new orbit and clock determination strategy, second order ionosphere modeling, and single station ambiguity resolution. The legacy products are no longer available; therefore, the accuracy formulation provided by Sanli and Tekic [2] is not applicable today.

To analyze the accuracy of GPS PPP from the currently available version of GIPSY (version 6.3), the data of the International GNSS Service (IGS) stations belonging to the same time interval (January 2008) used by Sanli and Tekic [2] were tested in this study. The PPP accuracy has been reformulated to be  $S_n = 7.8/\sqrt{T}$  mm,  $S_e = 6.8/\sqrt{T}$  mm and  $S_v = 29.9/\sqrt{T}$  mm for the GPS baseline components north, east and vertical, respectively, and named as the current PPP accuracy model. These results showed that, as expected, the previous positioning accuracy has been improved significantly. Moreover, the PPP accuracy was revised by using a recent 10 day long GPS dataset, from January 2014, belong to the same GPS stations. Eventually, the revised PPP accuracy results revealed the accuracy model equations as  $S_n = 5.9/\sqrt{T}$  mm,  $S_e = 7.0/\sqrt{T}$  mm and  $S_v = 22.1/\sqrt{T}$  mm. The revised accuracy model provided proximate results to the current PPP accuracy model; however, the Sanli and Tekic [2] model was improved by approximately 56%, 66% and 46% for the positioning components north, east and vertical, respectively.

Moreover, straightforward polynomial and logarithmic equations were tested for providing a better accuracy model. However, accuracy model equations of Sanli and Tekic [2] still provided better results.

The results mentioned above were obtained from globally distributed 11 IGS stations and 10 consecutive days of GPS data. However, increased number of GPS stations and using current GPS data were thought to be necessary for developing a better model and producing more reliable accuracy estimation results. Moreover, the PPP accuracy was decided to be analyzed regionally including equatorial area, middle latitude and high latitude areas for northern and southern hemispheres. For this reason, 67 globally distributed continuously operating GPS stations were selected for this study. By using 10 consecutive days of GPS data, the PPP accuracy results were obtained as  $S_n = 6.2/\sqrt{T}$  mm,  $S_e = 6.6/\sqrt{T}$  mm and  $S_v = 21.7/\sqrt{T}$  mm with applying the current accuracy model equations. These model equations are more reliable than the previous results and should be preferred for use when planning a field work. Regional accuracy model results will be provided in Results section.

**Key words:** GPS accuracy, Precise Point Positioning, GIPSY OASIS II, observing session duration, outlier detection

---

## GPS HASSAS NOKTA KONUMLAMA DOĞRULUĞUNU ARTIRMAK İÇİN MODELLEME STRATEJİLERİ GELİŞTİRME

Adem Gökhan HAYAL

Harita Mühendisliği Anabilim Dalı

Doktora Tezi

Tez Danışmanı: Prof. Dr. D. Uğur ŞANLI

Hassas konum belirlemeye olan ihtiyaç özellikle deformasyon belirleme çalışmaları gibi jeodezik çalışmalarda konum belirleme cihazlarındaki gelişmelere paralel olarak artmaktadır. Günümüzde GPS en yaygın olarak kullanılan üç boyutlu konum belirleme tekniğidir. Fakat, güvenilir konum veya deformasyon oranı bilgilerini belirli bir doğrulukta elde edebilmek için araştırmacıların arazi çalışmalarını planlamadan önce GPS'nin doğruluğunu bilmeleri gerekir. Bu yüzden GPS konum belirleme doğruluğunun tahmin edilmesi araştırmacılar için son zamanlarda önemli bir çalışma alanı olmuştur.

Başlangıçtaki çalışmalar genelde en hassas konum belirleme yöntemi olan statik GPS gözlemlerinin doğruluğunun belirlenmesi üzerine olmuştur. Son zamanlarda Hassas Nokta Konumlama Tekniği (PPP) rölatif konumlama tekniğine (RP) alternatif ortaya çıkmıştır. Yaygın olarak kullanılan RP tekniğinden farklı olarak PPP tekniğinde sadece bir GPS alıcısı kullanır ve bu durum PPP tekniğini daha verimli ve ekonomik yapar. GPS verilerinin değerlendirilmesi için ise GIPSY/OASIS II (veya GIPSY) yazılımı BERNESE ve GAMIT gibi yazılımlar arasında öne çıkmaktadır.

PPP doğruluğuna etki eden parametrelerin belirlenmesi için çeşitli çalışmalar yapılmış ve gözlem süresi Sanli ve Engin [1], Sanli ve Tekic [2], Ozturk ve Sanli [3] gibi araştırmacılar tarafından en anlamlı parametre olarak bulunmuştur. Sabit ve 24 saat gözlem yapan GPS istasyonları en doğru konum bilgilerini sunmasına rağmen finansal ve diğer sebeplerden dolayı kampanya veya dönemsel GPS ölçülerini dikkate almamız gerekmektedir. Bu yüzden, özellikle gözlem süresine dayalı GPS konumlama doğruluğunun tahmin edilmesi ölçüm planlama çalışmalarında faydalı olacaktır.

Daha önceki GIPSY PPP çalışmalarında NASA JPL'nin legacy ürünleri ve GIPSY versiyon 4.0 kullanılmış ve RP'ye göre daha kaba sonuçlar elde edilmiştir. JPL Ağustos



2007'de yeni modelleme ve analiz stratejilerinin kullanıldığı gelişmiş ürünlerini yayınlamaya başlamıştır. Bu yeni gelişmeler GIPSY versiyon 5.0 ve sonraki versiyonlara dahil edilmiştir. JPL'nin getirdiği ana gelişmeler yeni yörünge ve saat belirleme stratejisi, ikinci derece iyonosfer modelleme ve tek istasyon iyonosfer çözümüdür. JPL'nin legacy ürünleri artık mevcut değildir ve bu yüzden Sanli ve Tekic [2] tarafından geliştirilen PPP doğruluğu modeli günümüzde artık geçerli değildir.

GPS PPP'nin doğruluğunu mevcut en güncel GIPSY versiyonunu (versiyon 6.3) kullanarak analiz etmek için Sanli ve Tekic [2] tarafından kullanılan IGS istasyonlarının yine aynı zaman dilimine ait (Ocak 2008) GPS gözlem verileri test edilmiştir. PPP doğruluğu kuzey, doğu ve düşey konum bileşenleri için sırasıyla  $S_n = 7.8/\sqrt{T}$  mm,  $S_e = 6.8/\sqrt{T}$  mm ve  $S_v = 29.9/\sqrt{T}$  mm olarak yeniden formüle edilmiştir, bu modele güncel PPP doğruluğu modeli adı verilmiştir. Beklenildiği gibi bu sonuçlar mevcut konumlama doğruluğunun anlamlı bir şekilde iyileştiğini göstermiştir. Bunlara ek olarak, PPP doğruluğu yine aynı IGS istasyonları fakat daha güncel (Ocak 2014) 10 günlük GPS verileri kullanılarak revize edilmiştir. Sonuç olarak revize edilmiş PPP doğruluğu modeli  $S_n = 5.9/\sqrt{T}$  mm,  $S_e = 7.0/\sqrt{T}$  mm ve  $S_v = 22.1/\sqrt{T}$  mm olarak formüle edilmiştir. Bu model, sonuçları yukarıda bahsedilen güncel model sonuçlarına yakın değerler sağlamış, ayrıca Sanli ve Tekic [2] modeli kuzey, doğu ve düşey konum bileşenleri için sırasıyla 56%, 66% ve 46% oranlarında iyileştirilmiştir.

Ayrıca daha iyi ve güvenilir bir model geliştirebilmek için polinomsal ve logaritmik denklemler test edilmiştir. Fakat Sanli ve Tekic [2] tarafından sunulan modelin yine daha iyi sonuçları türettiği görülmüştür.

Yukarıda bahsedilen sonuçlar global olarak dağılmış 11 IGS istasyonu ve bu istasyonlara ait 10 ardışık gözlem gününe ait GPS verileri kullanılarak elde edilmiştir. Oysa ki GPS istasyon sayısını artırmanın ve güncel GPS verisi kullanmanın daha iyi bir model geliştirmek ve daha güvenilir doğruluk elde edebilmek için gerekli olduğu düşünülmektedir. Ayrıca PPP doğruluğunun ekvatorial bölge ve kuzey ve güney yarım küreler için orta ve yüksek enlemler alanları kapsayacak şekilde bölgesel olarak da analiz edilmesinin gerekli olduğuna karar verilmiştir, bu amaçla 67 global olarak dağılmış sürekli gözlem yapan GPS istasyonu bu çalışma için seçilmiştir. 10 ardışık güne ait GPS gözlem verileri ve mevcut model denklemleri kullanılarak PPP doğruluğu sonuçları  $S_n = 6.2/\sqrt{T}$  mm,  $S_e = 6.6/\sqrt{T}$  mm ve  $S_v = 21.7/\sqrt{T}$  mm olarak elde edilmiştir. Elde edilen sonuçlara göre bu model denklemleri öncekilerden daha güvenilirdir ve arazi çalışmaları planlanırken tercih edilmelidir. Bölgesel doğruluk model sonuçları tezin sonuç kısmında verilecektir.

**Anahtar Kelimeler:** GPS doğruluğu, Hassas Nokta Konumlama, GIPSY OASIS II, gözlem süresi, uyuşumsuz ölçü yakalama

### INTRODUCTION

#### 1.1 Literature Review

GPS Precise Point Positioning (PPP) has become very popular recently. In contrast to commonly used relative positioning (RP), PPP employs only one receiver which makes it more efficient and cost effective. For processing the GPS data, GIPSY/OASIS II (GOA-II or GIPSY), a well-established GPS software, has had a leading role among its counterparts.

However, global disturbances, unmodeled errors and biases affect the positioning accuracy. Nevertheless, with its world-wide continuously operating GPS stations, IGS helps with providing high-precision GPS information such as high accuracy orbit and clock data, earth orientation parameters, atmospheric correction parameters and station coordinates velocities in a unified reference frame [2].

Various studies have been conducted for analyzing the GPS positioning accuracy and also for determining the most significant parameters that the accuracy depends on, such as by Davis et al. [4], Dong and Bock [5], Larson and Agnew [6], Feigl et al. [7], Witchayang and Segantine [8], Eckl et al. [9], Fard and Dare [10], Soler et al. [11], Sanli and Engin [1], Sanli and Tekic [2], Bertiger et al. [12], Firuzabadi and King [13], Wang [14]. Based on the studies above, positioning accuracy studies can be classified into two groups: relative positioning (RP) accuracy and PPP accuracy. On the other hand, some of the researchers studied the accuracy results by using their GPS measurements while some considered the positioning accuracy as their main topic and produced accuracy estimation equations. The results of the studies mentioned above revealed that the GPS positioning accuracy mainly depends on observing session duration, baseline length and network geometry.

Eckl et al. [9] are among the first scientists who developed the GPS positioning accuracy formulation. They performed a study to investigate the dependency of accuracy of a derived three-dimensional relative position vector on the baseline length ( $L$ ) and the GPS observing session duration ( $T$ ). Using US National Continuously Operating Reference Stations (CORS) stations with baseline lengths varying from 25 to 300 km and using their in-house PAGES software, the authors tested the RP accuracy. They concluded that the dependency on baseline length is negligibly small and the accuracy only depends on observing session duration when  $L$  and  $T$  ranging from 26km to 300km and observing session durations from 4h to 24h, respectively. Eckl et al. [9] generated the prediction formulas as  $S_n(T) = 9.5/\sqrt{T}$  mm,  $S_e(T) = 9.9/\sqrt{T}$  mm and  $S_v(T) = 36.5/\sqrt{T}$  mm where  $S_n, S_e$  and  $S_v$  are the positioning accuracies for the position components of north, east and vertical, respectively, in mm when  $T$  inserted in the formulas as hours.

The formulas generated by Eckl et al. [9] enabled users to predict the positioning accuracy when  $T$  is at least 4 hour or long. However, the accuracy was unable to be predicted properly with the given equations above when  $T$  is shorter than 4 hours. On the other hand, Soler et al [11] attempted to model GPS positioning accuracy for  $T$  ranging from 1 hour to 4 hours. They used CORS operating in USA and processed the GPS data by using the On-line Positioning Users Service (OPUS). The authors concluded that at least 2 hours of static GPS data are required for obtaining results sufficiently accurate for surveying activities. Moreover, they stated that it is possible to obtain the accuracy of 0.8 cm, 2.1 cm and 3.4 cm for positioning components of north, east and vertical, respectively, when  $T$  is 2 hours.

In addition to Eckl et al. [9], Sanli and Engin [1] noted that baselines longer than 300 km might be required in some studies, like tectonic studies; therefore, they aimed to analyze GPS accuracies for baselines ranging from 300 km to 3000km. The GPS data were processed by using GIPSY research software and the estimated RMS values were used in the functional model developed by Eckl et al. [9]. However, they claimed that the formula derived by Eckl et al. [9] could not perform the accuracy estimates well for longer baselines. Therefore, a new prediction formula was derived by the authors. GIPSY is different from the other software because it employs precise orbits and clocks from NASA Jet Propulsion Laboratory (JPL) and mainly a single receiver is sufficient for mm positioning [15]. However, the authors did not apply PPP method alone. Instead, they fixed the ambiguities between station pairs using the ambiguity resolution technique

given by Blewitt [16], which produces results similar to those of the relative positioning. The authors concluded that the GPS positioning accuracy depends on both the observing session duration and the baseline length over the regional scale.

On the other hand, Ozturk and Sanli [3] aimed to develop a uniform accuracy model that can be used world-wide. They first researched the studies of Eckl et al. [9] and Sanli and Engin [1], which are mentioned above, and proved that their results are reliable within the given limitations. Then, the authors generated a new model that unifies these studies, which covers the baseline lengths ranging from 3km to 3000km. They used the same software, GIPSY, and applied the same processing technique as Sanli and Engin [1]. The authors claimed that the GPS positioning accuracy depends on both the observing session duration and the baseline length for the given baseline range.

Firuzabadi and King [13] performed a study to analyze the effect of network geometry, i.e. with respect to the number and distribution of the reference GPS sites and the observing session durations on positioning accuracy. Using the GAMIT/GLOBK software, the authors concluded that the current IGS accuracy is achievable using at least 4 reference stations and 6 hours of observing sessions. The authors also concluded that the dependency on baseline length and geometric distribution is weak for 4-station networks with flexible reference station choice.

Moreover, Sanli and Kurumahmut [17] tested the effect of the large height differences on the positioning accuracy. The authors claimed that the accuracy degrades when there are large height differences among the stations. They improved the accuracy model of Sanli and Engin [1] by including the height variation in the formula. The authors concluded that 20% of improvement in the prediction of the vertical positioning accuracy is possible for 6 hours of observing sessions when the two standard deviations obtained from the model of Sanli and Engin [1] and the model they developed were combined.

Contrasting the studies above, Sanli and Tekic [2] conducted a research study in order to analyze the accuracy of GPS by using the PPP technique. Therefore, instead of fixing the ambiguities between station pairs, they used the PPP module of the GIPSY software [15]. They first adopted the accuracy prediction equations of Eckl et al. [9] and modified the model so that it will be a function of observing session duration and station latitude. The GIPSY version 4.0 was employed for processing the GPS data by the authors. In contrast with previous studies, the authors arranged their GPS stations regarding to absolute values

of the station latitudes for the Least Squares (LS) analysis. Their goal was to see whether there is a dependency on station latitude or not. The authors detected dependency on latitude for east and vertical components for shorter sessions. Namely, the RMS of the solutions increased as the station gets closer to the equator. However, as done previously, they preferred to model the accuracy depending only on the observing session duration, and at least 6 hours of observing session duration was necessary for sufficiently accurate GPS applications. Moreover, the authors developed the prediction formulas as  $S_n = 13.5/\sqrt{T}$  mm,  $S_e = 20.7/\sqrt{T}$  mm and  $S_v = 40.8/\sqrt{T}$  mm where again  $S_n, S_e$  and  $S_v$  are the accuracies for north, east and vertical, respectively, and  $T$  is the observing session duration in hours.

## 1.2 Objective of the Thesis

The current accuracy model, Sanli and Tekic [2], is obsolete because JPL started using new modeling and analysis strategies while Sanli and Tekic [2] were studying the PPP accuracy and the legacy products they used in their study are no longer available. NASA's JPL recently adopted a new orbit determination strategy and introduced the models to eliminate the second order ionospheric errors modeled by Kedar et al. [18] and a single station ambiguity resolution given by Bertiger et al. [12]. These developments mainly improved the horizontal positioning accuracy and they were included in the GIPSY version 5.0 onwards by JPL. Moreover, JPL reprocessed all of their final orbit products considering the second order ionospheric corrections on Oct/Nov 2014.

Considering all of the developments mentioned above, it could be concluded that Sanli and Tekic [2] accuracy model is irrelevant today. Therefore, the current accuracy model is required to be refined based on the new and improved products.

This study aims to generate a new and reliable accuracy model for PPP. First, Sanli and Tekic [2] model will be remodeled by using the same GPS stations and by using the current available version of GIPSY/OASIS II software, version 6.3. In order for a direct comparison, the GPS data will be selected to be within the same time interval, January 2008, of Sanli and Tekic [2] to provide the same solar cycle conditions. The observations in 2008 coincided with the last solar cycle minimum whereas recent observations were collected during the solar cycle maximum. Then, effects of second order ionospheric correction and single station ambiguity resolution, the main developments advanced by JPL after August 2007, on positioning accuracy will be analyzed. After that, new model

approximations will be tested in order to see if it is possible to develop improved model equations for modeling PPP accuracy. Then, Sanli and Tekic [2] GPS stations with recent GPS data, data from January 2014, will be used to generate current positioning accuracy (revised PPP accuracy). Finally, a densified GPS network, different than the one used in Sanli and Tekic [2], with 67 globally scattered GPS stations will be used for producing a solid and more reliable PPP accuracy model (denser PPP accuracy). In addition, this study will also focus on analyzing the data regionally, and developing a new applicable accuracy estimation model for the regions of equatorial, middle latitude and high latitude areas.

### **1.3 Hypothesis**

The current accuracy model, Sanli and Tekic [2], does not meet today's needs. Once JPL's new products and the recent GPS data are used, the accuracy model equations should change. The coefficients of the accuracy model equations and the predicted accuracy model results should be improved parallel to the advancements in the IGS and JPL's products.

#### **1.3.1 Thesis Outline**

Chapter 2 comprises the basics of PPP as well as the general information about IGS, JPL and GIPSY while Chapter 3 presents the accuracy modeling methodology including relevant equations, outlier detection strategy and new model tests. Moreover, Chapter 4 includes current accuracy model results by using Sanli and Tekic [2] GPS stations and the denser network GPS stations. In addition, regional accuracy models will also be introduced in Chapter 4. Finally, Chapter 5 provides the conclusions and future suggestions.

### GENERAL INFORMATION

#### 2.1 Precise Point Positioning

Several techniques are available for GPS/GNSS positioning based on their positioning method, area of use and available accuracy. These techniques can basically be classified as Single Point Positioning (SPP), Relative Positioning (RP), Differential Positioning (DGNSS and RTK) and Precise Point Positioning (PPP) [19].

The SPP technique is the most basic positioning technique. It employs one GPS receiver and estimating the position by measuring the code pseudoranges as soon as at least four satellites are observable by the receiver. This technique uses the broadcast ephemeris and can generate the positioning information with a worst-case accuracy of about 3.5 m for horizontal and 4.5 m for vertical components (with 95% confidence as noted by [www.gps.gov](http://www.gps.gov)). Therefore, it is usually used for applications which do not require high accuracy such as recreational applications and low accuracy navigation [19], [20].

On the other hand, RP requires at least two receivers observing at least four mutual satellites simultaneously. This technique can provide the order of sub-centimeter level positioning accuracy; thus, this makes it the most preferred technique for high precision geodetic applications. In this technique, the carrier phase and/or pseudorange measurements are used and the error sources in the data, which are the satellite errors, atmospheric errors and the receiver errors, are removed by applying some mathematical models [19], [20], [21], [22], [23], [24].

The DGNSS and RTK techniques also require at least two receivers. They can be considered as relative positioning technique; however, the main difference is that they provide real time positioning information. The corrections are estimated at the base station and then transmitted to the rover. With DGNSS, it is possible to obtain the order

of decimeter level accuracy while RTK provides centimeter level accuracy [19], [24], [25].

In the late 1990's, NASA's Jet Propulsion Laboratory (JPL) scientists Zumberge et al. [15] established a new robust technique as an alternative to the traditional techniques mentioned above and named the technique as Precise Point Positioning (PPP). PPP provides millimeter level positioning accuracy by using only one GPS receiver which makes it comparable to RP [15], [21], [26]. NASA's precise orbits, clocks and earth orientation parameters are used for the processing. Although this method uses one GPS receiver for positioning as in SPP, described above, its philosophy is completely different. Ionosphere free combination of undifferenced code and carrier phase observations is used for positioning in PPP (see equations from (2.1) to (2.4)). The objective is to precisely estimate satellite orbits using several GPS stations without the user's station. This process does not degrade the precision of the orbits used in the data processing [2], [15].

The main difference between RP and PPP is how they handle the satellite and receiver clock errors. To eliminate the satellite clock errors, PPP uses highly precise satellite clock estimates derived from a solution by using data from IGS's network of globally distributed GPS stations instead of between-receiver differencing. Moreover, the receiver clock errors are eliminated by considering these errors as part of the least squares solution for the coordinates, instead of between-satellite differencing.

Sanli and Engin [1] and Sanli and Tekic [2] claim that PPP technique suffers when processing short observing session durations. The influences of global disturbances, which could easily be eliminated by relative positioning over shorter distances, will be observed on the solutions if they are not modeled properly [16].

As a result, a receiver station's position can be obtained without the need for a reference base station [21]. Moreover, because no base station is required in PPP, the datum for the ground site will be the satellite reference frame (datum), ITRF. Therefore, users need to apply a straightforward coordinate transformation in order to obtain the station coordinates in the desired frame [21].

PPP can produce positioning information by processing both static and kinematic data. In addition, this method can also process the data in post processing mode and real time if the proper equipment is available to generate, transmit, receive and process the precise satellite orbit and clock products [27].



PPP has become a favorite method for positioning in various areas in which there are no base stations available within proximity, or the establishment of base stations is difficult or not cost-effective [14]. Some of the applications that PPP has been employed for are exemplified as ground control establishment [28], deformation monitoring [29], [30], municipal surveying [31], hydrographic and marine applications [32], [33], measuring seismic waves [34] and landslide monitoring [14].

Numerous scientific software packages are available for PPP processing. The most famous ones are the GIPSY/OASIS software developed by JPL (see Chapter 2.4), the BERNESE GPS software (version 5.0 or higher) developed by Astronomical Institute of the University of Berne, WaPP developed by Lambert Wanniger, BNC developed by Bundesamt für Kartographie und Geodäsie (BKG) and RTK-LIB developed by Takasu. In addition, web based PPP services are also available for processing PPP data which are presented in Table 2.1 below [19].

Table 2.1 Web-based online PPP services [19], [35]

<b>Service Short Name</b>	<b>Service Long Name</b>	<b>Organizations</b>
CSRS-PPP	Canadian Spatial Reference System-Precise Point Positioning	Natural Resources Canada (NRCan)
GAPS	GPS Analysis and Positioning Software	University of New Brunswick (UNB)
APPS	Automatic Precise Positioning Service	NASA – Jet Propulsion Laboratory (JPL)
magicGNSS	magicPPP -Precise Point Positioning Solution	GMV Innovating Solutions
Trimble Center Point RTX	Trimble center Point RTX	Trimble

Main mathematical equations of PPP method are based on are given below.

$$\phi = \rho - (\delta t_r - \delta t_s)c + \lambda N + \delta_{trop} + \delta_{tide} + \delta_{rel} + \varepsilon_{pc} \quad (2.1)$$

$$R = \rho - (\delta t_r - \delta t_s)c + \delta_{trop} + \delta_{tide} + \delta_{rel} + \varepsilon_{cc} \quad (2.2)$$

$$N = f_1 N_1 - f_2 N_2 \quad (2.3)$$

$$\lambda = c / (f_1^2 - f_2^2) \quad (2.4)$$

where  $\phi$  and  $R$  are the carrier phase and pseudorange, respectively, and  $\rho$  is the geometric range between receiver and satellites.  $f_1$  and  $f_2$  symbolize the GPS L1 and L2 frequencies while  $N_1$  and  $N_2$  are the phase ambiguity terms on L1 and L2 frequencies. Also,  $c$  is the speed of light,  $\lambda$  is the wavelength of the combination,  $\delta t_r$  and  $\delta t_s$  are the receiver and satellite clock errors.  $\delta_{trop}$ ,  $\delta_{tide}$ , and  $\delta_{rel}$  are the tropospheric, tidal, and relativistic effects, respectively,  $\varepsilon_{pc}$  and  $\varepsilon_{cc}$  represents the residuals after the combination of phase and code, respectively [36], [37].

PPP method equations are also widely described in [15], [19], [30], [38]. In addition, Figure 2.1 presents the flowchart of PPP.

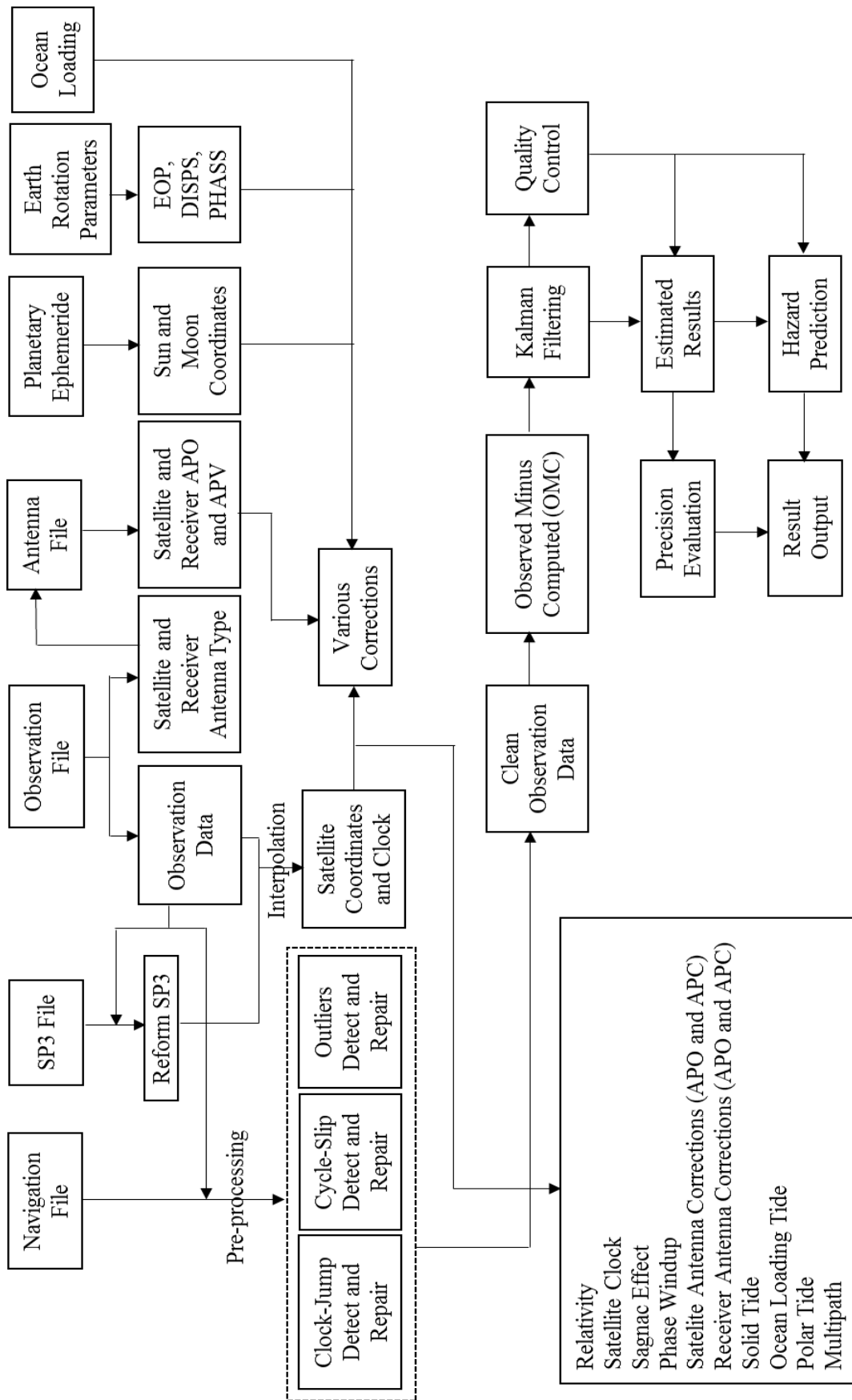


Figure 2.1 Flowchart of PPP [30]



Table 2.2 IGS GPS Satellite ephemerides / satellite & station clocks [39]

Type		Accuracy	Latency	Updates	Sample Interval
Broadcast	Orbits	~100 cm	Real Time	--	daily
	Sat. Clocks	~5 ns RMS ~2.5 ns SDev			
Ultra-Rapid (Predicted Half)	Orbits	~5 cm	Real Time	at 03, 09, 15, 21 UTC	15 min
	Sat. clocks	~3 ns RMS ~1.5 ns SDev			
Ultra-Rapid (Observed Half)	Orbits	~3 cm	3 - 9 hours	at 03, 09, 15, 21 UTC	15 min
	Sat. Clocks	~150 ps RMS ~50 ps SDev			
Rapid	Orbits	~2.5 cm	17 - 41 hours	at 17 UTC daily	15 min
	Sat. & Stn. Clocks	~75 ps RMS ~25 ps SDev			5 min
Final	Orbits	~2.5 cm	12 - 18 days	Every Thursday	15 min
	Sat. & Stn. Clocks	~75 ps RMS ~20 ps SDev			Sat.: 30s Stn.: 5 min

### 2.3 Jet Propulsion Laboratory

Jet Propulsion Laboratory (JPL) is a federally-funded research and development facility in the US. It was founded in the 1930s and has been managed by California Institute of Technology (CALTECH) for the National Aeronautics and Space Administration (NASA). JPL has developed tools for space exploration which later provided a useful source for understanding the Earth, its atmosphere, climate, oceans, geology and the biosphere [41]. JPL has also developed the GIPSY/OASIS II academic software (see Chapter 2.5) which was used in this thesis for studying the accuracy of the PPP technique, as well being used by so many scientists, especially for PPP related researches.

## 2.4 Advancements in JPL Analysis Strategy

In August 2007, JPL started releasing its products using new modeling and analysis strategies. Legacy products are no longer available [42].

The main developments provided by JPL includes:

- The new orbit and clock determination strategy,
- Second order ionosphere modeling
- Single station ambiguity resolution.

Therefore the accuracy formulation provided before August 2007 is not applicable today.

Figure 2.3 represents the effect of these advancements on the IGS Final Orbits.

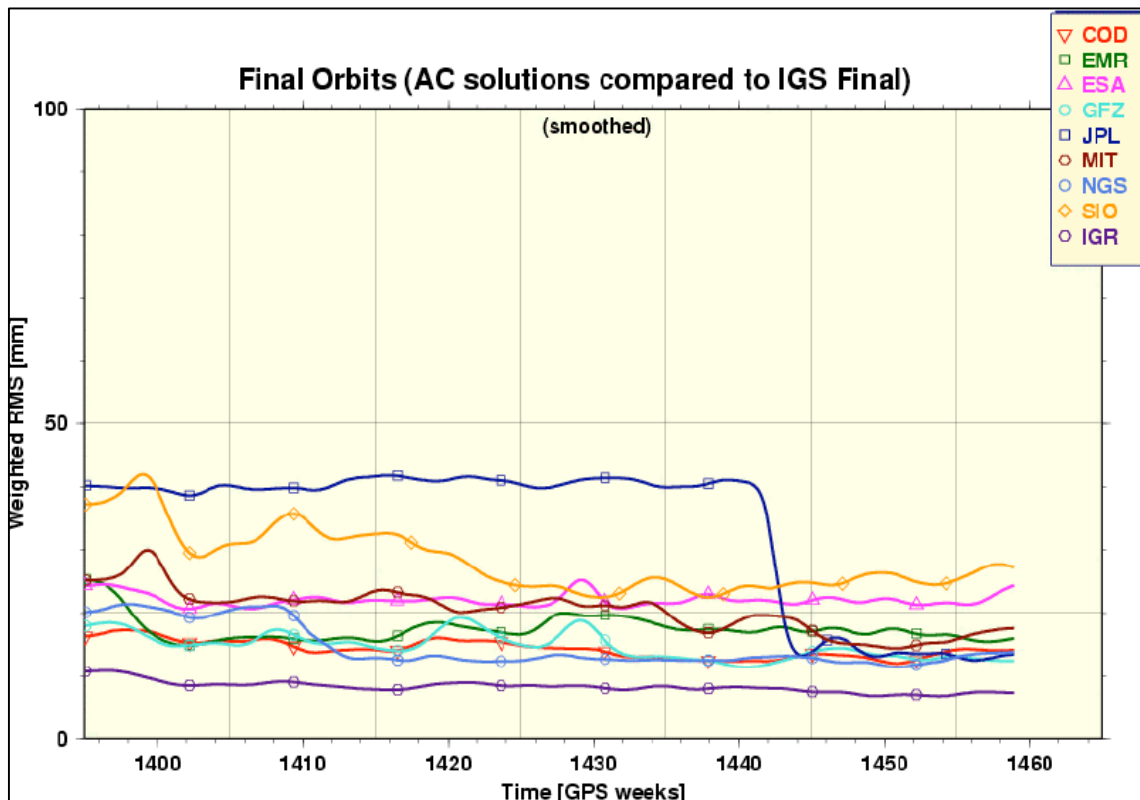


Figure 2.3 JPL orbits versus other IGS ACs [42]

In addition, JPL recently reprocessed all of their final orbit products with second order ionospheric corrections on Oct/Nov 2014. All of the orbit products downloaded before then did not have second order ionosphere corrections applied.

The effects of the ambiguity resolution and second order ionospheric correction on the positioning accuracy will be analyzed in Chapter 4.2.

## 2.5 GIPSY/OASIS II

GNSS-Inferred Positioning System and Orbit Analysis Simulation (GIPSY/OASIS II or GOA II) software was developed by the Jet Propulsion Laboratory (JPL) in mid-1980's and it has been maintained by the Near Earth Tracking Applications and Systems. GIPSY/OASIS II is an academic research software serving hundreds of research and educational licensed users from at least 20 countries. It was evolved from VLBI software package (MODEST) and runs on a UNIX system. GIPSY/OASIS II originally aimed to support GPS-based precise orbit determination of the Topex/Poseidon satellite altimeter mission. Currently, in addition to GPS, GIPSY/OASIS II is able to process observation data of Russian GLONASS, French DORIS and Satellite Laser Ranging (SLR) system [43], [44]. Actually, GIPSY and OASIS are two different software packages which use common modules; the first one was designed for standard geodetic applications while the latter is a covariance analysis package for Earth orbiting and deep space missions [45]. For convenience, this software will eventually be referred as GIPSY.

GIPSY can process the data in static, kinematic and Precise Point Positioning mode [15], [26], [45]. Instead of using double differences, GIPSY processes GPS observations in the undifferenced mode. Satellite and receiver clock biases are estimated stochastically by using a white noise estimation model while tropospheric zenith delay is estimated by random walk model [46], [47]. Since these biases are considered as stochastic variables during modeling, GIPSY does not use normal equations as a modeling algorithm [46]. Instead, GIPSY applies filtering and smoothing techniques in order to remove these biases. Filtering does forward processing of the measurements and generates the coefficients required in smoothing while smoothing applies backward processing and produces information for solving the stochastic parameters [26].

Square Root Information Filter (SRIF) is used for calculating the unknown parameters in GIPSY. SRIF has the advantage of handling all types of parameters as stochastic processes and uses small batches, instead of inversion of large matrices, when solving the parameters [46]. This filter is computationally efficient, numerically very stable, and a fast algorithm. By inverting small matrices successively produced for each cluster the round-off errors caused by big matrix inversions are avoided [26], [45].

Moreover, GIPSY conducts a series of sophisticated modeling specific to the research software; for example, accurate observation model with rigorous treatment of celestial

and terrestrial reference systems, reliable data editing (cycleslips, outliers), estimation of polar motion and Earth spin rate, estimation of reference frame transformation parameters and kinematic modeling of station positions to account for plate tectonics and co-seismic displacements, etc [26].

GIPSY uses GPS Data to Position (gd2p.pl) interface for processing GNSS data observed by a single receiver and performs static and kinematic positioning, precise orbit determination, better error detection, clock estimations and troposphere estimation [44]. GIPSY comprises several processing modules (programs) which are given in Figure 2.4. These modules were coded in FORTRAN or lately in C and they can be operated by using UNIX command lines. Each module generates output files that are used as input for the next module [26]. GIPSY uses gd2p.pl interface to automatically run these modules [44]. Detailed information about GIPSY modules and how they operate can be found in [26], [44], [45]. Figure 2.4 represents a typical work flow diagram for GIPSY GNSS-based terrestrial positioning.

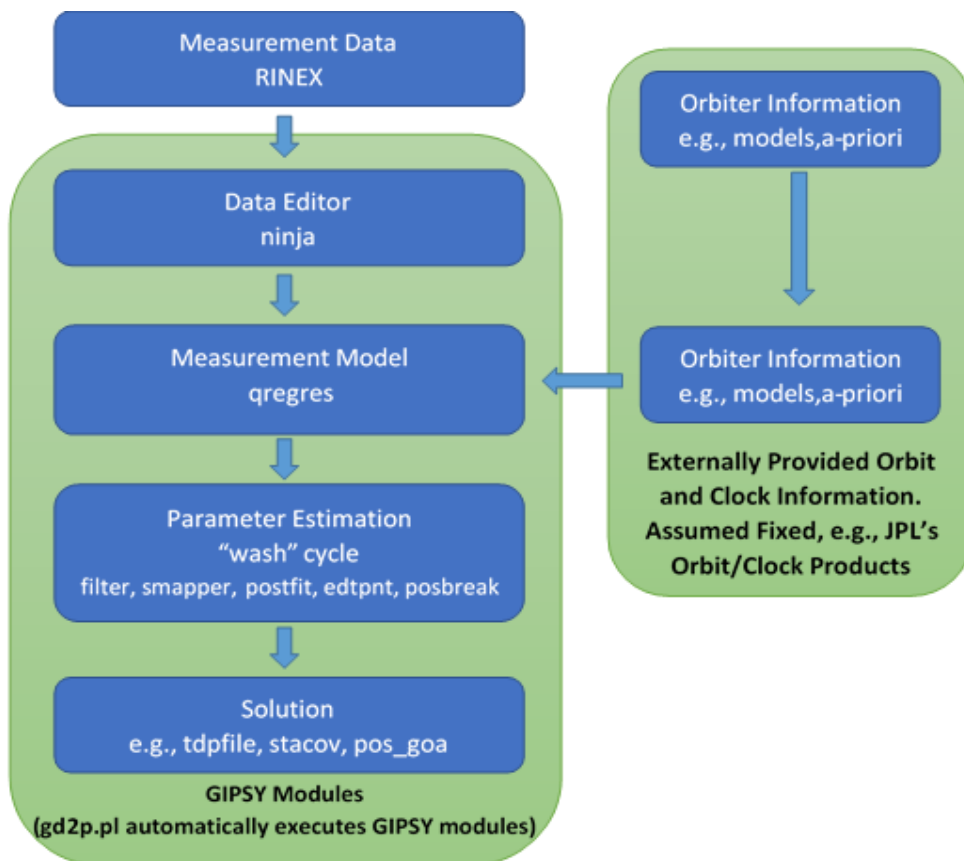


Figure 2.4 Workflow diagram for GIPSY GNSS-based terrestrial positioning [44]



#### 3.1 Data Set Management

The GPS data used in this thesis was downloaded from the Scripps Orbit and Permanent Array Center (SOPAC) data archive. SOPAC, a primary member of IGS, serves as a Global Data Center and a Global Analysis Center with the goal of supporting high precision geodetic and geophysical measurements by using GPS satellites. Precise, rapid, ultra-rapid, and hourly orbits are provided by SOPAC for IGS and NOAA's Forecast Systems Laboratory (FSL). Moreover, SOPAC web page comprises various services and tools related to GPS, such as SCOUT which is an ITRF Coordinates Generator, Site Information Manager (SIM), and a utility to check for unused 4-character site codes. SOPAC archive also contains 24-hour RINEX (Receiver Independent Exchange Format) data of about 800 continuous GPS sites distributed around the world [48].

The 24-hour RINEX GPS data, obtained from SOPAC, were first quality checked and then divided into hourly subset of GPS data for the observing session durations ( $T$ ) of 1, 2, 3, 4, 6, 8, 12 and 24 hours by using the TEQC (Translation, Editing, and Quality Check) software for evaluating different  $T$  in this thesis.

TEQC was developed by the scientists of the UNAVCO (University NAVSTAR Consortium), established in 1984 within the Cooperative Institute for Research in Environmental Sciences (CIRES) at the University of Colorado -Boulder then became an independent organization in 2001 [49]. TEQC is a free, simple but powerful and unified software designed for solving various pre-processing issues of positioning and navigation data, especially in RINEX or Binary Exchange Format (BINEX). TEQC performs three main functions including translation, editing and quality check. Translation applies binary data reading/translation of native binary formats. Editing performs time windowing, file

splicing, SV or other filtering; metadata extraction, editing, and/or correction of RINEX header metadata or BINEX metadata records. Quality check applies quality checking of GPS and/or GLONASS data (native binary, BINEX, or RINEX observation files; with or without ephemerides)[50].

### 3.2 GPS Data Processing

The GPS data used in this thesis study were sampled with elevation cut off angle of 7 degrees and the recording interval of 30 seconds. Moreover, during the analysis JPL final precise (flinnR) orbits and clocks were used. The advanced processing command given by [51] was used for processing with the precise point positioning mode of the GIPSY/OASIS software. Currently the highest available version (v 6.3) was used for processing the data.

A sample command is presented below which will be used for processing the GPS data used in this thesis.

```
gd2p.pl -i bogt0010.08o -n BOGT -r 300 -type s -d 2008-01-01 -add_ocnld -OcnldCpn -tides WahrK1 PolTid FreqDepLove OctTid -trop_z_rw 5E-8 -wetzgrad 5E-9 -w_elmin 7 -post_wind 5.0E-3 5.0E-5 -orb_clk flinnR -arp -ion_2nd -amb_res 1 -stacov > gd2p.log
```

In this command line, various options are provided as command line arguments. The meaning of options selected in thesis studies are listed in Table 3.1 which were obtained from the gd2p.pl help file and Desai and Bertiger [52]. In addition, antenna calibration procedure was not applied in this study since it was not going to effect our analysis results. However, one can perform the antenna calibration by simply including the antenna calibration function, `-AntCal station.xyz`, in the code.

The advanced processing command given above was used in a series of Linux commands in order to process required GPS data automatically. The command simply processes the data in a certain folder and generates the output stacov\_final files and places them in a desired folder. Each GPS observation data takes about 45 seconds to process with GIPSY and more than 66000 observation files were generated and processed in this thesis. Therefore, the researcher saved enormous time and effort by running the command above within a shell script.

Table 3.1 Summary of options used in GIPSY processing

Option	Definition
-i	Input rinex_file or compress_rinex
-n	Name_of_receiver
-d	Day to process (yyyy-mm-dd)
-r	Measurement data rate (sec), default 300
-type	Type of positioning method (s for static, k for kinematic)
-add_ocnld	Adds ocean loading coefficients to qregres.nml.
-OcnldCpn	Applies companion tides in the ocean tide loading displacement modeling. Cannot be used without -add_ocnld.
-tides	Adds additional solid tide models to the station qregres namelist. WahrK1, PolTid, FreqDepLove and OctTid models were selected.
-trop_z_rw	Random walk troposphere parameter for static solutions. Defaults to 1.7E-7 (km/sqrt(sec)).
-wetzgrad	If set, will solve for troposphere gradient parameters as a Random.
-w_elmin	Sets the minimum elevation cutoff angle. 7 degree was selected.
-post_wind	Final postfit range phase window for editing point cycle (in km). 5.0E-3 5.0E-5 (km) values were selected, which are typical values for well modeled objects and receivers
-orb_clk	Defines type and location of orbit and clock products for transmitting satellites. flinnR products were selected.
-ion_2nd	Turns on the 2nd-order ionosphere correction.
-amb_res	Number of iterations with ambiguity resolution with wlpb (wide lane and phase biases) file. Iteration number was set to 1.
-arp	Sets vector for the antenna reference point to the phase center to be identically 0.0.
-stacov	Generates a stacov_final file in the same reference frame as the orbits.

The results produced by GIPSY were represented by using the International Earth Rotation Service's reference system ITRS [53], with a realization of the reference frame ITRF2008 [54]. Tropospheric Zenith Wet Delay was modeled as a random-walk parameter with a variance rate of  $5 \text{ mm}^2$  per hour, and wet delay gradient as a random

walk with a variance rate of  $0.5 \text{ mm}^2$  per hour. GMF mapping function a priori zenith conditions was used when modeling the dry troposphere [55]. As explained in Chapter 2.1, the ionospheric delay was eliminated by using ionosphere free combination of undifferenced code and carrier phase observations from L1 and L2 frequencies. In addition, second order ionospheric correction given by Kedar et al. [18], ambiguity resolution introduced by Bertiger et al. [12] and ocean loading corrections were applied. Furthermore, satellite and receiver antenna phase centre variation (APV) maps were automatically applied following the IGS standards [56].

### **3.3 Outlier Removal Procedure**

GPS observations might be contaminated by outliers due to numerous reasons. For example, carrier phase observations may comprise cycle slips [30]. These outliers in the solutions degrade the quality of the accuracy modeling and they usually occur when the observation sessions are especially shorter than two hours. Classical/Traditional method and Median Method given in Tut et al. [57] were tested, and results are presented in this section.

#### **3.3.1 Traditional Method**

Outliers in data are identified and removed from the data as follows: First, the mean value and the standard deviation ( $\sigma$ ) of the solution set were computed. Then, residuals are estimated by subtracting the mean value from the individual data. Finally, the residuals which are larger than  $3\sigma$  are considered as outliers and removed from the dataset. The reduced data might still include outliers; therefore, this procedure is required to be repeated iteratively until the solution set did not contain any outlier [57].

Nevertheless, elimination of outliers can sometimes be inconvenient when the traditional method is used because it requires an iterative solution. This method could produce subjective results which might affect the statistical significance of the solutions [58]. This issue could be solved by using a robust outlier detection method such as the median method given by Tut et al. [57].

#### **3.3.2 Median Method**

This method is the simplest and because of its highest breakdown point (50%), it can be considered as the most efficient among the robust outlier detection methods [57], [59],

[60]. The median method does not require any iteration and the suspected outliers which are larger than threshold value of  $3\sigma_{mad}$  are removed in one run. As a result, it is possible to remove the problematic outliers by using the median method [61]. The required equations are given below.

$$m = \text{median}(\text{values}) \quad (3.1)$$

$$m2 = \text{values} - m \quad (3.2)$$

$$\sigma_{mad} = 1.483 \times \text{median}(\text{absolute}(m2)) \quad (3.3)$$

Detailed model description of the Median method can be found in [57], [59], [62], [63].

### 3.3.3 Outlier Detection Model Test Results

For analyzing the outlier detection models mentioned above, QUIN, an IGS CORS GPS station, was chosen because of its problematic outliers [61]. Two hours of non-overlapping sub sessions derived from 10 consecutive day data, within January of 2008, were used for this analyze.

The outlier detection method results were shown in Figure 3.1, Figure 3.2 and Figure 3.3 for north, east and vertical components of the local coordinate frame, respectively.

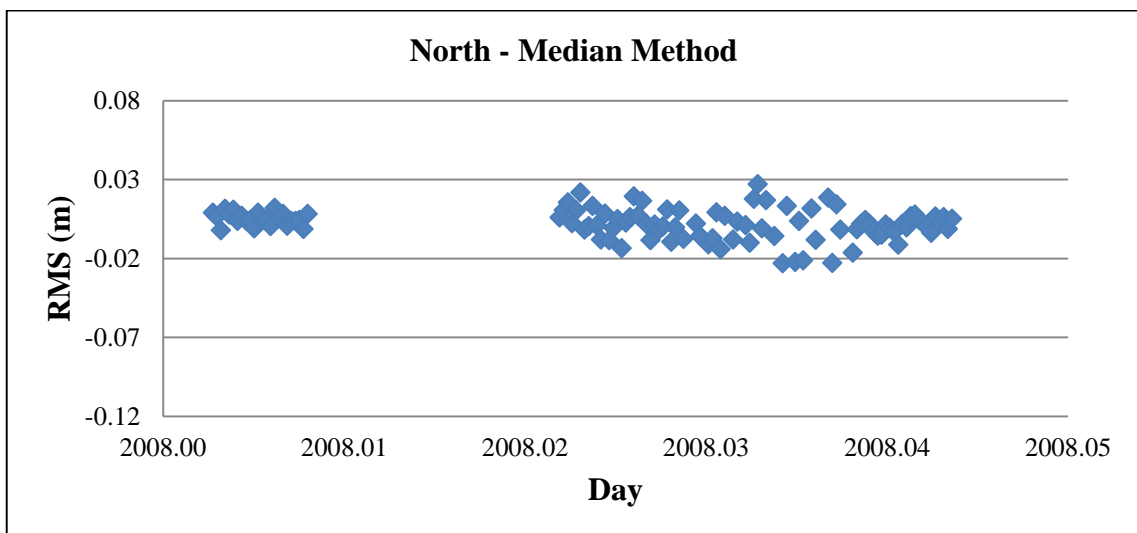
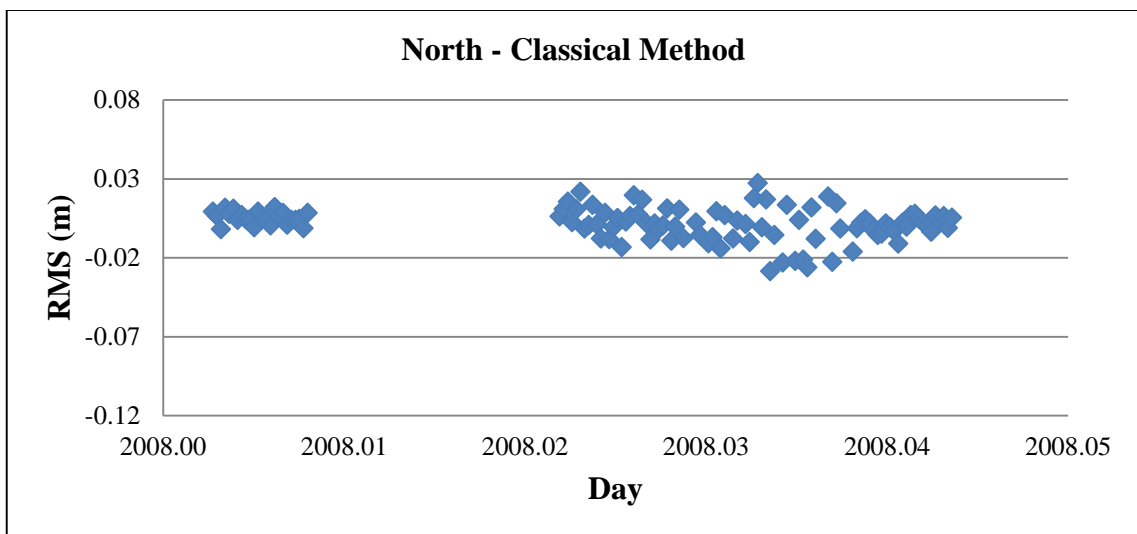
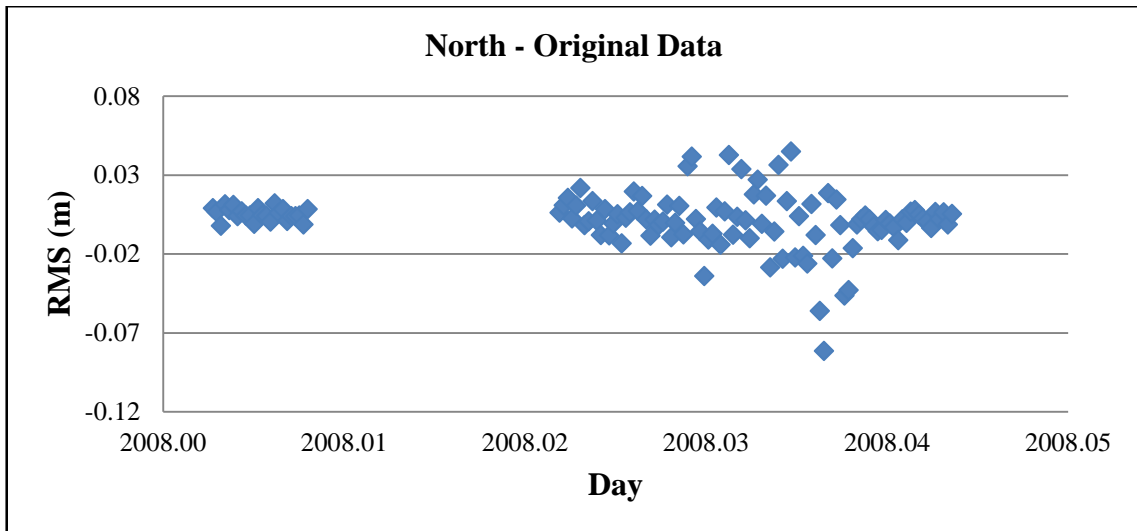


Figure 3.1 Outlier detection model results for north [61]

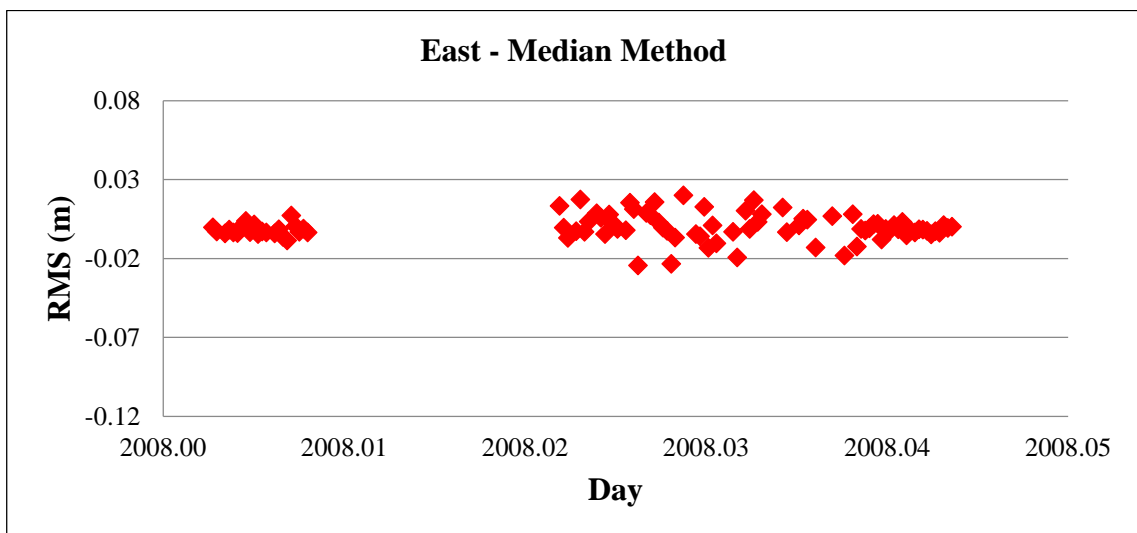
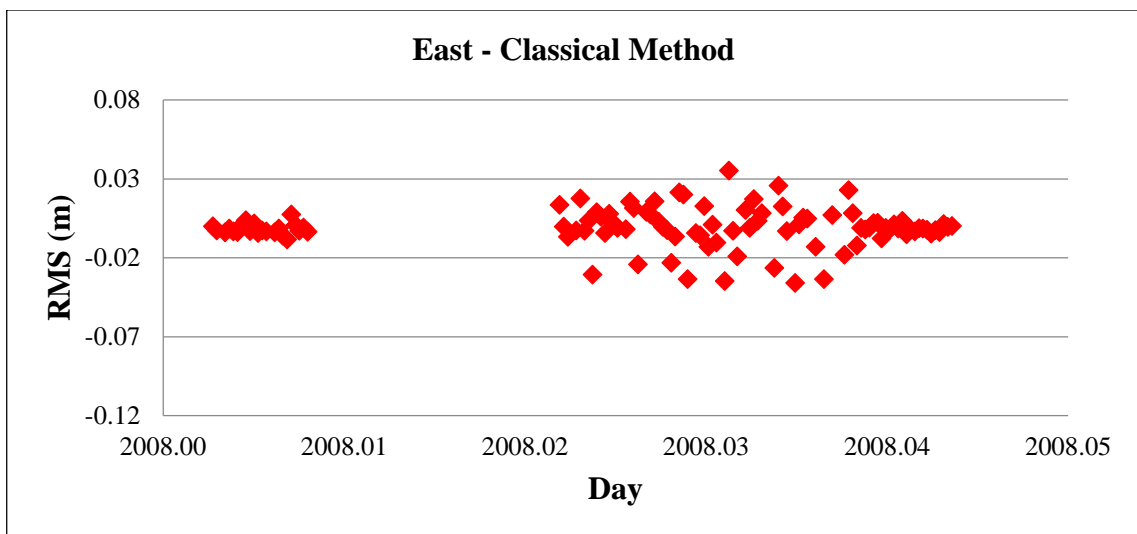
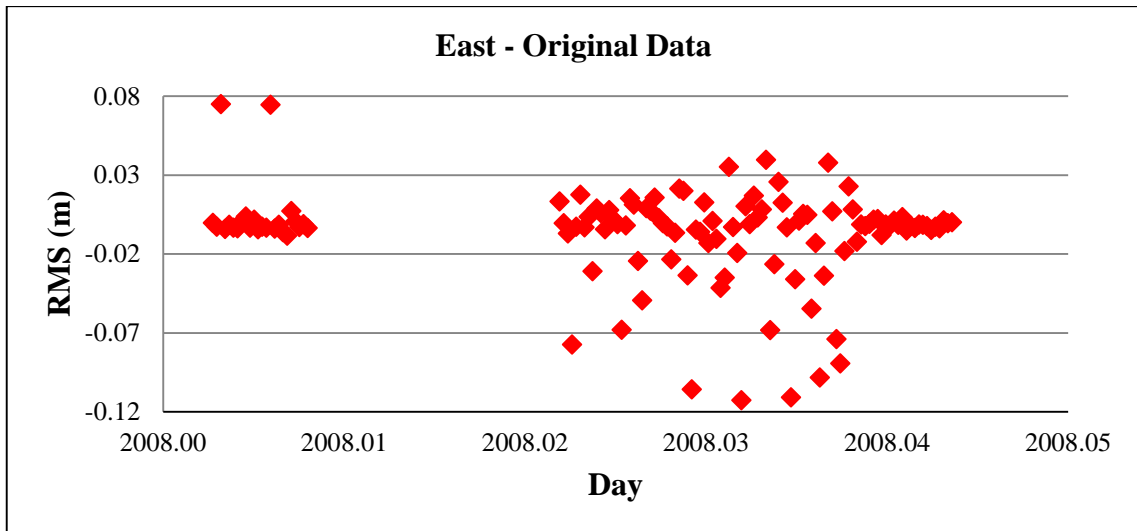


Figure 3.2 Outlier detection model results for east [61]

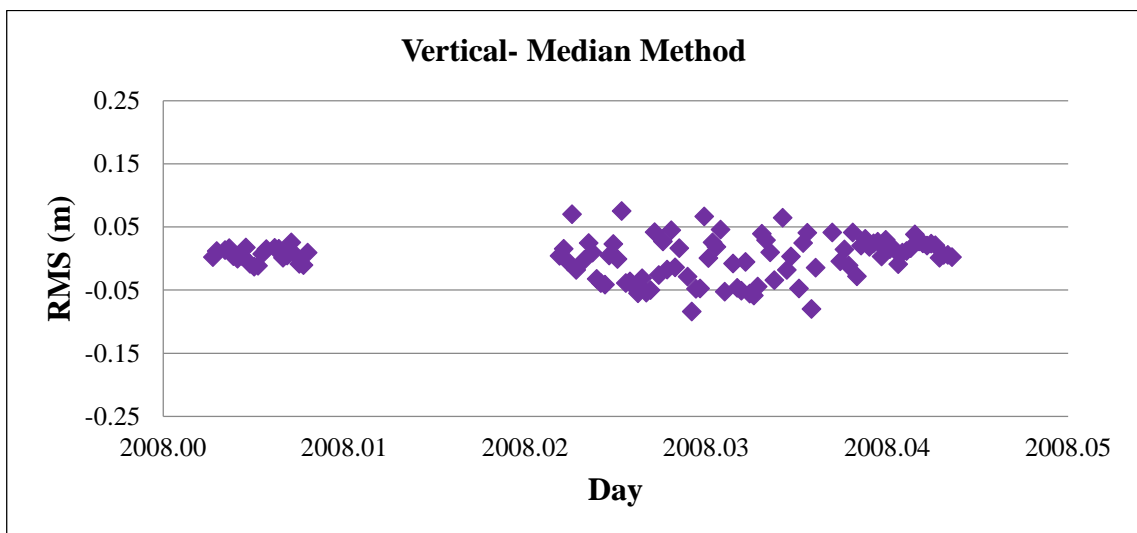
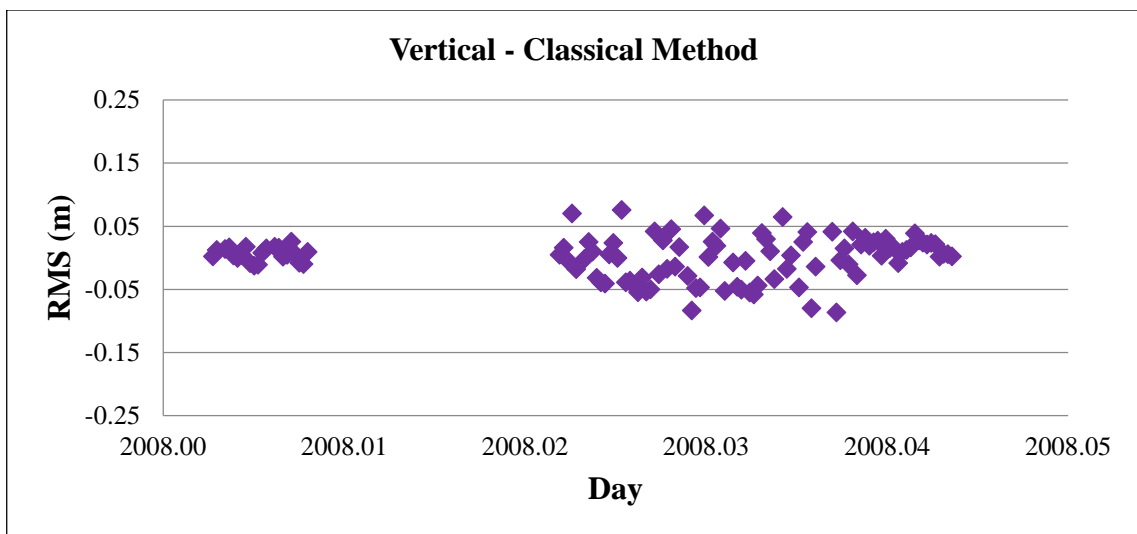
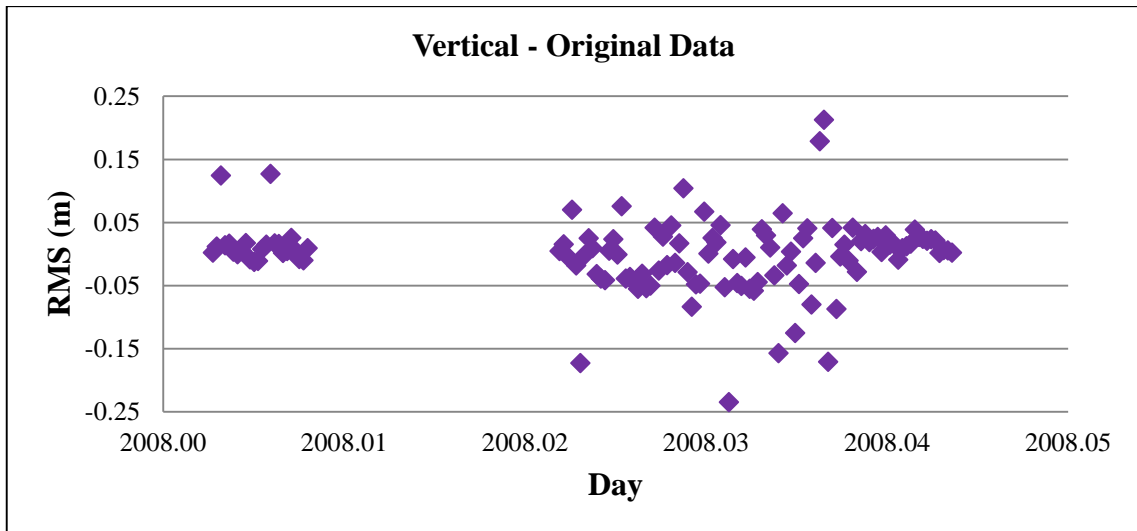


Figure 3.3 Outlier detection model results for vertical [61]

Here, with the Classical/Traditional Method, values larger than  $3\sigma$  were iteratively removed, which required 6, 7 and 4 iterations for north, east and vertical components,



respectively. On the other hand, no iteration was necessary for the median method which removed the outliers larger than  $3\sigma_{mad}$  at once. As a result, the outliers removed with the Classical method corresponded 9.2% of north, 13.3% of east and 8.3% of vertical component data. When the median method was used, these percentages were obtained as 10.8%, 21.7% and 9.2% for north, east and vertical components, respectively. These results and the RMS values estimated after the outliers were removed can be found in Table 3.2 below.

Table 3.2 Outlier detection model estimations

Coordinate Frame Component	Original Data	Outlier Detection Methods			
		Classical Method		Median Method	
	RMS (mm)	Outliers Removed (%)	RMS (mm)	Outliers Removed (%)	RMS (mm)
North	17.2	9.2	10.1	10.8	9.5
East	30.4	13.3	12.1	21.7	8.0
Vertical	57.1	8.3	32.6	9.2	31.7

### 3.4 PPP Accuracy Model

The accuracy results studied in this thesis were obtained by comparing the results of each station's short GPS observation sessions with their average of 24 hour sessions from 10 consecutive days by assuming the average of 24 hour results as the true (or the most accurate) values. Since an average of 24 hours results were considered as the true (or the most accurate) values, the term "accuracy" rather than the term "precision" was used in this thesis when evaluating the PPP accuracy [14].

Before introducing the PPP accuracy model, it is necessary to disclose some of its limitations. The accuracy model studies in this thesis will have some limitations as also mentioned by Eckl et al. [9] in their research methodology. This study will not be capable of comparing the accuracy of PPP with the accuracy of the other GPS positioning techniques, mentioned in Chapter 2.1, because each individual GPS solution was compared with the average of 24 hour solutions by estimating the RMS values in this study as mentioned above. In addition, this study will not be able to compare the GPS

results with the results of other terrestrial and space positioning techniques such as Electronic Distance Measurement Technology (EDM), Russian Global Navigation Satellite System (GLONASS), Very Long Baseline Interferometry (VLBI) and Satellite Laser Ranging (SLR). On the other hand, since 10 consecutive days of GPS data were used in this study, the accuracy results will not be able to represent the short term seasonal effects, such as the effects of variations in temperature and humidity, and long term seasonal effects, such as tidal effects and variations in solar activity. Furthermore, the GPS data will be processed by using the GIPSY and the accuracy results will not be compared with results of the other positioning software.

The Accuracy model developed by Sanli and Tekic [2] is given below.

$$S(\varphi, T) = \sqrt{\frac{a}{T} + \frac{b\varphi^2}{T} + c + d\varphi^2} \quad (3.4)$$

where  $S_n(\varphi, T)$  denotes the accuracy (estimated RMS values) of the north GPS positioning components north, east and vertical in mm as a function of station latitude  $\varphi$  in degrees and observation session length  $T$  in hours. The coefficients  $a, b, c$  and  $d$  are derived through a LS analysis [9].

By taking the square of both of sides of the equation we will obtain the linearized equation as below.

$$S^2 = \frac{a}{T} + \frac{b\varphi^2}{T} + c + d\varphi^2 \quad (3.5)$$

According to the given model in equation (3.5), the design matrix  $A$ , the unknown parameter vector  $X$  and the observation vector  $y$  are defined as below.

$$A = \begin{bmatrix} \frac{1}{T_1} & \frac{\varphi_1^2}{T_1} & 1 & \varphi_1^2 \\ \vdots & \vdots & \vdots & \vdots \\ \frac{1}{T_m} & \frac{\varphi_1^2}{T_m} & 1 & \varphi_1^2 \\ \frac{1}{T_1} & \frac{\varphi_2^2}{T_1} & 1 & \varphi_2^2 \\ \vdots & \vdots & \vdots & \vdots \\ \frac{1}{T_m} & \frac{\varphi_2^2}{T_m} & 1 & \varphi_2^2 \\ \vdots & \vdots & \vdots & \vdots \\ \frac{1}{T_m} & \frac{\varphi_l^2}{T_m} & 1 & \varphi_l^2 \end{bmatrix}_{k \times i} \quad (3.6)$$

where  $l$  is the number of observations,  $k = m \times l$  and  $i$  is the number of unknown coefficients, which is equal to 4 in equation (3.4),  $m$  is the observing session duration number, where  $T = 1, 2, 3, 4, 6, 8, 12, 24$  h.

$$X = \begin{bmatrix} a \\ b \\ c \\ d \end{bmatrix}_{i \times 1} \quad (3.7)$$

$$y = \begin{bmatrix} s_1^2 \\ \vdots \\ s_l^2 \end{bmatrix}_{k \times 1} \quad (3.8)$$

In addition, the observations have equal weights, so the weight matrix  $P$  is formed as  $P = I_{k \times k}$ , where  $I$  is the identity matrix.

The unknown coefficients ( $a$ ,  $b$ ,  $c$  and  $d$ ) in equation (3.5) can be estimated by using the LS solution in the Gauss Markov Model. The Gauss-Markov Model is defined by

$$y = AX + e, \quad e \sim (0, \sigma_0^2 P^{-1}) \quad (3.9)$$

where  $y$  is the  $k \times 1$  observation vector,  $A$  is the  $k \times i$  design matrix,  $X$  is the  $i \times 1$  unknown parameter vector,  $e$  is the  $k \times 1$  random error vector,  $P$  is the  $k \times k$  symmetric, positive-definite weight matrix,  $Q = P^{-1}$  is the  $k \times k$  cofactor matrix,  $\sigma_0^2$  is the unknown variance component. The least-squares estimates of parameters is obtained as

$$\hat{X} = (A^T P A)^{-1} A^T P y \quad (3.10)$$

with the residual vector

$$\tilde{e} = y - A\hat{X} \quad (3.11)$$

the estimated variance component is calculated as

$$\hat{\sigma}_0^2 = \frac{\tilde{e}^T P \tilde{e}}{k-m} \quad (3.12)$$

In their studies, Sanli and Tekic [2] tested the coefficients obtained by the equations above with the Students  $t$  test for the significance level of  $\alpha = 0.05$ . Then, coefficients that have the ratio value of larger than 2 (corresponding the confidence level of 95%, obtained from  $t$ -Table) were found to be significantly different than zero for the given significance level, which is the coefficient  $a$  for north, east and vertical positioning components, and the insignificant components  $b$ ,  $c$ , and  $d$  were eliminated by the authors. Then, the model

was regenerated (reduced) as in equation (3.13), which estimates the accuracy with respect to observing session duration and will be referred as the reduced PPP accuracy model afterwards.

$$S_n(T) = \sqrt{\frac{a_n}{T}} \quad (3.13)$$

After that, the authors reapplied the LS method for obtaining the final coefficient values. However, the design matrix ( $A$ ) was needed to be regenerated as below keeping the rest of the LS equations the same as given above.

$$A = \begin{bmatrix} \frac{1}{T_1} \\ \vdots \\ \frac{1}{T_m} \end{bmatrix}_{m \times 1} \quad (3.14)$$

$$X = [a_n]_{i \times 1}, (i = 1) \quad (3.15)$$

Moreover, the Reduced PPP Accuracy Model for the east and vertical components are derived again by replacing  $n$  with  $e$  and  $v$ , respectively.

### NUMERICAL STUDY AND RESULTS

In this section, the available model for PPP accuracy will be regenerated by taking the advancements of the JPL's modeling and analysis strategy into consideration. Then, attempts to produce a new and improved PPP accuracy model will be presented together with evaluations of the models tested. Moreover, the Revised Accuracy Model will be provided for both by using the same GPS stations of Sanli and Tekic [2] obtained by using a recent GPS data set and by a different and a denser GPS network consisting of 67 globally distributed GPS stations from IGS network. Finally, the denser accuracy model will be introduced regionally.

#### 4.1 Current PPP Accuracy Model

The model developed by Sanli and Tekic [2] is the only PPP accuracy model available today. However, this model lacks the integration of innovative advancements that JPL had brought to their modeling and analysis strategy (see Chapter 2.4 for more detail) because the authors used an older version of GIPSY (version 4.0) which does not contain the advancements. Therefore, it was aimed to rework the Sanli and Tekic [2] model in this section. The same GPS network of Sanli and Tekic [2] was adopted for this study. For a direct comparison of the results and also for providing the same ionospheric conditions, the experiments were carried out by using January 2008 GPS data as done in Sanli and Tekic [2]. For the same reason, the atmospheric conditions of the observation days were not taken into consideration when preparing the observation schedule, as it was not done by Sanli and Tekic [2]. The ionospheric conditions in 2008 coincided with the last solar minimum where current ionospheric corresponds to a solar cycle maximum [44]. The IGS stations used by Sanli and Tekic are presented in Figure 4.1 and the observation schedule was presented in Table 4.1 while detailed information about these GPS stations are given in Table A.1.

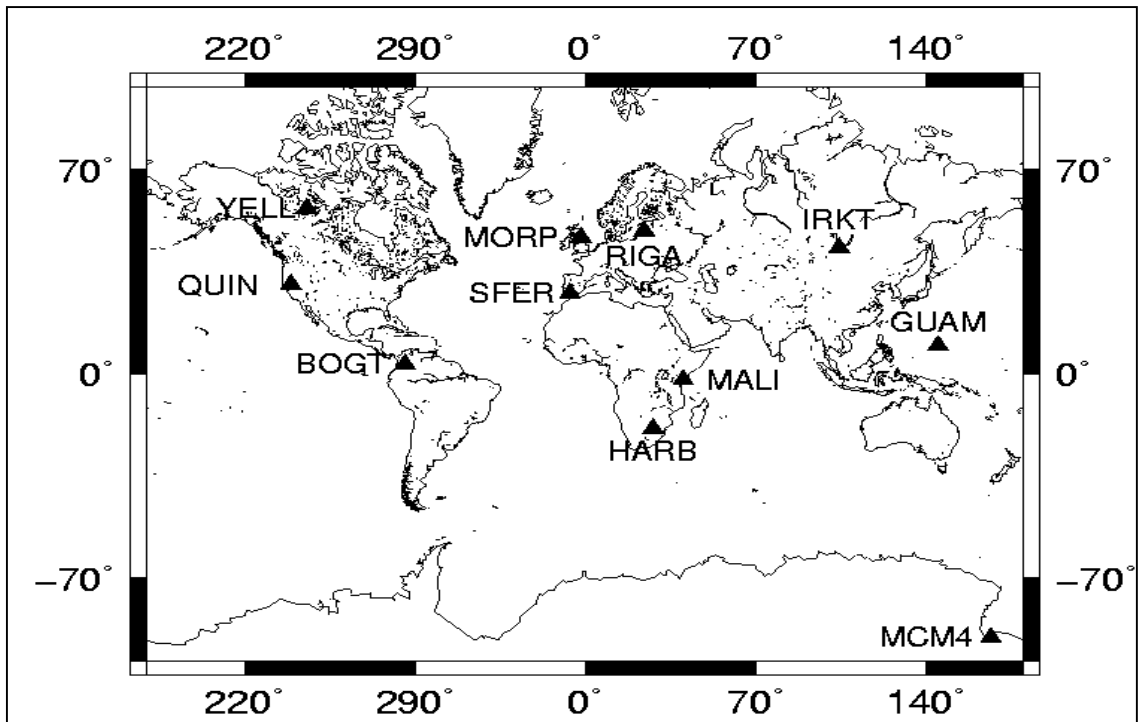


Figure 4.1 GPS stations used in Sanli and Tekic [2]

Table 4.1 Observation time schedule for the current accuracy model, X denotes that data from this day were included in the study

Site ID	Site Lat. (°)	Day of the Year (2008)											
		1	2	8	9	10	11	12	13	14	15	16	
BOGT	4.6	X	X	X	X	X	X	X	X	X	X	X	-
GUAM	13.6	X	X	X	X	X	X	X	X	X	X	X	-
HARB	-25	X	X	X	X	X	X	X	X	X	X	X	-
IRKT	52.2	X	X	X	X	X	X	X	X	X	X	X	-
MALI	-3	X	X	X	X	X	X	X	X	X	X	-	X
MCM4	-77.8	X	X	X	X	X	X	X	X	X	X	X	-
MORP	55.2	X	X	X	X	X	X	X	X	X	X	X	-
QUIN	40	X	X	X	X	X	X	X	X	X	X	X	-
RIGA	57	X	X	X	X	X	X	X	X	X	X	X	-
SFER	36.5	X	X	X	X	-	X	X	X	X	X	X	X
YELL	62.5	X	X	X	X	X	X	X	X	X	X	X	-

The daily GPS data was divided into non-overlapping sub-sessions generating the observation files with  $T$  equals to 1, 2, 3, 4, 6, 8, 12 and 24 hours. Then, these observation files were processed by using the highest available version of GIPSY (version 6.3) and three dimensional coordinates of the individual observation data were estimated. Next, these coordinates were transformed to the local North-East-Vertical (NEV) coordinate frame allowing us to analyze the positioning components individually. The possible outliers in the results were removed by using the median method, a reliable robust outlier detection method given by Tut et al. [57] and described in Chapter 3.3.2. Then, RMS values were estimated by considering the 24 hour data results as the true values. The RMS values get smaller as  $T$  increases. Table 4.2, Table 4.3 and Table 4.4 present the estimated RMS values for the positioning components of north, east and vertical, respectively.

Table 4.2 Estimated RMS values of the current accuracy model, for north (in mm)

Site ID	Observing Session Duration (T)							
	1 h	2 h	3 h	4 h	6 h	8 h	12 h	24 h
BOGT	15.19	3.75	2.88	2.36	1.86	1.45	1.34	1.46
GUAM	23.34	6.15	4.94	4.62	3.93	3.28	3.59	1.80
HARB	12.38	3.81	3.19	3.11	2.64	2.54	2.88	2.43
IRKT	24.35	5.47	3.66	3.14	2.13	1.93	1.66	1.35
MALI	30.64	6.88	4.80	3.52	2.50	2.03	1.51	1.47
MCM4	16.08	3.58	2.91	2.31	2.02	2.55	1.68	1.56
MORP	25.65	4.92	3.40	3.13	2.34	1.77	1.98	1.31
QUIN	29.32	10.63	10.67	8.36	6.90	6.79	4.99	4.43
RIGA	12.72	3.75	2.83	2.35	1.95	1.70	0.75	0.76
SFER	12.97	4.39	3.05	2.52	1.87	1.83	1.65	1.28
YELL	14.31	3.59	2.35	2.15	1.59	1.68	1.42	0.55

Table 4.3 Estimated RMS values of the current accuracy model, for east (in mm)

Site ID	Observing Session Duration (T)							
	1 h	2 h	3 h	4 h	6 h	8 h	12 h	24 h
BOGT	55.95	5.56	3.52	3.03	2.25	1.79	1.46	0.94
GUAM	63.17	8.29	6.10	4.31	4.24	4.79	4.18	3.44
HARB	33.14	4.49	3.37	2.59	2.79	2.43	2.28	1.85
IRKT	59.63	4.27	2.76	2.52	2.16	1.82	1.72	1.27
MALI	86.94	8.77	7.78	5.58	4.55	4.10	2.69	2.75
MCM4	14.75	3.33	2.24	2.16	1.98	1.75	1.45	1.20
MORP	47.13	3.66	2.57	2.22	1.80	1.49	0.66	1.12
QUIN	59.34	8.43	6.08	4.25	2.25	2.43	1.60	1.13
RIGA	26.34	2.80	2.19	2.19	1.88	1.90	1.66	1.60
SFER	34.54	4.21	2.81	2.47	1.85	1.63	1.12	1.29
YELL	22.48	3.41	2.37	2.25	2.04	1.79	1.63	1.55

These RMS values were used for estimating the current PPP accuracy model by following the estimation steps given in Chapter 3.4. Note that modeling the accuracy of the GPS with respect to observing session duration is just a preference. Sanli and Tekic [2] widely discussed the possible influences on the accuracy. For instance, they showed the effect of station latitude on solutions. However, in this study, following the tradition given in Eckl et al. [9] and Sanli and Tekic [2], the accuracy has been modeled only with respect to observing session duration. Various forms of mathematical representation concerning the observation session has been discussed in Section 4.3.

Accuracy model estimation results showed that 4-24 hour session solutions could be used for modeling the PPP accuracy while Sanli and Tekic [2] were able to use 6-24 hour session lengths in their study. This improvement was expected because of the improvements in JPL and IGS products. Therefore, RMS values obtained from 4-24 hour session results were used in estimating the accuracy model coefficients in this thesis.



Table 4.4 Estimated RMS values of the current accuracy model, for vertical (in mm)

Site ID	Observing Session Duration (T)							
	1 h	2 h	3 h	4 h	6 h	8 h	12 h	24 h
BOGT	67.84	22.26	10.62	9.31	6.50	6.70	4.88	2.17
GUAM	100.31	44.34	24.61	19.33	15.98	13.93	9.56	6.41
HARB	46.52	22.13	16.32	12.32	7.59	6.69	4.84	4.57
IRKT	67.60	24.55	16.32	14.44	9.53	7.54	6.79	6.58
MALI	105.04	36.99	27.98	21.36	22.36	14.37	9.17	6.59
MCM4	37.89	14.68	11.19	10.66	10.13	6.47	7.00	3.77
MORP	58.27	19.77	15.39	12.19	10.74	9.47	7.06	5.03
QUIN	87.65	29.67	30.26	24.56	18.61	17.60	17.71	15.11
RIGA	37.24	15.99	13.79	12.60	9.82	9.90	6.66	4.77
SFER	44.68	16.12	9.02	8.17	7.31	4.51	4.27	2.22
YELL	29.92	14.47	10.41	10.16	6.05	5.67	5.76	2.83

The unknown coefficients  $a$ ,  $b$ ,  $c$ , and  $d$  (3.7) for each positioning component were estimated by using the LS technique and the test statistics were generated by dividing the estimated values to their standard deviations (formal errors or 1-sigma uncertainties). These values were presented in Table 4.5.

Table 4.5 Estimated coefficients, their 1-sigma uncertainties and ratio values of the current accuracy model, for position components north, east and vertical

<b>Coefficient</b>	<b>Estimate</b>	<b>Uncertainty</b>	<b>Ratio</b>
$a_n(mm^2 \cdot h)$	65.39	34.47	1.90
$a_e(mm^2 \cdot h)$	53.08	14.43	3.68
$a_v(mm^2 \cdot h)$	1239.07	318.74	3.89
$b_n(mm^2 \cdot h/degree^2)$	-7.08E-03	1.25E-02	-0.57
$b_e(mm^2 \cdot h/degree^2)$	-8.69E-03	5.22E-03	-1.66
$b_v(mm^2 \cdot h/degree^2)$	-1.63E-01	1.15E-01	-1.41
$c_n$	2.06	5.22	0.40
$c_e$	2.82	2.18	1.29
$c_v$	-7.93	48.25	-0.16
$d_n(mm^2/degree^2)$	-2.00E-04	1.89E-03	-0.11
$d_e(mm^2/degree^2)$	-5.40E-04	7.91E-04	-0.68
$d_v(mm^2/degree^2)$	3.24E-03	1.75E-02	0.19

After applying the Students t test for  $\alpha = 0.05$  significance level, the coefficients having the ratio values smaller than 2 ( $b$ ,  $c$  and  $d$ ) were eliminated as described in Chapter 3.4. Then, the accuracy model was reduced to be as in equation (3.13), which only has the coefficient  $a$ ; the only one that depends on  $T$ . Then by applying the LS technique again, coefficient  $a$  for the three dimensional positioning components and their statistical values are estimated as below.

Table 4.6 Estimated coefficients, their 1-sigma uncertainties and ratio values of the current accuracy model, for position components north, east and vertical

<b>Coefficient</b>	<b>Estimate</b>	<b>Uncertainty</b>	<b>Ratio</b>
$a_n(mm^2 \cdot h)$	60.31	10.72	5.63
$a_e(mm^2 \cdot h)$	44.97	5.35	8.40
$a_v(mm^2 \cdot h)$	894.01	103.50	8.64

By using the coefficients in Table 4.6, the current PPP accuracy model was generated as below.

$$\begin{aligned}
 S_n &= \frac{7.8}{\sqrt{T}} \left[ \frac{mm\sqrt{h}}{\sqrt{h}} \right] \\
 S_e &= \frac{6.8}{\sqrt{T}} \left[ \frac{mm\sqrt{h}}{\sqrt{h}} \right] \\
 S_v &= \frac{29.9}{\sqrt{T}} \left[ \frac{mm\sqrt{h}}{\sqrt{h}} \right]
 \end{aligned} \tag{4.1}$$

where  $S_n$ ,  $S_e$ ,  $S_v$  are the accuracy estimates (for north, east and vertical components) and  $T$  is the observing session duration in hours.

Comparing equation (4.1) with the accuracy model estimations of Sanli and Tekic [2], it follows that the accuracy of GPS PPP improved about 42% for the north, 67% the east, and 27% for the vertical coordinate due to the advancements in JPL's new orbit determination strategy and modeling strategy, especially the ambiguity resolution technique and 2<sup>nd</sup> order ionosphere modeling.

The solid black line superimposed through the RMS values in Figure 4.3 and Figure 4.5 represents the model derived using equation (4.1).

## 4.2 Contributions of Ambiguity Resolution and Second Order Ionospheric Correction

In order to analyze the effects of the ambiguity resolution and second order ionospheric correction on the positioning accuracy, GPS data from the same GPS stations and the same time interval (January 2008) of Sanli and Tekic [2], studied in the Chapter 4.1, were processed based on four different scenarios by using the LS steps given in Chapter 3.4. First, both of these solutions were not considered during the process. Second, only the second order ionospheric correction was included in the process. Third, only the ambiguity resolution was considered when processing the data. The final process included both of the solutions which was already done in the Chapter 4.1.

Table 4.7 presents the results obtained by using the reduced accuracy model (3.13). Results from the first, second, third and the final scenarios were given in the columns named none, ion, amb and all, respectively.

Table 4.7 Accuracy model estimates of the ambiguity resolution and second order ionospheric correction

<b>Parameter</b>	<b>none</b>	<b>ion</b>	<b>amb</b>	<b>all</b>
$S_n$ (mm)	$\frac{9.9}{\sqrt{T}}$	$\frac{9.8}{\sqrt{T}}$	$\frac{7.8}{\sqrt{T}}$	$\frac{7.8}{\sqrt{T}}$
$S_e$ (mm)	$\frac{19.7}{\sqrt{T}}$	$\frac{19.6}{\sqrt{T}}$	$\frac{6.8}{\sqrt{T}}$	$\frac{6.8}{\sqrt{T}}$
$S_u$ (mm)	$\frac{35.6}{\sqrt{T}}$	$\frac{35.5}{\sqrt{T}}$	$\frac{29.7}{\sqrt{T}}$	$\frac{29.9}{\sqrt{T}}$

These results showed that the second order ionospheric correction did not affect the positioning accuracy while the ambiguity resolution significantly improves the horizontal positioning accuracy, especially in the east direction (see Table 4.7 and Figure 4.2). It can be concluded from Table 4.7 that positioning accuracies could be improved by 21%, 65% and 17% for positioning components north, east and vertical, respectively, when the ambiguity resolution was employed.

Moreover, when the daily geomagnetic activity prepared by the U.S. Dept. of Commerce, NOAA, Space Weather Prediction Center [64] and (see Table B.1) was examined for the observation days, it can be seen that the low geomagnetic activity (K-indices are lower than 5) is observed for the middle latitude areas for all the observation days and for the majority of the days belong to the high latitude areas. Therefore, second order ionospheric correction was already expected not to have a large effect on positioning accuracy.

The RMS values estimated from these four scenarios are depicted in Figure 4.2 below for the IGS station of QUIN while Figure 4.3 represents these predicted RMS values together with the RMS values of the GPS stations used in this study.

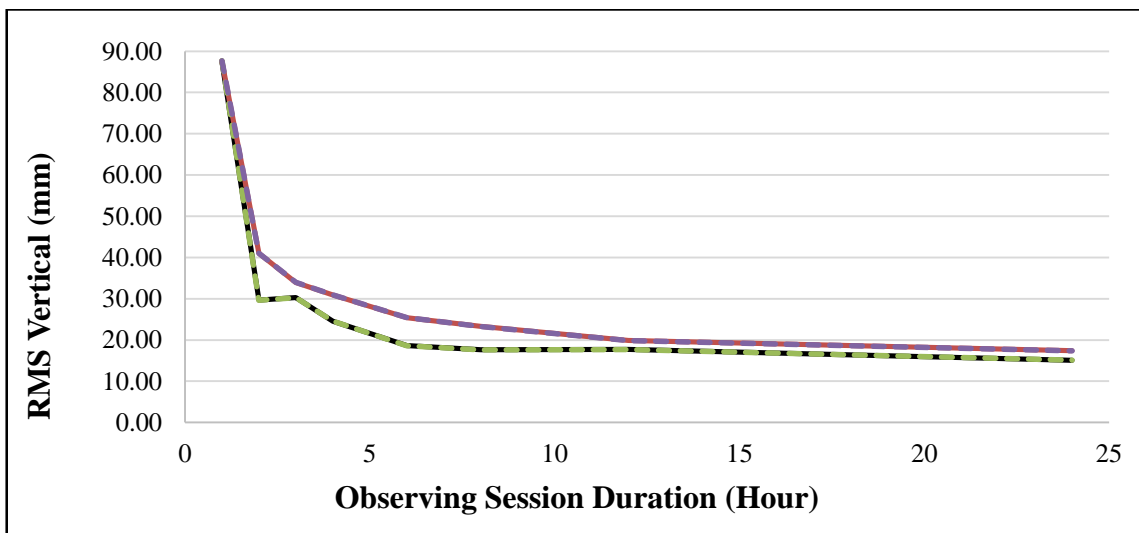
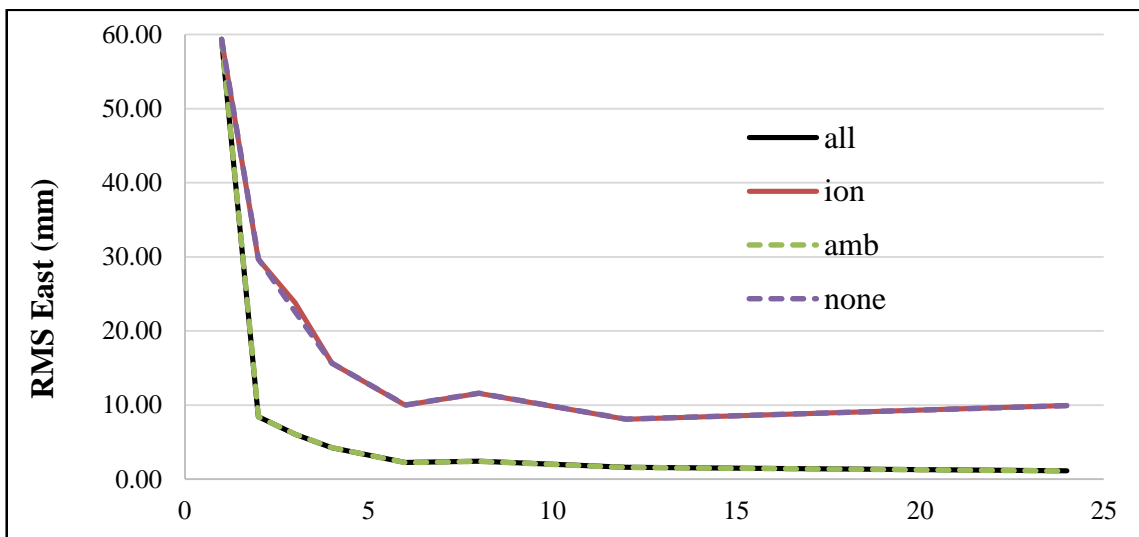
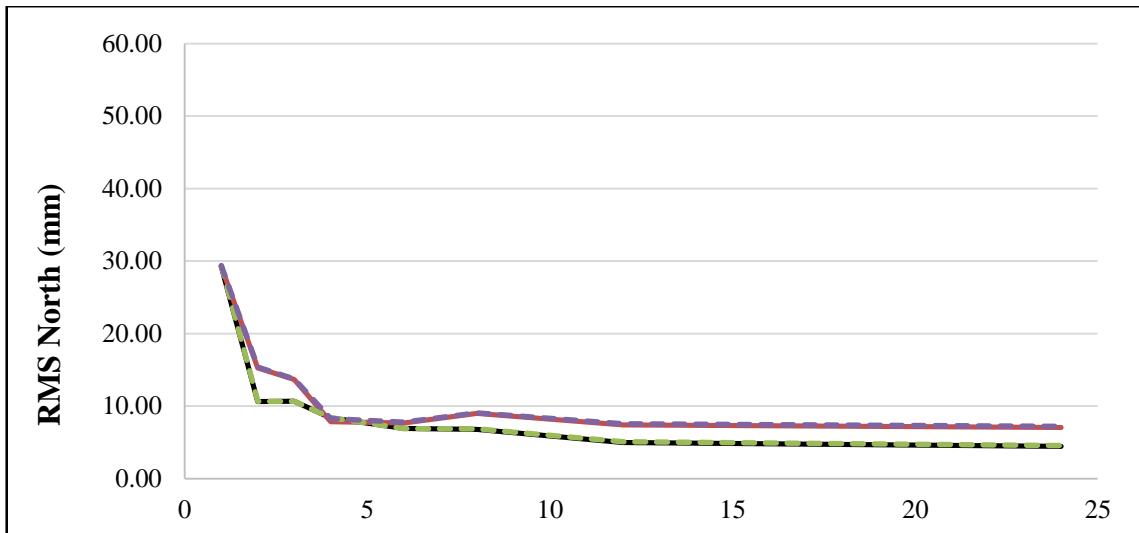


Figure 4.2 RMS estimations of QUIN based on the four scenarios

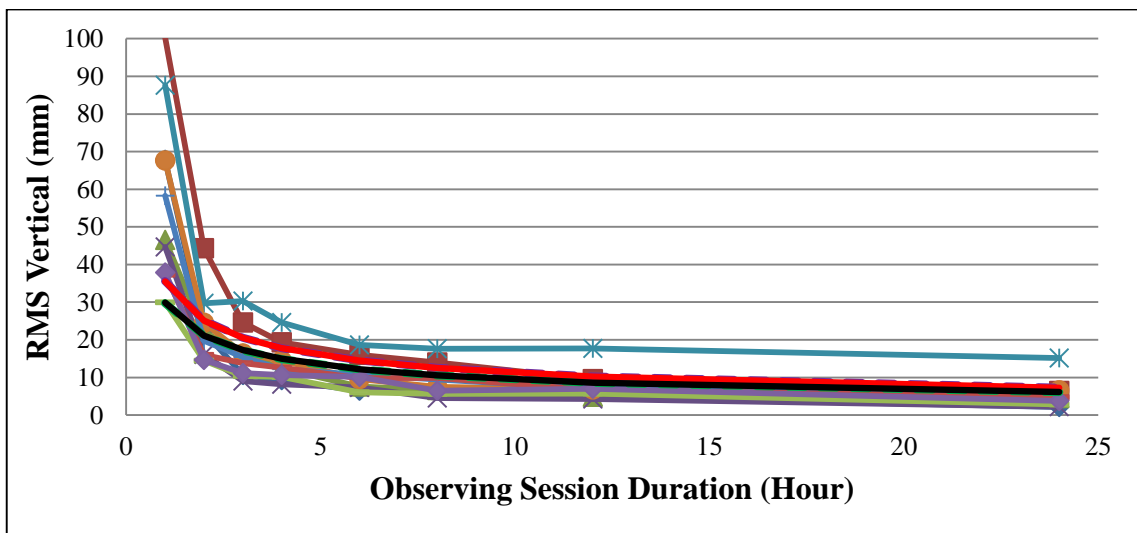
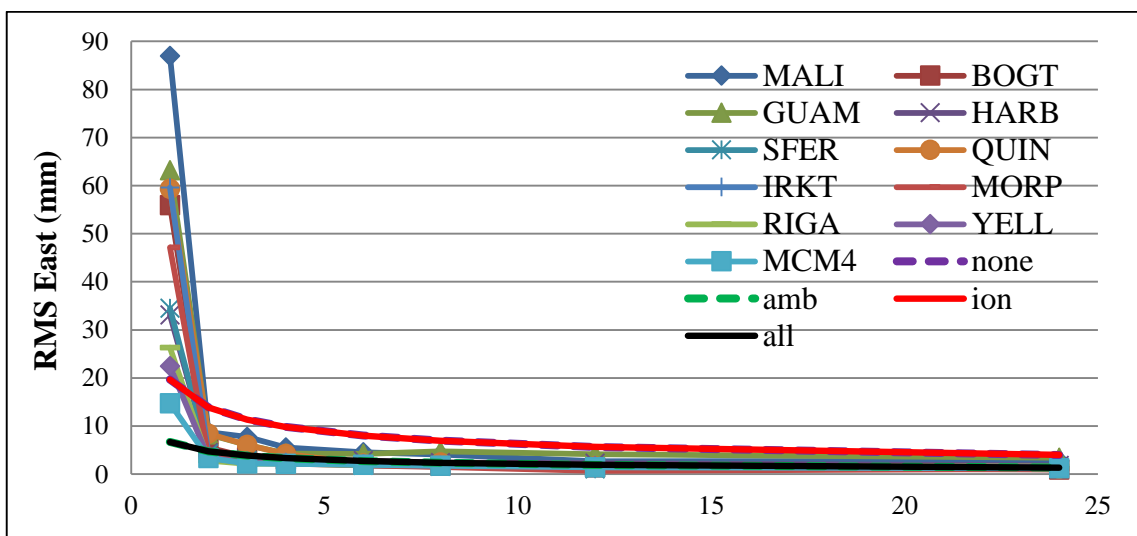
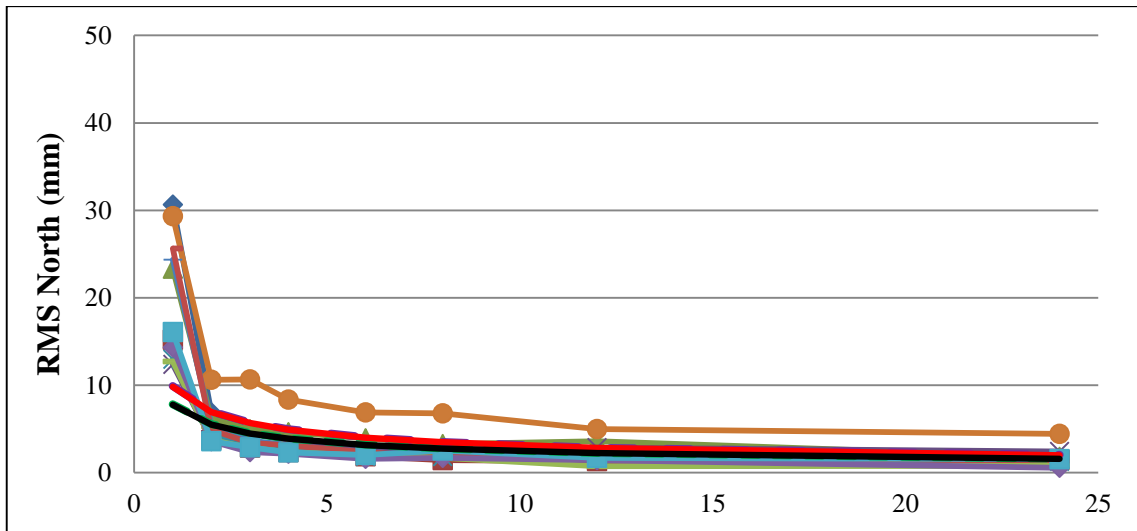


Figure 4.3 Prediction/model fit of the accuracy models of the four scenarios to the RMS values of this study, from observing session durations of 1 through 24 h

Figure 4.4, below, presents the effects of JPL’s new modeling and analysis strategy on accuracy model (3.13) coefficients comparing the results of the Sanli and Tekic [2] model, the model without the corrections stated in this section (none) and the model including these corrections as well as the model generated by using the denser GPS network data given in Chapter 4.2.

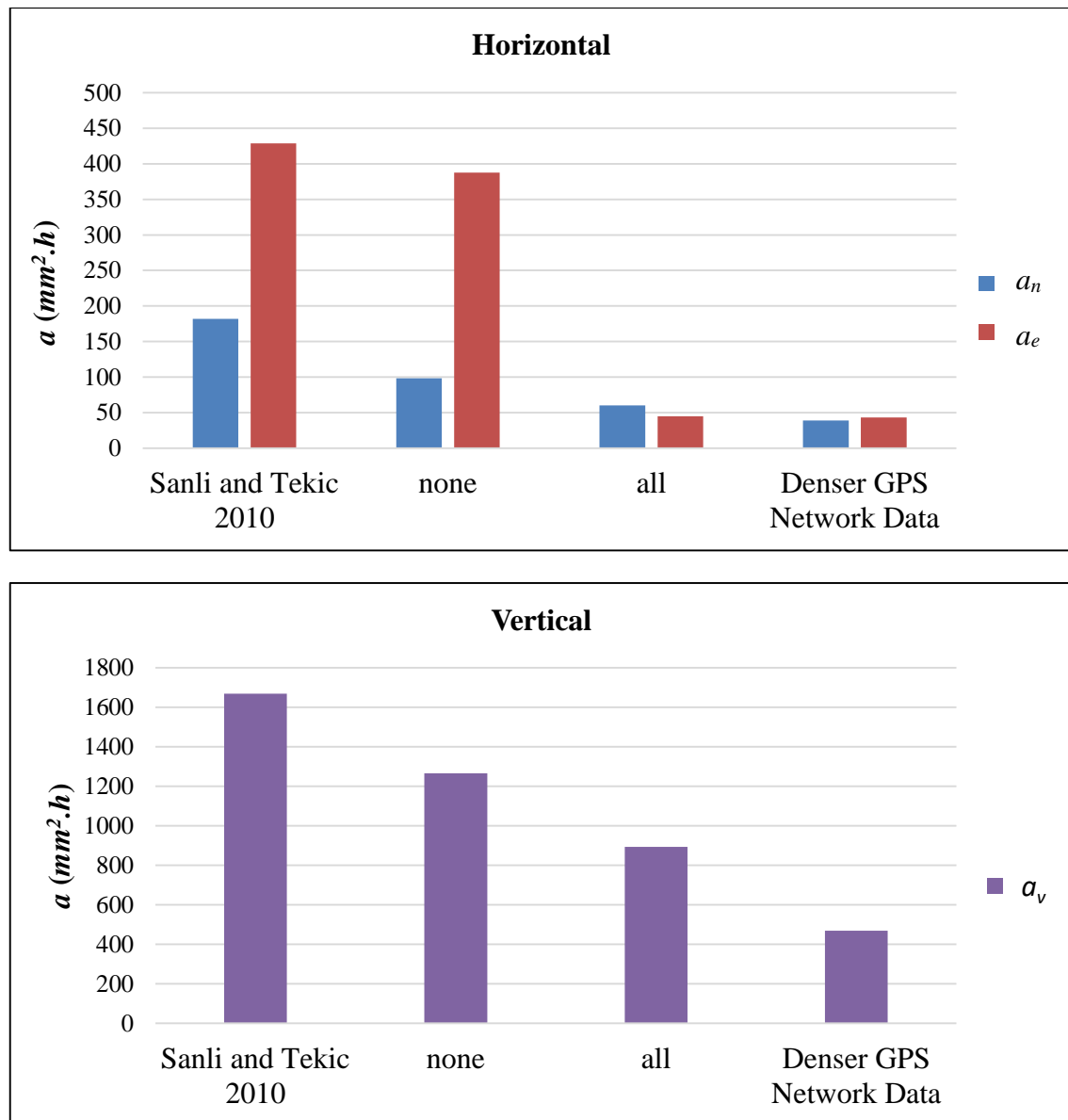


Figure 4.4 Effects of the JPL’s new modeling and analysis strategy on positioning accuracy coefficients

Here  $a_n$ ,  $a_e$  and  $a_v$  represent the coefficients for north, east and vertical components, respectively. Moreover, the accuracy prediction model values are obtained by equation (3.13).

It can be concluded from the results presented above that the advancements in JPL's analyze strategy has significantly improved the positioning accuracy, especially for horizontal positioning components.

### 4.3 New Accuracy Model Trials

New accuracy models were tested out in this section. The main motivation behind this effort is the current PPP accuracy model (4.1), as well as Sanli and Tekic [2] model, appears convoluted compared to a straightforward polynomial expansion and a logarithmic function. Therefore, less complicated and straightforward models need to be tested in order to generate a better accuracy model. Moreover, observing session durations of 4-24 h were only comprised in the current accuracy model (see Figure 4.5). The remaining 1-3 h sessions were predicted by using the model in equation (4.1). In addition, the predicted model does not fit well for the 1-4 hour sessions. Another reason for investigating new accuracy models is to examine if it is possible to generate a model that fits better for the shorter session durations.

#### 4.3.1 Straightforward Polynomial Accuracy Model

First and second degree polynomial models were tested as below.

- **First Order Polynomial Model**

In this section, it will be shown that the PPP accuracy could also be modeled using a straightforward polynomial expansion rather than the convoluted formulation adopted by Sanli and Tekic [2]. The new model, i.e. the corresponding form of equation (3.4), can be reformulated as:

$$P(|\varphi|, T) = a_{00} + a_{10}|\varphi| + a_{01}T + a_{11}|\varphi|T \quad (4.2)$$

where  $a_{00}$ ,  $a_{10}$ ,  $a_{01}$ , and  $a_{11}$  are to be estimated through the LS analysis.  $T$  indicates the observing session duration, and  $\varphi$  is the station latitude.

Similar LS analysis and statistical testing procedure were applied for the polynomial model given in equation (4.2) and found the significant parameters as given in Table 4.8 below.



Table 4.8 Significant constants and their formal 1-sigma uncertainties for the position components north, east, and up from the least squares analysis of the polynomial modeling performed as a function of observing session duration

Component	Constant	Estimate	Uncertainty	Ratio
North	$a_{00}$	3.279	0.350	9.379
	$a_{01}$	-0.073	0.027	-2.717
East	$a_{00}$	2.951	0.243	12.137
	$a_{01}$	-0.061	0.019	-3.260
Vertical	$a_{00}$	13.639	1.122	12.156
	$a_{01}$	-0.377	0.087	-4.343

Hence, the polynomial equation given in (4.2) turned into a first degree polynomial, i.e. a simple linear, equation as follows.

$$P(T) = a_{00} + a_{01}T \quad (4.3)$$

By including the estimated coefficients in the equation, the model is generated below for all three GPS coordinates north, east and vertical:

$$\begin{aligned} P_n(mm) &= 3.279 - 0.073T \\ P_e(mm) &= 2.951 - 0.061T \\ P_v(mm) &= 13.639 - 0.377T \end{aligned} \quad (4.4)$$

- **Second Order Polynomial Model**

Then a second order polynomial function formulated below (4.5) was tested and predicted values based on this model fit into the RMS values of the north, east and vertical coordinates (Figure 4.5):

$$P(T) = a_0 + a_1T + a_2T^2 \quad (4.5)$$

where  $P(T)$  denotes the accuracy of the RMS derived from the second order polynomial model.  $a_0$ ,  $a_1$  and  $a_2$  are estimated through least squares analysis, and  $T$  indicates the observing session duration. Similar LS analysis and statistical testing procedures were applied again for the polynomial model given in equation (4.5).

Estimated coefficient values for the second order polynomial accuracy model are given below for the north, east and vertical components, respectively.

$$\begin{aligned}
 P_n(mm) &= 4.1973 - 0.256T + 0.006T^2 \\
 P_e(mm) &= 3.882 - 0.247T + 0.006T^2 \\
 P_v(mm) &= 18.585 - 1.362T + 0.034T^2
 \end{aligned}
 \tag{4.6}$$

### 4.3.2 Logarithmic Accuracy Model

The log function fitted into the RMS values of the north, east and vertical coordinates is:

$$L(T) = a \times \ln(T) + b \tag{4.7}$$

where  $L(T)$  denotes the RMS derived from the polynomial and logarithmic models respectively. Coefficients  $a$  and  $b$  are estimated through the LS analysis, and  $T$  indicates the observing session duration. We applied similar least squares analysis and statistical testing procedures for the logarithmic model given in equation (4.7).

Estimated prediction formulas for the logarithmic accuracy model are given for north, east and vertical components below.

$$\begin{aligned}
 L_n(mm) &= -0.928 \times \ln(T) + 4.512 \\
 L_e(mm) &= -0.785 \times \ln(T) + 4.004 \\
 L_v(mm) &= -4.765 \times \ln(T) + 19.977
 \end{aligned}
 \tag{4.8}$$

### 4.3.3 Internal Model Assessment

Comparison of the predicted values by using the models defined above and the mean RMS values estimated by using the RMS values given in Figure 4.5 is presented in Table 4.9 for all three GPS coordinates north, east, and vertical.

Figure 4.5 comprises predicted model results and the estimated RMS values. The model fit for the reduced accuracy model (4.1) is presented with a black straight line, the 1<sup>st</sup> order polynomial model fit is depicted by a black dotted line and the 2<sup>nd</sup> order polynomial is represented with a dashed red line whereas the model fit for the log function is represented with a dashed blue line in Figure 4.5.

It can be concluded that the polynomial and logarithmic models are only capable of predicting the accuracy of 4-24 hour solutions. On the other hand, 2-24 hour sessions can

successfully be predicted by using equation (4.1). However, all four models fail to predict the actual mean RMS of 1h solutions. Apparently, the refined model given in equation (4.1) occurs to be the best model in predicting the mean RMS for 2-24 hour sessions.

Table 4.9 Comparison of the predicted accuracy from three different models with the actual mean RMS

Component	Session (h)	Mean RMS (mm)	Model (mm)			
			1 <sup>st</sup> order Polynomial	2 <sup>nd</sup> order Polynomial	Logarithmic	$a/\sqrt{T}$
North	1	19.7	3.2	3.9	4.5	7.8
	2	5.2	3.1	3.7	3.9	5.5
	3	4.1	3.1	3.5	3.5	4.5
	4	3.4	3.0	3.3	3.2	3.9
	6	2.7	2.8	2.9	2.8	3.2
	8	2.5	2.7	2.6	2.6	2.7
	12	2.1	2.4	2.0	2.2	2.2
	24	1.7	1.5	1.7	1.6	1.6
East	1	45.8	2.9	3.6	4.0	6.7
	2	5.2	2.8	3.4	3.5	4.7
	3	3.8	2.8	3.2	3.1	3.9
	4	3.0	2.7	3.0	2.9	3.4
	6	2.5	2.6	2.6	2.6	2.7
	8	2.4	2.5	2.3	2.4	2.4
	12	1.8	2.2	1.8	2.1	1.9
	24	1.6	1.5	1.7	1.5	1.4

Table 4.9 Comparison of the predicted accuracy from three different models with the actual mean RMS (cont'd)

Component	Session (h)	Mean RMS (mm)	Model (mm)			
			1 <sup>st</sup> order Polynomial	2 <sup>nd</sup> order Polynomial	Logarithmic	$a/\sqrt{T}$
Vertical	1	62.1	13.3	17.3	20.0	29.9
	2	23.7	12.9	16.0	16.7	21.1
	3	16.9	12.5	14.8	14.7	17.3
	4	14.1	12.1	13.7	13.4	15.0
	6	11.3	11.4	11.6	11.4	12.2
	8	9.3	10.6	9.9	10.1	10.6
	12	7.6	9.1	7.1	8.1	8.6
	24	5.4	4.6	5.5	4.8	6.1

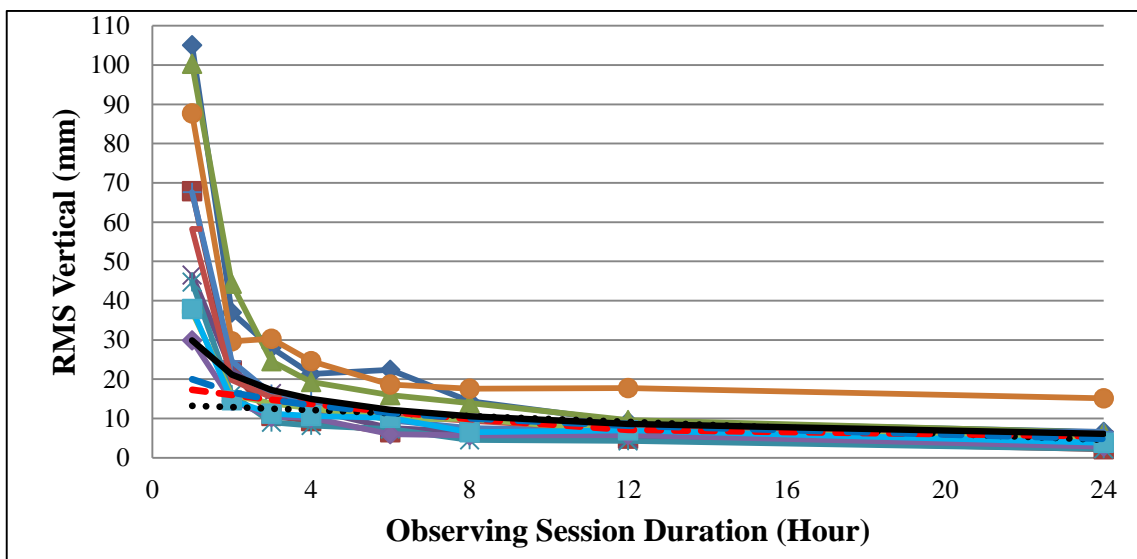
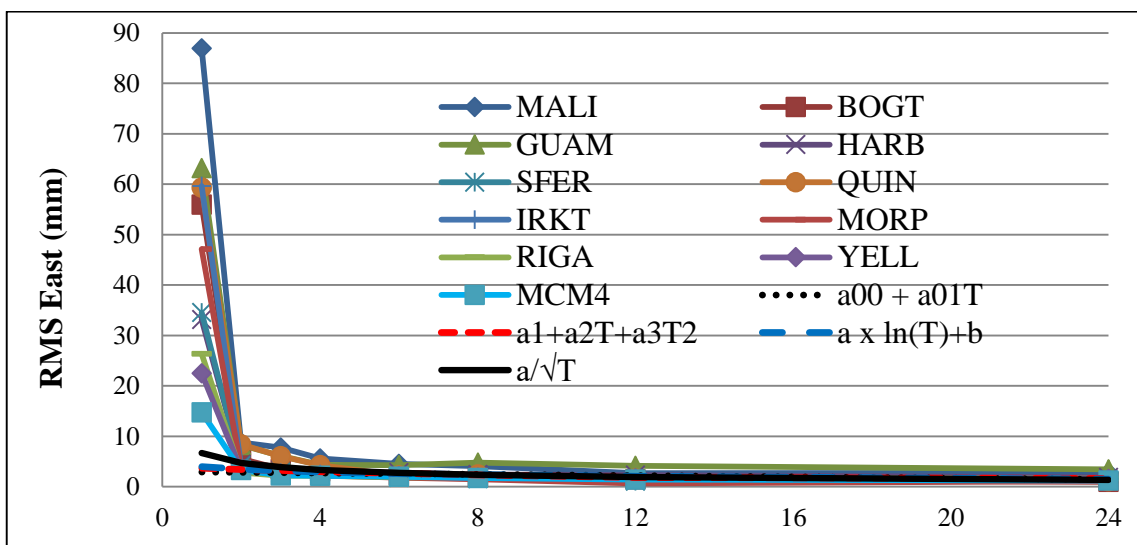
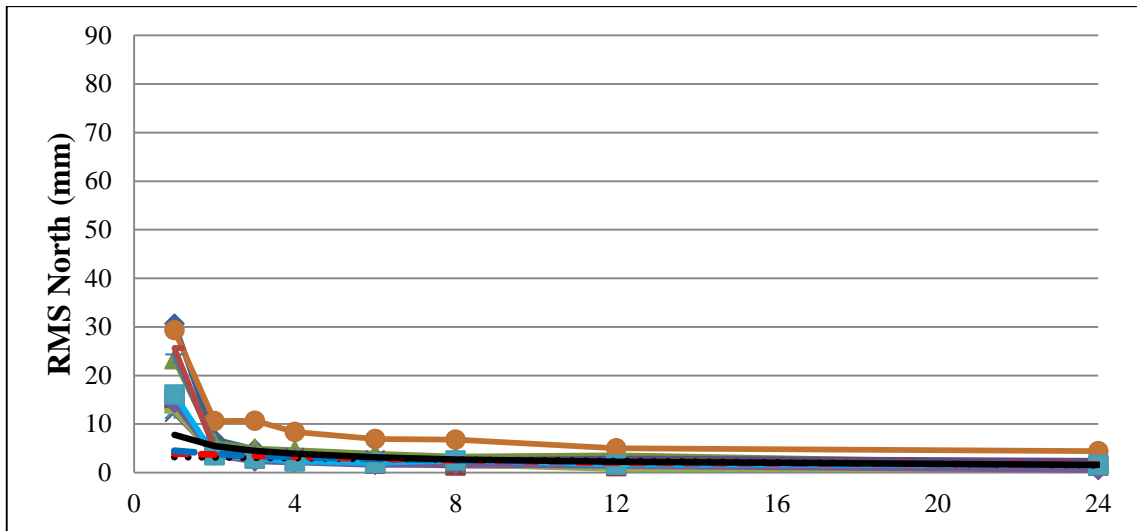


Figure 4.5 Prediction/model fit of the accuracy models to the RMS values of this study, from observing session durations of 1 through 24 h

#### 4.3.4 External Model Assessment

In this section the 24 hour predictions which are derived from equation (4.1) were compared with the evidence from previous studies. In addition, the empirical evidence produced in this study and the current IGS positioning accuracies obtained from <https://igsb.jpl.nasa.gov/> were also appended (see Table 4.10).

Table 4.10 Comparison of the results from this study with those of the published work previously (predictions of 24 hours are compared)

Accuracy	North (mm)	East (mm)	Vertical (mm)
Current accuracy model (4.1)	1.6	1.4	6.1
Average RMS	1.7	1.6	5.4
Bertiger et al. [12]	2.1	1.9	6.0
Sanli and Tekic [2] (the available model)	2.8	4.2	8.3
IGS Continuous (January 2016)	3.0	3.0	6.0

It can be concluded from the above table that the Sanli and Tekic [2] prediction exhibits the highest deviation when representing the empirical evidence produced in this study. Part of their deviation can be attributed to fact that Sanli and Tekic [2] used an older software release which lacked refined second order ionosphere model, single receiver ambiguity solution developed by Bertiger et al. [12], which were introduced with the latest available software release version 6.3. Moreover, with the single receiver ambiguity solution developed by Bertiger et al. [12], prediction of the east component from Sanli and Tekic [2] became much better. Furthermore, for the new models tested in this section, the GIPSY positioning accuracies of 3-4 mm horizontal and 12-15 mm vertical generated by using 4 hour observing session durations do not satisfy the IGS accuracy given in Table 4.10. Also note that, even for the 12 hour session data, the positioning accuracy still fails to satisfy the IGS vertical positioning accuracy. Akarsu et al. [65] stated that the estimated velocities are effected when short observation sessions are used in positioning. Users who are dealing with GPS campaign measurements and employing 8-12 hour of observation sessions should keep this in mind.

#### 4.4 Revised PPP Accuracy Model

The current PPP accuracy model was aimed to be revised by using a recent GPS dataset. The same GPS stations given in Chapter 4.1 were used and 10 consecutive days within

January of 2014 were selected when determining the observation schedule (see Table 4.11). Daily geomagnetic activity prepared by NOAA [64] was examined and the days with K-indices lower than 5 were selected for this study. Geomagnetic activity K-indices for January 2014 are given in Table B.2.

Table 4.11 Observation time schedule of the revised accuracy model, X denotes that data from this day were included in the study

Site ID	Site Lat. (°)	Day of the Year (2014)													
		5	6	7	8	9	10	11	12	13	15	16	17	21	24
BOGT	4.6	X	X	X	X	X	X	X	X	X	X	-	-	-	-
GUAM	13.6	X	X	-	-	X	X	X	X	X	X	X	X	-	-
HARB	-25	X	X	X	X	X	X	X	X	X	X	-	-	-	-
IRKT	52.2	X	X	X	X	X	X	X	X	X	X	-	-	-	-
MALI	-3	X	X	X	X	X	X	X	-	X	X	X	-	-	-
MCM4	-77.8	X	X	X	X	X	X	X	X	X	X	-	-	-	-
MORP	55.2	-	-	X	X	X	X	X	X	X	X	-	-	X	X
QUIN	40	X	X	X	X	X	X	X	X	X	X	-	-	-	-
RIGA	57	X	X	X	X	X	X	X	X	X	X	-	-	-	-
SFER	36.5	-	X	X	X	X	X	X	X	-	X	X	X	-	-
YELL	62.5	X	X	X	X	X	X	X	X	X	X	-	-	-	-

Then, by following the same processing steps when generating the current PPP accuracy model (Chapter 4.1), the daily GPS observation data was divided into non-overlapping hourly observation data and processed by GIPSY v6.3. Next, the possible outliers in the data were removed by using the Median method [57] and the RMS values were estimated, which were given in Table C.1, C.2 and C.3.

By using the RMS values from 4-24 hour session solutions, which were found to be significant again, the accuracy model coefficients (3.7) were estimated as given in Table 4.12.

Table 4.12 Estimated coefficients, their 1-sigma uncertainties and ratio values of the revised accuracy model, for position components north, east and vertical

<b>Coefficient</b>	<b>Estimate</b>	<b>Uncertainty</b>	<b>Ratio</b>
$a_n(mm^2 \cdot h)$	29.51	8.93	3.30
$a_e(mm^2 \cdot h)$	42.38	21.28	1.99
$a_v(mm^2 \cdot h)$	615.25	184.43	3.34
$b_n(mm^2 \cdot h/degree^2)$	-4.85E-05	3.23E-03	-0.02
$b_e(mm^2 \cdot h/degree^2)$	-6.22E-03	7.70E-03	-0.81
$b_v(mm^2 \cdot h/degree^2)$	-6.21E-02	6.67E-02	-0.93
$c_n$	1.35	1.35	1.00
$c_e$	3.08	3.22	0.96
$c_v$	1.77	27.92	0.06
$d_n(mm^2/degree^2)$	-2.34E-04	4.89E-04	-0.48
$d_e(mm^2/degree^2)$	1.46E-04	1.17E-03	0.12
$d_v(mm^2/degree^2)$	-6.43E-04	1.01E-02	-0.06

As it can be seen in Table 4.12, only the coefficient “a” values provided significant results based on the Students t test (see Chapter 3.4). Therefore, the reduced model in equation (3.13) was used in the LS estimations and the significant coefficient values for north, east and vertical positioning components were calculated as in Table 4.13.

Table 4.13 Estimated coefficients, their 1-sigma uncertainties and ratio values of the revised accuracy model, for position components north, east and vertical

<b>Coefficient</b>	<b>Estimate</b>	<b>Uncertainty</b>	<b>Ratio</b>
$a_n(mm^2 \cdot h)$	34.45	2.77	12.43
$a_e(mm^2 \cdot h)$	49.18	6.77	7.26
$a_v(mm^2 \cdot h)$	489.17	58.49	8.36

By using the coefficients in Table 4.13, the revised PPP accuracy model was generated as below.



$$\begin{aligned}
S_n &= \frac{5.9}{\sqrt{T}} \left[ \frac{mm\sqrt{h}}{\sqrt{h}} \right] \\
S_e &= \frac{7.0}{\sqrt{T}} \left[ \frac{mm\sqrt{h}}{\sqrt{h}} \right] \\
S_v &= \frac{22.1}{\sqrt{T}} \left[ \frac{mm\sqrt{h}}{\sqrt{h}} \right]
\end{aligned}
\tag{4.2}$$

where  $S_n$ ,  $S_e$ ,  $S_v$  are the accuracy estimates for north, east and vertical components, respectively and  $T$  is the observing session duration in hours.

The revised accuracy model provided comparative results to the current PPP accuracy model. On the other hand, these results showed that Sanli and Tekic [2] model could be improved by approximately 56%, 66% and 46% for the positioning components north, east and vertical, respectively. These results make it possible to predict the accuracy for session durations of 2 through 24 h sufficiently.

Figure 4.6 represents the prediction/model fit of the accuracy models to the RMS values of the revised accuracy model.

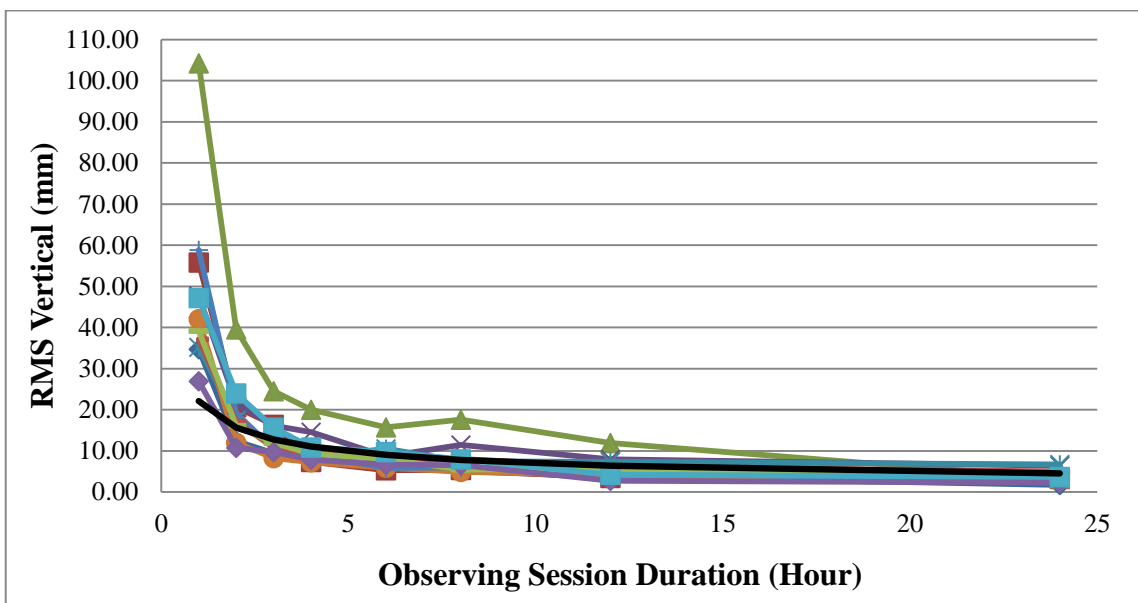
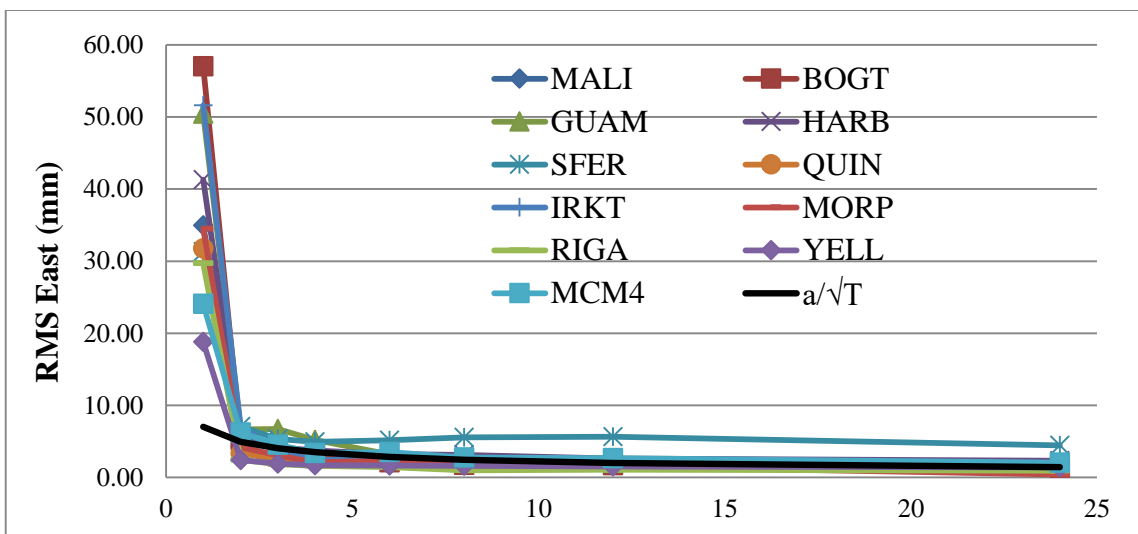
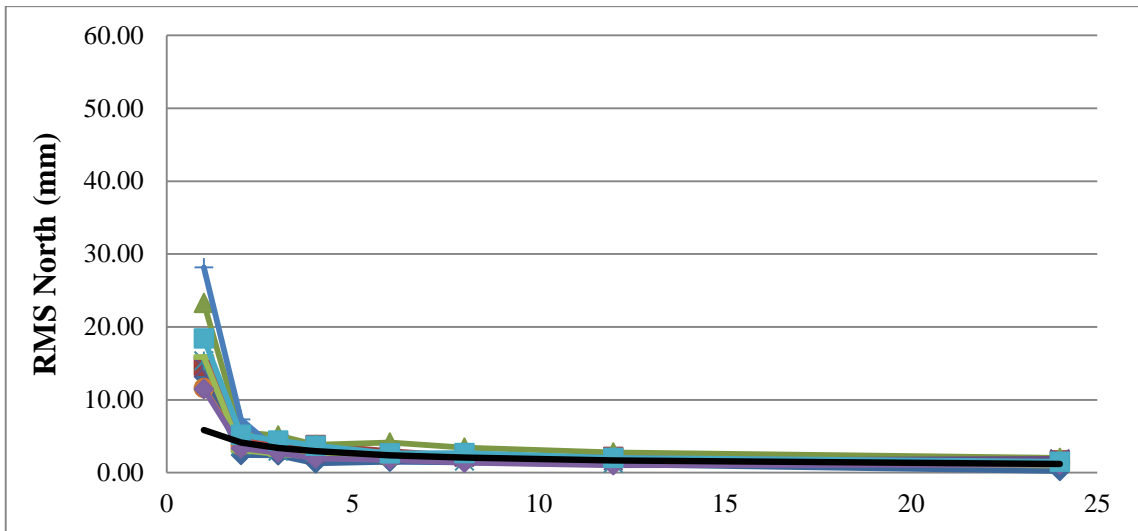


Figure 4.6 Prediction/model fit of the revised accuracy model to the RMS values, from observing session durations of 1 through 24 h

#### 4.5 PPP Accuracy Model from a Densified Network

In order to develop a better and more reliable PPP accuracy model, a densified GPS network with more and wisely distributed GPS stations was planned to use. Therefore, a GPS network was designed to cover high latitude area where  $\varphi > 60^\circ$ , the middle latitude area where  $50^\circ > \varphi > 40^\circ$  for the north and south hemispheres, and the equatorial area where  $-10^\circ > \varphi > 10^\circ$ . In total, 67 GPS stations were selected for this study. The GPS network and the stations are shown in Figure 4.7 and the WGS84 ellipsoidal coordinates of the densified GPS network stations are given in Table A.2.

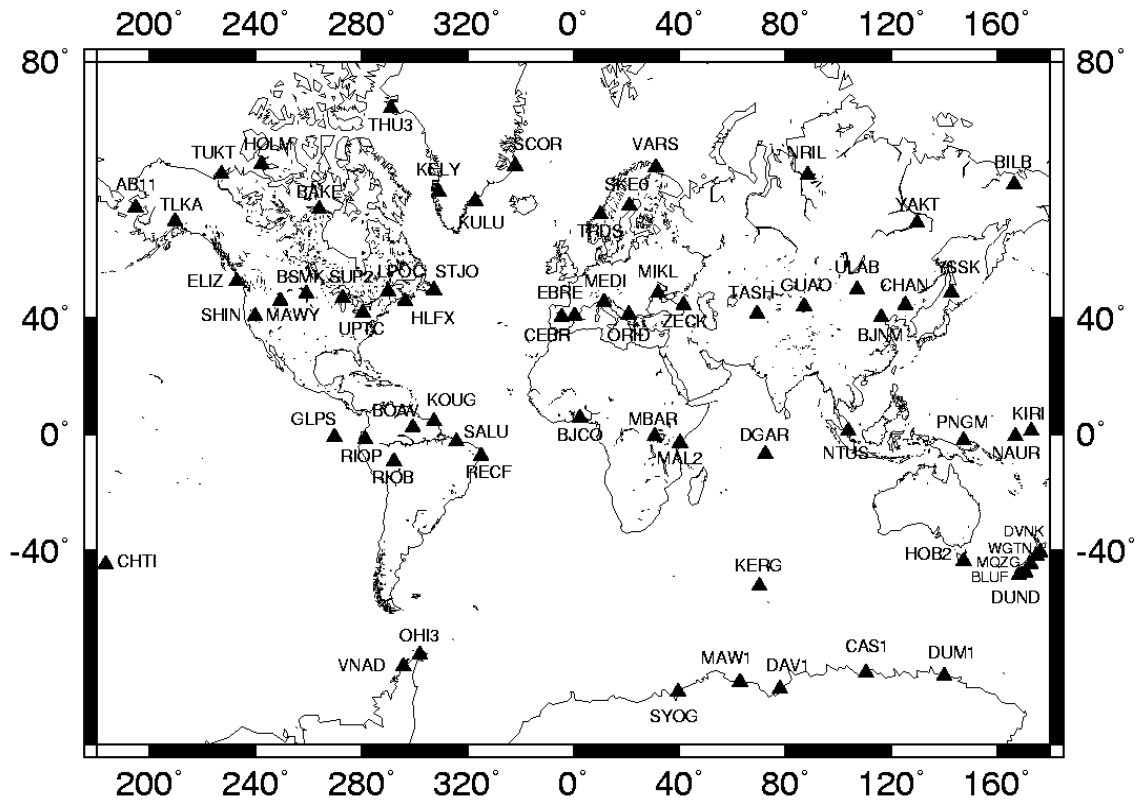


Figure 4.7 Densified GPS network

After selecting the GPS stations, 10 consecutive observation days in which GPS data are available were determined for the study. The summarized observation time schedule is presented in Table 4.14 whereas the detailed observation schedule is presented in Table B.3. In addition, geomagnetic activity was also examined when determining the observation time schedule and the days with K-indices lower than 5 were selected for this study. Geomagnetic activity K-indices for the selected days are given in Table B.4.

Table 4.14 Summarized observation time schedule for the denser accuracy model, X denotes that data from this day were included in the study

SITE ID	Day of the Year (2013)												
	61	62	63	64	65	66	67	68	69	70	71	72	73
AB11, BAKE, BILB, BJNM BLUF, BOAV, BSMK, CAS1 CEBR, CHAN, CHTI, DAV1 DGAR, DNVK, DUM1, DUND ELIZ, GLPS, GUAO, HOB2 HOLM, HLFX, KELY, KOUG KULU, LPOC, MAL2, MAW1 MAWY, MBAR, MCM4, MEDI MIKL, MQZG, NAUR, NTUS OHI3, ORID, RECF, RIOB RIOP, SALU, SCOR, SHIN STJO, SKE0, SUP2, SYOG TASH, THU3, TLKA, TUKT ULAB, VARS, VNAD, WGTN YSSK, ZECK	X	X	X	X	X	X	X	X	X	X	-	-	-
BJCO	X	-	-	X	X	X	X	X	X	X	X	X	-
EBRE	X	X	X	-	-	-	X	X	X	X	X	X	X
KERG	X	-	X	X	-	X	-	X	X	X	X	X	X
KIRI	X	X	X	X	X	X	X	X	X	-	X	-	-
NRIL, UPTC	X	X	-	X	X	X	X	X	X	X	X	-	-
PNGM	X	X	X	X	X	-	X	X	X	X	X	-	-
TRDS	X	X	X	X	X	X	-	X	X	X	X	-	-
YAKT	X	X	X	X	X	X	X	X	-	X	X	-	-

The selected 10 days of GPS data for 67 stations was downloaded from SOPAC archives and divided into 1h (hour), 2h, 3h, 4h, 6h, 8h, 12h data by using TEQC as described in previous sections. Then the observation data was processed by using GIPSY (version 6.3). Then, the RMS values (see Table C4, C.5 and C.6) were estimated after removing

the outliers with the Median method [57]. By again using the RMS values from 4-24 hour session solutions, which were found to be significant again, the coefficients in equation (3.7) were estimated and presented in Table C.7 together with their statistical parameters. Based on the the Students  $t$  test results, the PPP accuracy model was reformulated to include only the observing session durations. By using the reduced accuracy model in equation (3.13) with the LS technique (Chapter 3.4) the significant coefficients for the reduced accuracy model are given in Table 4.15 for the densified GPS network data.

Table 4.15 Estimated coefficients, their 1-sigma uncertainties and ratio values of the denser accuracy model, for position components north, east and vertical

<b>Coefficient</b>	<b>Estimate</b>	<b>Uncertainty</b>	<b>Ratio</b>
$a_n(mm^2 \cdot h)$	39.03	1.84	21.21
$a_e(mm^2 \cdot h)$	43.04	5.17	8.33
$a_v(mm^2 \cdot h)$	469.21	21.50	21.83

By using the coefficients in Table 4.15, the denser PPP accuracy model was generated as below.

$$\begin{aligned}
 S_n &= \frac{6.2}{\sqrt{T}} \left[ \frac{mm\sqrt{h}}{\sqrt{h}} \right] \\
 S_e &= \frac{6.6}{\sqrt{T}} \left[ \frac{mm\sqrt{h}}{\sqrt{h}} \right] \\
 S_v &= \frac{21.7}{\sqrt{T}} \left[ \frac{mm\sqrt{h}}{\sqrt{h}} \right]
 \end{aligned} \tag{4.3}$$

where  $S_n$ ,  $S_e$ ,  $S_v$  are the accuracy estimates and  $T$  is the observing session duration.

These results are almost identical with the revised model results given in equation (4.2). The accuracy model results generated in equation (4.3) should be preferred for the later studies requiring precise positioning, such as when planning GPS campaign measurements, since these estimates were obtained by using 67 GPS stations, six times larger than the stations used in previous sections. This model will be referred as the denser PPP accuracy model from now on.

Figure 4.8 represents the model fit of the denser PPP accuracy model to the RMS values of this study. The model fit for the denser accuracy model (4.3) is presented with black

straight line. The accuracy can satisfactorily be predicted for session durations of 2 through 24 h.

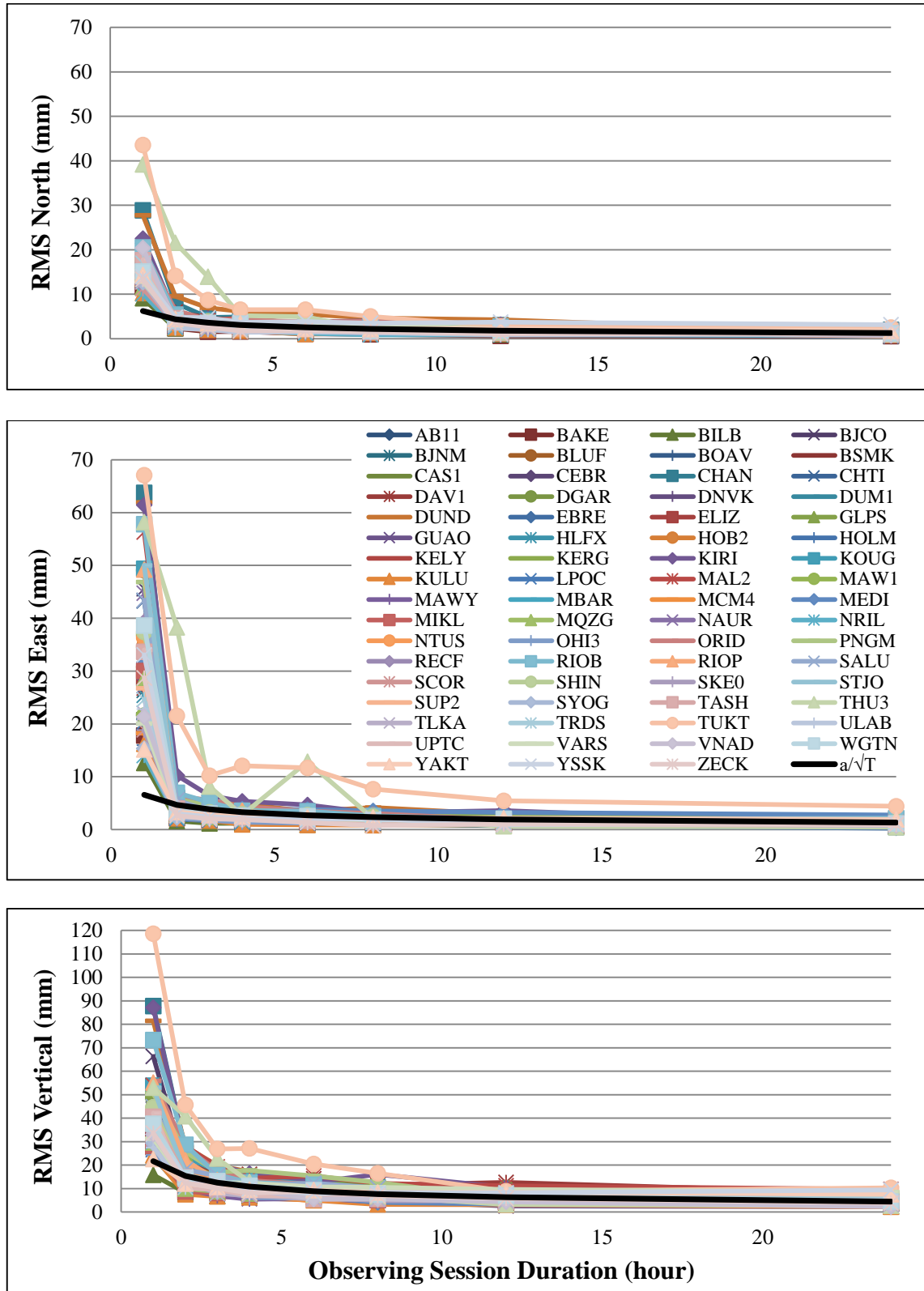


Figure 4.8 Prediction/model fit of the denser accuracy model to the RMS values of this study, from observing session durations of 1 through 24 h

#### 4.6 Regional PPP Accuracy Models

The former studies of Eckl et al. [9] and Sanli and Tekic [2], and the accuracy model studies performed in previous chapters formulated the accuracy with respect to observing session duration. Therefore, PPP accuracy models for the equatorial, middle latitude and high latitude areas for northern and southern hemispheres were generated by using the reduced accuracy model (3.13). Table 4.16 and Figure 4.9 present the coefficients for the regional accuracy model results together with the denser accuracy model while Table 4.17 gives the accuracy model prediction values for the mentioned regions.

Table 4.16 Estimated coefficients from the denser and the regional accuracy models, for position components north, east and vertical

Coefficients	Global (Denser)	Equatorial	Northern Hemisphere		Southern Hemisphere	
			Middle Latitude	High Latitude	Middle Latitude	High Latitude
$a_n(mm^2 \cdot h)$	39.03	43.14	34.49	38.53	50.67	32.52
$a_e(mm^2 \cdot h)$	43.04	49.20	26.81	71.38	36.65	27.32
$a_v(mm^2 \cdot h)$	469.21	700.70	321.30	491.65	464.54	392.62

Table 4.17 Denser and regional accuracy model prediction values

Accuracy Model	Global (Denser)	Northern Hemisphere		Equatorial	Southern Hemisphere	
		Middle Latitude	High Latitude		Middle Latitude	High Latitude
$S_n(mm)$	$\frac{6.2}{\sqrt{T}}$	$\frac{5.9}{\sqrt{T}}$	$\frac{6.2}{\sqrt{T}}$	$\frac{6.6}{\sqrt{T}}$	$\frac{7.1}{\sqrt{T}}$	$\frac{5.7}{\sqrt{T}}$
$S_e(mm)$	$\frac{6.6}{\sqrt{T}}$	$\frac{5.2}{\sqrt{T}}$	$\frac{8.4}{\sqrt{T}}$	$\frac{7.0}{\sqrt{T}}$	$\frac{6.1}{\sqrt{T}}$	$\frac{5.2}{\sqrt{T}}$
$S_v(mm)$	$\frac{21.7}{\sqrt{T}}$	$\frac{17.9}{\sqrt{T}}$	$\frac{22.2}{\sqrt{T}}$	$\frac{26.5}{\sqrt{T}}$	$\frac{21.6}{\sqrt{T}}$	$\frac{19.8}{\sqrt{T}}$

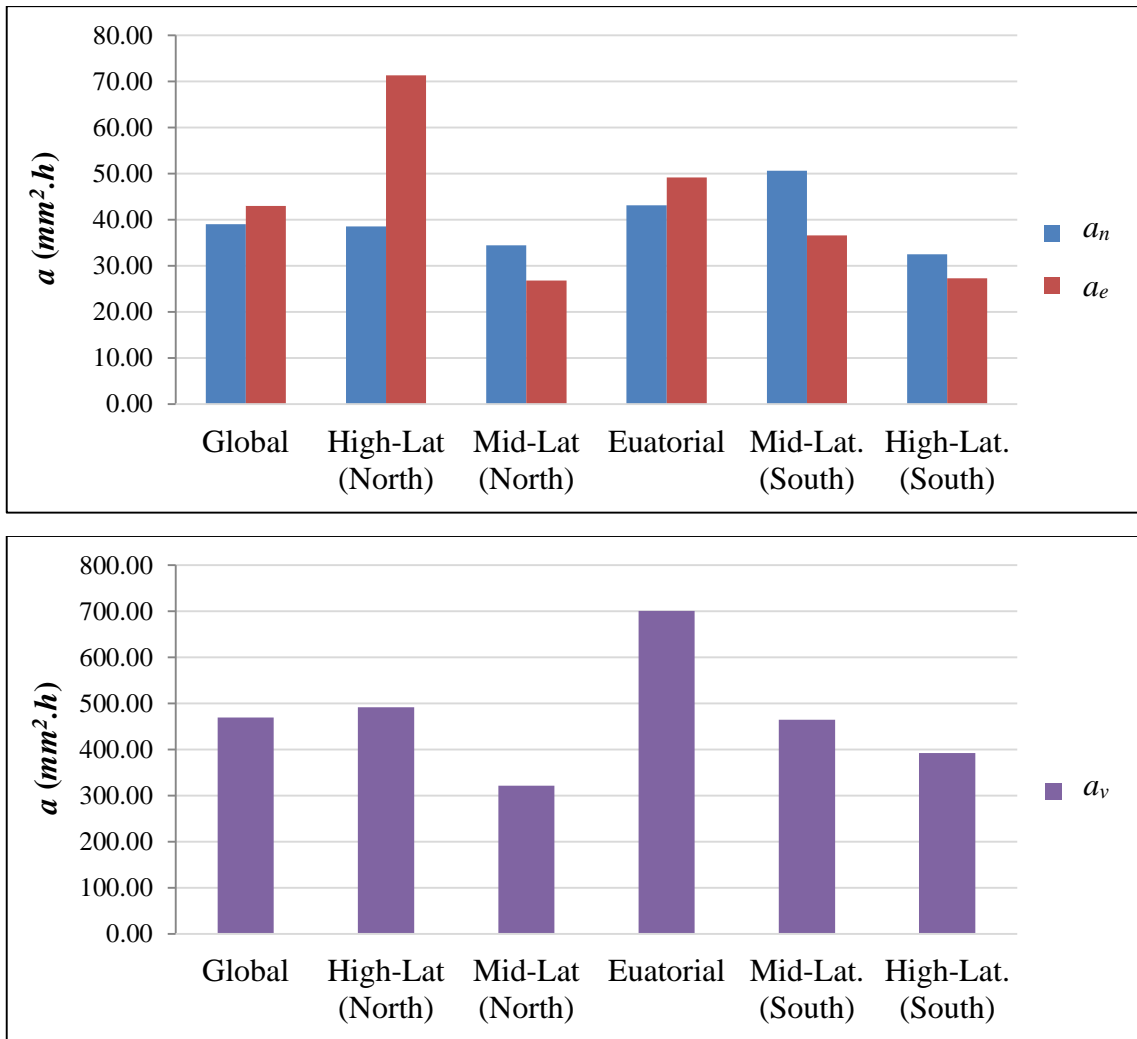


Figure 4.9 Estimated coefficients for position components north ( $a_n$ ), east ( $a_e$ ), and vertical ( $a_v$ )

The coarser/poorer accuracy modeling has occurred in the equatorial regions in which the effect of the magnetic field of the earth is possibly encountered [2]. Note that this affects all GPS baselines especially the vertical component. The accuracy of the GPS appears to be the best (i.e. with smaller coefficients) over the mid-latitudes in the northern hemisphere. To the user in mid-latitudes in the northern hemisphere and to the user in higher latitudes in the southern hemisphere, it is one recommended to use the regional models developed here.

The related figures of the prediction/model fit of the regional accuracy models to the RMS values of this study are presented in Figure D.1, D.2, D.3, D.4 and D.5.



### CONCLUSIONS AND SUGGESTIONS

The currently available GPS Precise Point Positioning (PPP) accuracy model, Sanli and Tekic [2] model, is obsolete because it utilizes JPL's legacy products, and these legacy products are no longer available. In recent years, NASA's JPL started to advance their modeling and analysis strategy for data processing and included these improvements to their processing software, GIPSY/OASIS II, starting from the version 5.0, which is a later version of the one that was used in Sanli and Tekic [2]. The main advancements developed by JPL included single station ambiguity resolution and second order ionosphere modeling. Moreover, in October/November 2014, JPL reprocessed all of their final orbit products with second order ionospheric corrections. Therefore, the studies before this time would not contain the second order ionosphere corrections. Because of the abovementioned reasons, users will not be able to obtain realistic results when they used the accuracy model of Sanli and Tekic [2] in their studies.

Therefore, renovating the current PPP accuracy model and developing a better model were the objective of this thesis. For this reason, the highest available version of GIPSY/OASIS II software (version 6.3) that comprises new and enhanced JPL and IGS products was used for the accuracy model estimations. Problematic outliers in solutions were removed by using the median method, a robust and efficient outlier detection method given in Tut et al. [57]. In addition, the modeling could be performed by using observation lengths from 6 to 24 hours previously while it is possible to use observation lengths from 4 to 24 hours with the new ambiguity resolution.

The former PPP accuracy model [2] was first refined to be  $S_n = 7.8/\sqrt{T}$  mm,  $S_e = 6.8/\sqrt{T}$  mm and  $S_v = 29.9/\sqrt{T}$  mm for the GPS baseline components north, east and vertical, respectively, by using the same GPS network and same observation time interval. These results provided significant improvement in model prediction coefficients.

Then, new model tests were performed including straightforward polynomial and logarithmic functions; however, the refined model of Sanli and Tekic [2] still provided better results such as the accuracy can satisfactorily be predicted for the observation session durations from 2 hours to 24 hours with this model.

The PPP accuracy model was revised by using the same GPS network but with a recent observation dataset, from January 2014. The revised accuracy model equations were obtained as  $S_n = 5.9/\sqrt{T}$  mm,  $S_e = 7.0/\sqrt{T}$  mm and  $S_v = 22.1/\sqrt{T}$  mm which were almost identical with the refined model results, but improved the positioning accuracy about by 56%, 66% and 46% for the positioning components north, east and vertical, respectively.

However, the studies above were obtained from only 11 GPS stations. An increase in the station numbers with a better network design was thought to be necessary for providing a more reliable accuracy model. Thus, 10 consecutive days of GPS data from globally scattered 67 IGS stations were used and the accuracy model, named as the denser PPP accuracy model, was obtained as  $S_n = 6.2/\sqrt{T}$  mm,  $S_e = 6.6/\sqrt{T}$  mm and  $S_v = 21.7/\sqrt{T}$  mm for north, east and vertical, respectively. These results were only slightly varied from the revised accuracy model results, but were statistically more significant than that of the original accuracy model provided by Sanli and Tekic [2]. Regional models including the equatorial area, middle latitude and high latitude areas were also generated in this study. Moreover, with the accuracy models generated in this thesis, the accuracy can satisfactorily be predicted for session durations of 2 through 24 h.

The denser accuracy model is believed to be more reliable than the previous results because of its GPS network design and should be preferred by users who wish to plan their GPS campaigns prior to field works.

For future studies, it is planned to develop a better accuracy model which would also enable a fit to 1 h sessions. For example, including a non-linear coefficient  $c$  in the model (i.e.  $L(T) = a + \ln(T \times c) + b$ ) might help to improve the PPP accuracy model.

## REFERENCES

---

- [1] Sanli, D.U. and Engin, C., (2009). "Accuracy of GPS Positioning over Regional Scales", *Survey Review*, 41: 192-200.
- [2] Sanli, D.U. and Tekic, S., (2010). *Accuracy of GPS Precise Point Positioning: A Tool for GPS Accuracy Prediction*, LAP Lambert Academic Publishing, Saarbrücken.
- [3] Ozturk, D. and Sanli, D.U., (2011). "Accuracy of GPS Positioning from Local to Regional Scales: A Unified Prediction Model", *Survey Review*, 43: 579-589.
- [4] Davis, J.L. Prescott, W.H. Svarc, J.L. and Wendt, K.J., (1989). "Assessment of Global Positioning System Measurements for Studies of Crustal Deformation", *Journal of Geophysical Research-Solid Earth and Planets*, 94: 13635-13650.
- [5] Dong, D.N. and Bock, Y., (1989). "Global Positioning System Network Analysis with Phase Ambiguity Resolution Applied to Crustal Deformation Studies in California", *Journal of Geophysical Research-Solid Earth and Planets*, 94: 3949-3966.
- [6] Larson, K.M. and Agnew, D.C., (1991). "Application of the Global Positioning System to Crustal Deformation Measurement: 1. Precision and Accuracy", *Journal of Geophysical Research-Solid Earth*, 96: 16547-16565.
- [7] Feigl, K.L. Agnew, D.C. Bock, Y. Dong, D. Donnellan, A. Hager, B.H. Herring, T.A. Jackson, D.D. Jordan, T.H. King, R.W. Larsen, S. Larson, K.M. Murray, M.H. Shen, Z.K. and Webb, F.H., (1993). "Space Geodetic Measurement of Crustal Deformation in Central and Southern California, 1984-1992", *Journal of Geophysical Research-Solid Earth*, 98: 21677-21712.
- [8] Witchayangkoon, B. and Segantine, P.C., (1999). "Testing JPL's PPP Service", *GPS Solutions*, 3: 73-76.
- [9] Eckl, M.C. Snay, R.A. Soler, T. Cline, M.W. and Mader, G.L., (2001). "Accuracy of GPS-Derived Relative Positions as a Function of Interstation Distance and Observing-Session Duration", *Journal of Geodesy*, 75: 633-640.
- [10] Ghoddousi-Fard, R. and Dare, P., (2006). "Online GPS Processing Services: An Initial Study", *GPS Solutions*, 10: 12-20.
- [11] Soler, T. Michalak, P. Weston, N.D. Snay, R.A. and Foote, R.H., (2006). "Accuracy of OPUS Solutions for 1-to 4-h Observing Sessions", *GPS Solutions*, 10: 45-55.
- [12] Bertiger, W. Desai, S.D. Haines, B. Harvey, N. Moore, A.W. Owen, S. and Weiss, J.P., (2010). "Single Receiver Phase Ambiguity Resolution with GPS Data", *Journal of Geodesy*, 84: 327-337.

- [13] Firuzabadi, D. and King, R.W., (2012). "GPS Precision as a Function of Session Duration and Reference Frame Using Multi-Point Software", *GPS Solutions*, 16: 191-196.
- [14] Wang, G., (2013). "Millimeter-Accuracy GPS Landslide Monitoring Using Precise Point Positioning with Single Receiver Phase Ambiguity (PPP-SRPA) Resolution: A Case Study in Puerto Rico", *Journal of Geodetic Science*, 3: 22-31.
- [15] Zumberge, J.F. Heflin, M.B. Jefferson, D.C. Watkins, M.M. and Webb, F.H., (1997). "Precise Point Positioning for the Efficient and Robust Analysis of GPS Data from Large Networks", *Journal of Geophysical Research-Solid Earth*, 102: 5005-5017.
- [16] Blewitt, G., (1989). "Carrier Phase Ambiguity Resolution for the Global Positioning System Applied to Geodetic Baselines up to 2000 Km", *Journal of Geophysical Research-Solid Earth and Planets*, 94: 10187-10203.
- [17] Sanli, D.U. and Kurumahmut, F., (2011). "Accuracy of GPS Positioning in the Presence of Large Height Differences", *Survey Review*, 43: 162-176.
- [18] Kedar, S. Hajj, G.A. Wilson, B.D. and Heflin, M.B., (2003). "The Effect of the Second Order GPS Ionospheric Correction on Receiver Positions", *Geophysical Research Letters*, 30 (16).
- [19] Ocalan, T., (2015). GNSS Ağlarında GPS Hassas Nokta Konumlama (GPS-PPP) Tekniği Yaklaşımli Çözümler, PhD Thesis. Yıldız Technical University, Graduate School of Natural and Applied Sciences, Istanbul.
- [20] El-Rabbany, A., (2002). *Introduction to GPS: The Global Positioning System*, Artech House, Boston.
- [21] King, M. Edwards, S. and Clarke, P., (2002). "Precise point positioning: Breaking the monopoly of relative GPS processing", *Engineering Surveying Showcase*: 40-41.
- [22] Kouba, J. and Héroux, P., (2001). "Precise Point Positioning Using IGS Orbit and Clock Products", *GPS Solutions*, 5: 12-28.
- [23] Hofmann-Wellenhof, B. Lichtenegger, H. and Wasle, E., (2007). *GNSS–Global Navigation Satellite Systems: GPS, GLONASS, Galileo, and More*, Springer Science & Business Media, Mörlenbach.
- [24] Ebner, R., (2008). *Validation and Application of Free-Online and Commercial Post-Processing PPP Packages*, MSc. Thesis, Graz University of Technology Institut für Geodäsie Arbeitsgruppe Navigation , Graz.
- [25] Kaplan, E. and Hegarty, C., (2005). *Understanding GPS: Principles and Applications*, Artech House, Norwood.
- [26] Sanli, D.U., (1999). *GPS Strategies for Tide Gauge Monitoring with Assessment of Sea Level Analysis Models*, PhD Thesis, University of Newcastle upon Tyne, Newcastle.
- [27] Bisnath, S. and Gao, Y., (2009). "Precise Point Positioning", *GPS World*, 20: 43-50.
- [28] Satirapod, C. and Homniam, P., (2006). "GPS Precise Point Positioning Software for Ground Control Point Establishment in Remote Sensing Applications", *Journal of Surveying Engineering*, 132(1): 11-14.

- [29] Rayan, A. Fernandes, R. Khalil, H. Mahmoud, S. Miranda, J. and Tealab, A., (2010). "Evaluation of the Crustal Deformations in the Northern Region of Lake Nasser (Egypt) Derived from 8 Years of GPS Campaign Observations", *Journal of Geodynamics*, 49: 210-215.
- [30] XU, C.-h. WANG, J.-l. GAO, J.-x. Jian, W. and Hong, H., (2011). "Precise Point Positioning and its Application in Mining Deformation Monitoring", *Transactions of Nonferrous Metals Society of China*, 21: 499-505.
- [31] El-Hattab, A., (2014). "Assessment of PPP for Establishment of CORS Network for Municipal Surveying in Middle East", *Survey Review*, 46: 97-103.
- [32] Abdallah, A. and Schwieger, V., (2015). "Kinematic Precise Point Positioning (PPP) Solution for Hydrographic Applications", *FIG Working Week 2015*, 17–21 May 2015, Sofia.
- [33] Alkan, R.M. and Ocalan, T., (2013). "Usability of The GPS Precise Point Positioning Technique in Marine Applications", *The Journal of Navigation*, 66(4): 579.
- [34] Xu, P. Shi, C. Fang, R. Liu, J. Niu, X. Zhang, Q. and Yanagidani, T., (2013). "High-Rate Precise Point Positioning (PPP) to Measure Seismic Wave Motions: An Experimental Comparison of GPS PPP with Inertial Measurement Units", *Journal of Geodesy*, 87: 361-372.
- [35] Ocalan, T. Erdogan, B. and Tunalioglu, N., (2013). "Analysis of Web-Based Online Services for GPS Relative and Precise Point Positioning Techniques", *Boletim De Ciencias Geodesicas*, 19: 191-207.
- [36] Mohamed, H.F., (2015). "Assessment of Factors Influencing Static GNSS Precise Point Positioning: A Case Study in Egypt", *International Journal of Applied Sciences and Engineering Research*, 4(5): 692-701.
- [37] Xu, G., (2007). *GPS: Theory, Algorithms and Applications*, Springer Science & Business Media, Meppel.
- [38] Heroux, P. and Kouba, J., (2001). "GPS Precise Point Positioning Using IGS Orbit Products", *Physics and Chemistry of the Earth Part a-Solid Earth and Geodesy*, 26: 573-578.
- [39] About the IGS, <http://www.igs.org/about>. 01 January 2016.
- [40] IGS Reference Stations, <http://kb.igs.org/hc/en-us/articles/202484696-IGS-tracking-network>. 26 January 2016.
- [41] Jet Propulsion Laboratory, [http://www.jpl.nasa.gov/news/fact\\_sheets/jpl.pdf](http://www.jpl.nasa.gov/news/fact_sheets/jpl.pdf). 21 January 2016.
- [42] Desai, S., (2008). "GIPSY and JPL's GPS Products: Status and Plans for 2008", A Course Material Prepared by Jet Propulsion Laboratory, California Institute of Technology.
- [43] GIPSY OASIS (GNSS-Inferred Positioning System and Orbit Analysis Simulation Software package), <https://gipsy-oasis.jpl.nasa.gov/>, 05 January 2016.
- [44] Desai, S. Kuang, D. and Bertiger, W., (2014). "GIPSY/OASIS (GIPSY) Overview and Under The Hood", A Course Material Prepared by Jet Propulsion Laboratory, California Institute of Technology.

- [45] Gregorius, T., (1996). "GIPSY-OASIS II: How it Works", Department of Geomatics, University of Newcastle Upon Tyne, 109.
- [46] Kaniuth, K. and Volksen, C., (2003). "Comparison of the BERNESE and GIPSY/OASIS II Software Systems Using EUREF Data", *Mitt. Des Bundesamtes für Kartographie und Geodasie*, 29: 314-319.
- [47] Tralli, D.M. and Lichten, S.M., (1990). "Stochastic Estimation of Tropospheric Path Delays in Global Positioning System Geodetic Measurements", *Bulletin géodésique*, 64: 127-159.
- [48] Description of SOPAC, <http://sopac.ucsd.edu/sopacDescription.shtml>, 25 January 2016.
- [49] About UNAVCO, <https://www.unavco.org/about/about.html>, 25 January 2016.
- [50] TEQC - The Toolkit for GPS/GLONASS/Galileo/SBAS/Beidou/QZSS Data, <https://www.unavco.org/software/data-processing/teqc/teqc.html>, 25 January 2016.
- [51] JPL, (2010). "Introduction to gd2p.pl", GIPSY User Group Meeting/Class, California Institute of Technology, Pasadena.
- [52] Desai, S. and Bertiger, W., (2014). "Static and Kinematic Precise Point Positioning with gd2p.pl", A Course Material Prepared by Jet Propulsion Laboratory. California Institute of Technology.
- [53] Petit, G. and Luzum, B., (2010). IERS conventions (2010), DTIC Document.
- [54] Altamimi, Z. Collilieux, X. and Métivier, L., (2011). "ITRF2008: an Improved Solution of the International Terrestrial Reference Frame", *Journal of Geodesy*, 85: 457-473.
- [55] Böhm, J. Niell, A. Tregoning, P. and Schuh, H., (2006). "Global Mapping Function (GMF): A New Empirical Mapping Function based on Numerical Weather Model Data", *Geophysical Research Letters*, 33.
- [56] Haines, B. Bar-Sever, Y. Bertiger, W. Desai, S. Harvey, N. and Weiss, J., (2010). "Improved Models of the GPS Satellite Antenna Phase and Group-Delay Variations Using Data from Low-Earth Orbiters", AGU Fall Meeting, 17 December 2010, San Francisco.
- [57] Tut, I. Sanli, D.U. Erdogan, B. and Hekimoglu, S., (2013). "Efficiency of BERNESE Single Baseline Rapid Static Positioning Solutions with Search Strategy", *Survey Review*, 45: 296-304.
- [58] Hayal, A.G. and Sanli, D.U., (2013). Accuracy of GIPSY PPP from Version 6, GNSS Precise Point Positioning Workshop: Reaching Full Potential, 13-14 June 2013, Ottawa.
- [59] Hampel, F.R. Ronchetti, E.M. Rousseeuw, P.J. and Stahel, W.A., (2011). "Robust statistics: The Approach Based on Influence Functions", Vol. 114, John Wiley & Sons, New York.
- [60] Hekimoglu, S., (1997). "The Finite Sample Breakdown Points of the Conventional Iterative Outlier Detection Procedures", *Journal of Surveying Engineering*, 123(1): 15-31.

- [61] Hayal, A.G. and Sanli, D.U., (2014). "Accuracy of GIPSY PPP from Version 6.2: A Robust Method to Remove Outliers", EGU General Assembly, 27 April - 2 May 2014, Vienna.
- [62] Yang, Y. Cheng, M. Shum, C. and Tapley, B., (1999). "Robust Estimation of Systematic Errors of Satellite Laser Range", Journal of Geodesy, 73: 345-349.
- [63] Yang, Y. Wen, Y. Xiong, J. and Yang, J., (1999). "Robust Estimation for a Dynamic Model of the Sea Surface", Survey Review, 35: 2-10.
- [64] Current Quarter Daily Geomagnetic Data, Prepared by the U.S. Dept. of Commerce, NOAA, Space Weather Prediction Center, [ftp://ftp.swpc.noaa.gov/pub/indices/old\\_indices/](ftp://ftp.swpc.noaa.gov/pub/indices/old_indices/), 20 February 2015.
- [65] Akarsu, V. Sanli, D.U. and Arslan, E., (2015). "Accuracy of Velocities from Repeated GPS Measurements", Natural Hazards and Earth System Sciences, 15: 875-884.

**APPENDIX-A****GPS STATION INFORMATION**

Table A.1 GPS stations used in Sanli and Tekic [2]

<b>Site ID</b>	<b>Site Name</b>	<b>Country</b>	<b>Latitude (°)</b>	<b>Longitude (°)</b>	<b>Ell. Ht. (m)</b>
BOGT	Bogota	Colombia	4.64007343	-74.08093952	2576.5139
GUAM	USGS Guam Observatory	Guam	13.58932947	144.86836073	201.9283
HARB	Hartebeest- hoek	Rep. of S. Africa	-25.88696215	27.70724533	1558.0911
IRKT	IRKUTSK	Russia	52.21902398	104.31624201	502.3539
MALI	Malindi	Kenya	-2.99591000	40.19440000	-23.3382
MCM4	McMurdo GPS Station	Antarctica	-77.83834982	166.66933012	97.9642
MORP	Morpeth	England	55.21279093	-1.68549527	144.4531
QUIN	Quincy	USA	39.97455399	-120.94442980	1105.7748
RIGA	RIGA Permanent GPS	Latvia	56.94862021	24.05877515	34.7264
SFER	San Fernando	Spain	36.46434617	-6.20564492	84.1759
YELL	Yellowknife	Canada	62.48089338	-114.48070296	180.9175



Table A.2 GPS stations from the densified GPS network

Region	Site ID	Site Name	Country	Latitude (°)	Longitude (°)	Ell. Ht. (m)
Equatorial Area	RIOB	Rio Branco	Brazil	-9.96545744	-67.80281211	172.5776
	RECF	Recife	Brazil	-8.05096212	-34.95151699	20.1277
	DGAR	Diego Garcia Island	UK	-7.26968253	72.37024287	-64.9377
	MAL2	Malindi	Kenya	-2.99605388	40.19414498	-20.9207
	SALU	São Luis	Brazil	-2.59345776	-44.21247935	18.9680
	PNGM	Lombrum	Papua N. Guinea	-2.04322833	147.36600583	116.3329
	RIOP	Riobamba	Ecuador	-1.65059560	-78.65110710	2817.1918
	GLPS	Puerto Ayora	Ecuador	-0.74299846	-90.30366784	1.7761
	MBAR	Mbarara	Uganda	-0.60146780	30.73787782	1337.5319
	NAUR	Nauru, Yaren District	Nauru	-0.55172827	166.92554504	46.2306
	NTUS	Singapore	Singapore	1.34580120	103.67995897	75.3869
	KIRI	Betio	Kiribati	1.35458450	172.92289039	36.1637
	BOAV	Boa Vista	Brasil	2.84518398	-60.70111540	69.5037
	KOUG	Kourou	French Guiana	5.09847120	-52.63975028	107.2334
BJCO	Cotonou	Benin	6.38466542	2.45002292	30.7224	
Middle Latitude Area	KERG	Port aux Francais	French S. Territ.	-49.35146698	70.25552293	73.0083
	BLUF	Bluff	N. Zealand	-46.58506023	168.29208130	124.6228
	DUND	Dunedin	N. Zealand	-45.88366199	170.59716412	386.9058
	CHTI	Wharekauri	N. Zealand	-43.73547201	-176.61711822	75.6615

Table A.2 GPS stations from the densified GPS network (cont'd)

Region	Site ID	Site Name	Country	Latitude (°)	Longitude (°)	Ell. Ht. (m)
Middle Latitude Area	KERG	Christchurch	N. Zealand	-43.70273198	172.65469688	154.6391
	HOB2	Hobart	Australia	-42.80470799	147.43873605	41.0434
	WGTM	Wellington	N. Zealand	-41.32345273	174.80588980	26.0062
	DNVK	Dannevirke	N. Zealand	-40.29885374	176.16665535	457.6280
	BJNM	Beijing	China	40.24532448	116.22413034	109.1253
	CEBR	Cebreros	Spain	40.45342978	-4.36785158	775.7732
	SHIN	SHIN_BRGN _CN1996	USA	40.59167840	-120.22504532	1377.3260
	EBRE	Roquetes	Spain	40.82088948	0.49236434	107.7963
	ORID	Ohrid	Macedonia	41.12731262	20.79405296	773.0054
	TASH	Tashkent	Uzbekistan	41.32804952	69.29556923	439.6967
	UPTC	UNIVERSITY OF PIT	USA	41.62881482	-79.66406821	341.9752
	GUAO	URUMQI	China	43.47110817	87.17731046	2028.7255
	ZECK	Zelenchukskaya	Russia	43.78839386	41.56506924	1166.2918
	CHAN	CHANGCHUN	China	43.79068557	125.44420272	273.2585
	MEDI	Medicina	Italy	44.51995878	11.64681755	50.0093
	HLFX	Halifax	Canada	44.68355025	-63.61128144	3.0964
	MAWY	MAWY_EBRY _WY1998	USA	44.97342727	-110.68930270	1824.2591
	SUP2	Escanaba	USA	45.74948334	-87.07350957	153.8052
	BSMK	BSC Base	USA	46.82112571	-100.81669239	551.2142
	MIKL	Mykolaiv	Ukraine	46.97278561	31.97284350	93.9110
YSSK	Yuzhno -Sakhalinsk	Russia	47.02973384	142.71672209	91.2976	

Table A.2 GPS stations from the densified GPS network (cont'd)

Region	Site ID	Site Name	Country	Latitude (°)	Longitude (°)	Ell. Ht. (m)
Middle Latitude Area	LPOC	La Pocatiere	Canada	47.34139407	-70.00855870	103.2611
	STJO	St. John's	Canada	47.59524098	-52.67775141	152.8372
	ULAB	Ulaanbataar	Mongolia	47.86506732	107.05232870	1575.5483
	ELIZ	Eliza Dome	Canada	49.87305275	-127.12266498	164.7259
High Latitude Area	MCM4	Ross Island	Antarctica	-77.83835034	166.66933231	97.9578
	SYOG	East Ongle Island	Antarctica	-69.00695698	39.58374251	49.9913
	DAV1	Davis	Antarctica	-68.57732347	77.97261248	44.3876
	MAW1	Mawson	Antarctica	-67.60476675	62.87071441	59.1149
	DUM1	Antarctic base of "Dumont d'Urville"	Antarctica	-66.66508567	140.00193526	-1.3562
	CAS1	Casey	Antarctica	-66.28336026	110.51970634	22.4641
	VNAD	Vernadsky Station	Antarctica	-65.24600470	-64.25416109	21.0194
	OHI3	O'Higgins	Antarctica	-63.32109160	-57.90138318	32.6173
	YAKT	Yakutsk	Russia	62.03095897	129.68030655	103.3921
	TLKA	Talkeetna	USA	62.30765240	-150.42029930	166.0020
	TRDS	TRONDHEIM	Norway	63.37138513	10.31916000	317.7869
	BAKE	Baker Lake	Canada	64.31781971	-96.00234856	4.5603
	AB11	Nome_ AnvilAK2006	USA	64.56449485	-165.37345880	349.4452
	SKE0	Skelleftea	Sweden	64.87919865	21.04829389	81.3887
	KULU	Kulusuk GPS	Greenland	65.57933601	-37.14935936	67.5162
	KELY	Kangerlussuaq	Greenland	66.98741947	-50.94484219	229.8576
	BILB	Bilibino	Russia	68.06531235	166.45338345	315.7566

Table A.2 GPS stations from the densified GPS network (cont'd)

<b>Region</b>	<b>Site ID</b>	<b>Site Name</b>	<b>Country</b>	<b>Latitude (°)</b>	<b>Longitude (°)</b>	<b>Ell. Ht. (m)</b>
<b>High Latitude Area</b>	NRIL	Norilsk	Russia	69.36183315	88.35978589	47.9269
	TUKT	Tuktoyaktuk	Canada	69.43823364	-132.99435212	-1.5422
	VAR5	VARDOE	Norway	70.33637408	31.03119915	174.9194
	SCOR	Scoresbysund /Ittoqqoormiit	Greenland	70.48533531	-21.95033893	128.5326
	HOLM	Ulukhaktok, formerly Holman (Victoria Island)	Canada	70.73630315	-117.76123969	0.4513
	THU3	Thule Airbase	Greenland	76.53704797	-68.82504494	36.1774

**APPENDIX-B**

**GPS OBSERVATION SCHEDULE INFORMATION**

Table B.1 Quarter daily geomagnetic data for January 2008 prepared by the U.S. Dept. of Commerce, NOAA, Space Weather Prediction Center [64]

Day	Middle Latitude (Fredericksburg)									High Latitude (College)									Estimated (Planetary)								
	A	K-indices								A	K-indices								A	K-indices							
01	2	1	1	0	0	0	1	1	0	2	1	0	1	1	1	0	0	0	3	1	1	0	0	1	1	0	1
02	1	0	0	0	0	0	1	1	0	0	0	0	0	1	0	0	0	0	1	0	0	0	0	0	0	0	0
03	1	0	0	0	0	0	1	1	0	1	0	0	1	1	0	0	0	0	1	0	0	0	0	0	0	0	0
04	2	0	0	0	1	1	1	1	2	1	0	0	0	2	0	0	0	1	2	0	0	0	0	0	1	0	2
05	13	2	2	3	3	3	2	2	4	29	1	2	3	5	6	5	3	3	18	2	2	4	4	4	4	3	4
06	12	2	4	2	2	2	3	3	2	21	3	2	3	4	5	4	3	3	13	2	4	2	2	3	3	3	
07	10	4	3	2	2	2	1	1	2	23	3	3	3	6	5	1	0	2	12	4	4	2	3	3	0	1	2
08	11	3	2	2	3	1	3	3	2	16	1	2	3	4	3	4	4	2	13	2	3	2	2	1	4	4	2
09	6	3	1	2	1	1	1	2	1	9	3	2	3	3	3	1	1	1	6	3	2	2	1	1	0	1	1
10	2	2	0	1	0	1	1	1	0	2	0	0	0	2	2	0	1	0	3	2	0	0	1	1	1	0	1
11	2	1	1	1	2	0	0	1	0	1	0	0	0	2	0	0	1	0	2	1	0	1	1	0	0	1	1
12	4	0	0	1	1	1	3	2	1	11	0	0	1	3	2	5	3	1	9	0	0	1	1	2	4	3	2
13	9	3	2	1	1	3	3	2	1	24	1	1	1	3	6	5	4	3	11	3	2	2	1	3	3	3	2
14	14	3	2	2	4	3	2	3	3	30	2	2	4	6	4	5	4	3	16	3	3	3	4	3	3	3	3
15	7	3	2	2	1	2	2	1	1	19	3	2	3	5	5	3	0	1	8	3	2	2	2	3	2	0	2
16	9	3	2	2	2	2	2	1	3	22	2	2	4	5	5	3	2	3	11	3	3	3	3	2	2	2	3
17	7	2	1	1	1	2	2	2	3	16	3	1	2	4	5	3	2	1	10	3	1	1	2	2	2	2	3
18	10	3	3	3	2	2	2	2	1	20	3	2	3	3	5	5	2	1	10	3	3	3	1	2	3	2	2
19	6	1	1	2	2	2	3	1	1	28	1	1	5	6	5	4	2	2	9	1	1	3	3	3	3	1	2
20	4	0	2	2	1	2	1	1	1	5	0	2	2	2	2	0	1	2	6	1	3	2	1	2	1	2	2
21	3	0	1	1	1	1	1	2	1	6	0	1	2	3	3	1	2	0	4	1	1	1	1	1	1	1	1
22	2	0	1	0	0	0	1	1	1	0	0	0	0	0	0	1	0	0	2	0	1	0	0	0	1	0	1
23	3	0	0	1	1	2	2	1	1	1	0	0	0	0	0	0	1	1	3	0	0	1	0	0	1	1	2
24	3	2	1	1	1	1	1	1	0	4	0	0	2	2	3	1	1	0	5	1	1	2	1	2	1	2	2
25	8	2	3	3	2	1	1	2	1	8	1	3	3	3	1	1	1	2	11	2	4	3	2	1	1	3	2
26	6	3	2	1	2	1	2	0	1	8	2	1	1	4	3	1	2	0	5	2	2	1	2	2	1	1	1
27	2	1	0	0	0	0	1	1	1	1	0	0	0	0	1	1	1	1	2	1	0	0	0	0	1	1	2
28	2	0	1	0	1	1	1	1	1	4	0	0	0	3	2	0	1	1	2	1	1	0	1	0	0	0	2
29	3	1	2	2	1	1	0	0	0	3	1	2	2	2	1	0	0	0	4	1	2	1	2	1	0	0	0
30	1	0	1	0	0	0	1	0	0	1	1	2	0	0	0	0	0	0	2	1	2	0	0	0	0	0	1
31	3	0	0	0	0	1	2	2	2	2	0	0	0	0	0	1	2	2	5	0	0	0	0	1	2	3	3

Table B.2 Quarter daily geomagnetic data for January 2014 prepared by the U.S. Dept. of Commerce, NOAA, Space Weather Prediction Center [64]

Day	Middle Latitude (Fredericksburg)									High Latitude (College)								Estimated (Planetary)									
	A	K-indices								A	K-indices							A	K-indices								
01	11	0	1	1	3	4	3	3	2	33	0	0	2	5	7	5	2	3	12	1	2	2	3	4	3	3	3
02	15	3	3	3	2	3	3	4	2	29	2	4	3	4	6	5	4	1	20	3	4	4	2	3	3	5	3
03	7	2	2	2	2	2	2	2	1	13	1	1	3	4	4	3	2	1	10	3	2	2	3	3	3	3	2
04	6	1	1	1	2	2	2	3	1	12	1	0	2	5	4	1	1	1	6	1	1	1	2	2	2	2	1
05	4	1	1	2	1	1	2	2	0	2	0	0	2	2	1	0	0	0	4	1	1	2	1	1	1	1	0
06	4	0	1	2	0	2	2	2	1	0	0	0	1	0	0	0	0	0	4	0	1	1	0	1	1	2	2
07	7	0	2	0	1	2	3	3	2	4	0	1	0	1	0	3	2	1	8	1	2	0	1	1	3	3	3
08	8	3	3	1	1	2	2	2	1	4	2	2	0	1	1	2	1	1	8	3	3	1	1	1	1	1	2
09	7	2	2	2	1	2	2	3	1	10	2	1	3	3	3	1	3	1	10	3	3	2	2	1	1	3	2
10	4	1	1	1	1	2	2	1	1	3	0	0	0	0	3	2	0	0	5	2	2	1	1	1	2	1	1
11	3	0	0	0	0	2	2	2	1	2	0	0	0	0	0	1	2	1	4	0	0	0	0	1	1	3	2
12	7	1	1	1	1	2	1	3	3	9	0	1	0	4	3	1	2	3	9	1	1	2	1	2	1	3	4
13	6	2	2	2	1	2	2	1	1	5	3	1	1	2	2	0	0	1	7	3	3	2	1	1	1	0	1
14	8	3	2	1	1	3	2	1	2	17	2	1	3	1	6	3	1	2	11	4	2	2	1	3	2	1	3
15	3	1	1	1	0	1	2	1	0	3	1	1	1	2	0	1	1	0	4	2	1	1	1	0	1	1	1
16	2	0	0	1	1	1	1	1	0	1	0	0	1	2	0	0	0	0	3	0	0	1	1	1	0	1	0
17	2	0	0	0	0	1	2	1	1	1	0	0	0	0	2	0	0	0	4	1	1	1	0	1	1	1	2
18	1	0	0	0	0	1	1	1	0	0	0	0	0	0	0	0	1	0	2	1	0	0	0	0	0	1	0
19	2	0	0	0	0	2	2	1	0	0	0	0	0	0	0	0	0	0	2	1	0	0	0	1	1	1	0
20	4	0	0	1	1	2	2	2	1	3	0	0	3	2	1	0	0	0	3	0	0	1	1	1	1	1	0
21	6	2	1	1	1	2	2	2	2	11	0	0	2	4	4	3	2	1	8	3	1	2	2	2	2	2	2
22	8	1	1	3	3	2	2	1	2	19	0	0	3	6	5	2	1	0	9	2	2	3	3	2	1	2	3
23	5	2	1	2	1	1	2	2	1	3	1	1	2	2	1	1	0	0	6	3	2	2	1	1	1	2	1
24	3	2	1	0	0	1	2	1	0	2	1	1	0	1	0	0	1	0	5	3	2	1	1	1	1	1	1
25	-1	3	2	1	1	1	2	-1	-1	-1	0	0	0	1	2	-1	-1	-1	8	3	2	2	1	1	2	2	3
26	3	0	2	2	1	0	1	1	1	4	0	1	2	3	0	1	1	0	6	2	3	2	1	0	2	1	1
27	3	0	1	1	0	2	2	0	1	1	0	0	0	0	1	1	0	0	4	1	1	1	0	1	1	1	1
28	3	0	0	1	1	1	2	2	1	3	0	0	1	2	0	1	2	1	5	0	0	2	1	1	2	2	2
29	6	1	2	2	2	2	2	2	1	10	0	1	3	4	3	3	1	0	7	2	2	2	2	2	2	2	2
30	4	2	3	1	0	1	1	1	0	1	1	1	1	0	0	0	0	0	5	2	3	1	0	0	0	1	1
31	2	0	0	0	1	1	1	1	0	0	0	0	0	1	0	0	0	0	3	0	0	1	1	1	0	1	1

Table B.3 Observation time schedule of the denser accuracy model, X denotes that data from this day were included in the study

Region	Site ID	Day of the Year (2013)													
		61	62	63	64	65	66	67	68	69	70	71	72	73	
Equatorial Area	RIOB	X	X	X	X	X	X	X	X	X	X	X	-	-	-
	RECF	X	X	X	X	X	X	X	X	X	X	X	-	-	-
	DGAR	X	X	X	X	X	X	X	X	X	X	X	-	-	-
	MAL2	X	X	X	X	X	X	X	X	X	X	X	-	-	-
	SALU	X	X	X	X	X	X	X	X	X	X	X	-	-	-
	PNGM	X	X	X	X	X	-	X	X	X	X	X	X	-	-
	RIOP	X	X	X	X	X	X	X	X	X	X	X	-	-	-
	GLPS	X	X	X	X	X	X	X	X	X	X	X	-	-	-
	MBAR	X	X	X	X	X	X	X	X	X	X	X	-	-	-
	NAUR	X	X	X	X	X	X	X	X	X	X	X	-	-	-
	NTUS	X	X	X	X	X	X	X	X	X	X	X	-	-	-
	KIRI	X	X	X	X	X	X	X	X	X	X	-	X	-	-
	BOAV	X	X	X	X	X	X	X	X	X	X	X	-	-	-
	KOUG	X	X	X	X	X	X	X	X	X	X	X	-	-	-
BJCO	X	-	-	X	X	X	X	X	X	X	X	X	X	-	
Middle Latitude Area	KERG	X	-	X	X	-	X	-	X	X	X	X	X	X	X
	BLUF	X	X	X	X	X	X	X	X	X	X	-	-	-	-
	DUND	X	X	X	X	X	X	X	X	X	X	-	-	-	-
	CHTI	X	X	X	X	X	X	X	X	X	X	-	-	-	-
	MQZG	X	X	X	X	X	X	X	X	X	X	-	-	-	-
	HOB2	X	X	X	X	X	X	X	X	X	X	-	-	-	-
	WGTN	X	X	X	X	X	X	X	X	X	X	-	-	-	-

Table B.3 Observation time schedule of the denser accuracy model, X denotes that data from this day were included in the study (cont'd)

Region	Site ID	Day of the Year (2013)												
		61	62	63	64	65	66	67	68	69	70	71	72	73
Middle Latitude Area	DNVK	X	X	X	X	X	X	X	X	X	X	-	-	-
	BJNM	X	X	X	X	X	X	X	X	X	X	-	-	-
	CEBR	X	X	X	X	X	X	X	X	X	X	-	-	-
	SHIN	X	X	X	X	X	X	X	X	X	X	-	-	-
	EBRE	X	X	X	-	-	-	X	X	X	X	X	X	X
	ORID	X	X	X	X	X	X	X	X	X	X	-	-	-
	TASH	X	X	X	X	X	X	X	X	X	X	-	-	-
	UPTC	X	X	-	X	X	X	X	X	X	X	X	-	-
	GUAO	X	X	X	X	X	X	X	X	X	X	-	-	-
	ZECK	X	X	X	X	X	X	X	X	X	X	-	-	-
	CHAN	X	X	X	X	X	X	X	X	X	X	-	-	-
	MEDI	X	X	X	X	X	X	X	X	X	X	-	-	-
	HLFX	X	X	X	X	X	X	X	X	X	X	-	-	-
	MAWY	X	X	X	X	X	X	X	X	X	X	-	-	-
	SUP2	X	X	X	X	X	X	X	X	X	X	-	-	-
	BSMK	X	X	X	X	X	X	X	X	X	X	-	-	-
	MIKL	X	X	X	X	X	X	X	X	X	X	-	-	-
	YSSK	X	X	X	X	X	X	X	X	X	X	-	-	-
	LPOC	X	X	X	X	X	X	X	X	X	X	-	-	-
	STJO	X	X	X	X	X	X	X	X	X	X	-	-	-
ULAB	X	X	X	X	X	X	X	X	X	X	-	-	-	
ELIZ	X	X	X	X	X	X	X	X	X	X	-	-	-	



Table B.3 Observation time schedule of the denser accuracy model, X denotes that data from this day were included in the study (cont'd)

Region	Site ID	Day of the Year (2013)												
		61	62	63	64	65	66	67	68	69	70	71	72	73
High Latitude Area	MCM4	X	X	X	X	X	X	X	X	X	X	-	-	-
	SYOG	X	X	X	X	X	X	X	X	X	X	-	-	-
	DAV1	X	X	X	X	X	X	X	X	X	X	-	-	-
	MAW1	X	X	X	X	X	X	X	X	X	X	-	-	-
	DUM1	X	X	X	X	X	X	X	X	X	X	-	-	-
	CAS1	X	X	X	X	X	X	X	X	X	X	-	-	-
	VNAD	X	X	X	X	X	X	X	X	X	X	-	-	-
	OHI3	X	X	X	X	X	X	X	X	X	X	-	-	-
	YAKT	X	X	X	X	X	X	X	X	-	X	X	-	-
	TLKA	X	X	X	X	X	X	X	X	X	X	-	-	-
	TRDS	X	X	X	X	X	X	-	X	X	X	X	-	-
	BAKE	X	X	X	X	X	X	X	X	X	X	-	-	-
	AB11	X	X	X	X	X	X	X	X	X	X	-	-	-
	SKE0	X	X	X	X	X	X	X	X	X	X	-	-	-
	KULU	X	X	X	X	X	X	X	X	X	X	-	-	-
	KELY	X	X	X	X	X	X	X	X	X	X	-	-	-
	BILB	X	X	X	X	X	X	X	X	X	X	-	-	-
	NRIL	X	X	-	X	X	X	X	X	X	X	X	-	-
	TUKT	X	X	X	X	X	X	X	X	X	X	-	-	-
	VARS	X	X	X	X	X	X	X	X	X	X	-	-	-
	SCOR	X	X	X	X	X	X	X	X	X	X	-	-	-
HOLM	X	X	X	X	X	X	X	X	X	X	-	-	-	
THU3	X	X	X	X	X	X	X	X	X	X	-	-	-	

Table B.4 Quarter daily geomagnetic data for March 2013 prepared by the U.S. Dept. of Commerce, NOAA, Space Weather Prediction Center [64]

Day	Middle Latitude (Fredericksburg)									High Latitude (College)								Estimated (Planetary)									
	A	K-indices								A	K-indices							A	K-indices								
61	23	4	4	3	4	4	3	3	4	64	5	4	7	7	5	6	4	1	27	4	4	3	5	4	4	4	4
62	14	4	3	3	2	2	2	3	3	17	3	4	4	2	3	4	2	2	12	4	3	2	1	2	2	3	3
63	6	2	2	1	2	2	2	1	1	10	3	3	1	4	2	2	1	1	7	3	3	2	2	1	2	1	2
64	4	2	1	1	1	2	0	1	1	6	2	1	0	4	2	0	0	0	4	2	1	1	1	1	1	0	1
65	3	3	0	0	0	1	1	1	1	1	1	0	1	0	0	1	0	0	4	3	1	0	1	1	0	1	1
66	4	1	2	0	1	1	2	1	1	1	0	1	0	0	0	0	1	0	3	1	2	0	0	0	1	1	1
67	2	0	1	1	1	1	1	1	0	1	0	0	0	2	1	0	0	0	4	1	1	1	1	1	1	1	1
68	3	0	0	1	1	1	1	2	1	1	0	0	0	0	0	0	1	1	3	0	0	1	1	1	1	1	1
69	6	2	1	2	2	2	2	2	1	4	1	0	1	2	3	1	1	0	6	2	1	1	2	2	1	2	1
70	3	1	0	1	1	2	1	1	1	0	1	0	0	0	0	0	0	0	4	1	0	1	1	1	1	1	2
71	4	2	2	2	0	1	1	1	1	2	2	1	1	0	0	0	0	0	5	2	2	2	1	1	1	1	1
72	6	1	1	2	1	3	2	2	1	4	1	0	2	0	3	0	1	0	5	1	1	2	1	2	1	2	1
73	3	2	1	1	1	1	1	1	0	3	1	1	2	2	0	0	0	0	4	1	1	1	1	1	1	1	1
74	4	0	1	0	1	3	1	1	1	4	0	0	0	3	2	1	1	0	5	0	1	0	2	2	1	1	1
75	5	0	3	2	2	2	1	0	1	11	0	1	4	5	1	0	0	1	6	0	3	2	2	1	1	0	1
76	8	3	3	2	2	2	2	1	1	13	2	3	4	4	3	2	1	1	10	3	3	3	2	2	2	1	2
77	32	2	1	5	5	5	5	4	4	79	1	0	6	7	7	7	6	5	46	2	1	6	5	5	6	6	5
78	6	2	2	2	1	2	2	2	1	7	2	2	3	2	1	1	2	1	7	3	2	2	2	1	1	2	2
79	4	1	1	1	1	1	1	2	2	3	2	1	0	0	0	1	2	2	5	2	1	1	0	0	1	2	2
80	7	1	2	2	1	2	2	2	3	18	2	4	2	1	5	4	2	3	9	2	2	2	1	2	2	3	3
81	11	3	4	4	1	1	1	1	1	14	3	5	4	2	1	1	1	1	12	4	4	4	1	1	1	1	1
82	2	0	0	0	1	1	1	2	1	2	0	0	0	1	0	1	2	1	4	1	0	0	1	1	1	2	2
83	10	2	1	2	2	2	2	3	4	15	2	1	2	4	5	2	3	2	11	2	1	2	2	3	2	3	4
84	6	2	1	2	2	2	2	2	1	11	2	1	2	5	2	3	1	0	5	2	1	2	2	1	1	2	1
85	3	0	0	1	1	2	1	2	1	2	0	0	0	1	1	0	1	1	4	0	0	1	1	1	1	2	1
86	2	1	0	0	1	1	2	1	0	0	1	0	0	0	0	0	0	0	3	1	1	0	1	0	1	1	0
87	9	1	2	2	2	3	2	2	3	29	2	2	3	5	6	5	3	3	14	1	2	2	3	3	4	3	4
88	10	4	1	1	2	2	3	2	2	15	3	2	4	5	1	2	2	1	9	4	1	1	2	1	2	2	2
89	19	3	3	4	4	3	4	2	3	51	2	4	7	6	5	6	3	2	23	3	3	4	4	3	5	3	3
90	12	4	4	2	2	2	2	2	2	21	4	6	2	4	2	2	2	1	17	5	5	2	2	1	2	3	2
91	3	1	0	0	1	1	2	1	1	4	2	1	1	1	0	2	1	1	4	1	0	1	1	1	2	1	1

---

**PPP ACCURACY MODEL ESTIMATIONS**

Table C.1 Estimated RMS values of the revised accuracy model, for north (in mm)

Site ID	Observing Session Duration (T)							
	1 h	2 h	3 h	4 h	6 h	8 h	12 h	24 h
BOGT	14.66	4.13	4.01	3.81	2.93	2.26	2.16	1.68
GUAM	23.32	5.53	5.12	3.83	4.13	3.43	2.80	2.02
HARB	14.39	4.42	3.58	2.55	2.42	2.12	1.65	1.88
IRKT	28.18	7.30	2.95	2.15	1.98	1.59	1.25	1.16
MAL2	13.18	2.44	2.37	1.30	1.48	1.43	1.16	0.24
MCM4	18.40	5.18	4.38	3.72	2.65	2.70	2.01	1.51
MORP	15.84	5.37	3.08	2.77	2.30	2.35	1.97	1.46
QUIN	11.59	3.71	3.24	2.79	2.15	1.88	1.95	1.43
RIGA	15.88	3.08	2.58	2.21	1.76	1.68	1.57	0.98
SFER	15.35	3.64	2.96	2.82	2.76	1.57	1.26	1.43
YELL	11.46	3.35	2.74	1.96	1.75	1.39	1.04	1.09

Table C.2 Estimated RMS values of the revised accuracy model, for east (in mm)

Site ID	Observing Session Duration (T)							
	1 h	2 h	3 h	4 h	6 h	8 h	12 h	24 h
BOGT	57.02	5.17	4.24	3.19	2.10	1.76	1.72	1.33
GUAM	50.45	6.67	6.74	5.23	3.21	2.33	2.03	1.51
HARB	41.30	5.32	4.19	3.74	3.28	3.13	2.66	2.33
IRKT	51.61	6.98	3.70	2.36	2.83	1.73	2.58	1.44
MAL2	34.95	4.28	2.82	2.69	2.46	1.99	1.80	1.36
MCM4	24.07	6.22	4.54	3.39	3.55	2.79	2.69	2.07
MORP	34.52	4.21	3.09	2.11	2.31	1.66	1.53	0.42
QUIN	31.75	3.37	2.49	2.41	2.20	2.12	1.98	1.83
RIGA	29.70	2.46	1.85	1.63	1.44	1.01	1.08	0.94
SFER	31.29	7.10	5.37	4.93	5.18	5.58	5.68	4.48
YELL	18.77	2.42	1.91	1.71	1.68	1.61	1.54	1.38

Table C.3 Estimated RMS values of the revised accuracy model, for vertical (in mm)

Site ID	Observing Session Duration (T)							
	1 h	2 h	3 h	4 h	6 h	8 h	12 h	24 h
BOGT	55.83	20.62	16.35	7.32	5.28	5.34	3.44	3.17
GUAM	104.23	39.53	24.52	19.99	15.73	17.56	11.92	3.35
HARB	47.75	21.49	16.12	14.58	8.61	11.42	7.92	6.38
IRKT	58.87	19.10	10.54	9.07	5.86	5.99	4.90	2.34
MAL2	34.68	12.34	9.42	9.79	7.76	5.09	3.76	1.73
MCM4	47.20	23.96	15.68	10.85	9.69	7.96	4.17	3.64
MORP	37.14	17.12	10.83	9.44	7.96	8.02	6.17	4.98
QUIN	42.04	12.00	8.24	7.27	5.95	4.91	4.02	3.06
RIGA	39.19	16.11	11.91	9.23	7.98	5.42	5.56	4.66
SFER	35.22	17.53	11.35	8.35	10.54	7.47	7.32	6.68
YELL	26.96	10.75	9.70	7.89	6.61	6.55	2.75	2.29

Table C.4 Estimated RMS values of the denser accuracy model, for north (in mm)

Region	Site ID	Observing Session Duration (T)							
		1 h	2 h	3 h	4 h	6 h	8 h	12 h	24 h
Equatorial Area	RIOB	20.54	5.41	3.43	3.72	3.31	2.77	2.71	1.72
	RECF	12.19	3.50	2.38	2.18	1.67	1.25	1.28	0.74
	DGAR	17.62	4.27	4.05	3.40	2.60	2.52	1.85	1.74
	MAL2	19.89	5.44	4.10	4.65	3.29	3.15	1.80	0.63
	SALU	16.86	4.27	3.13	3.04	2.23	2.36	1.67	1.38
	PNGM	16.00	4.42	3.44	3.29	3.24	2.02	1.80	1.54
	RIOP	19.58	4.02	3.45	2.34	2.06	1.97	1.74	1.35
	GLPS	13.51	5.28	3.96	3.31	2.73	2.21	1.38	1.23
	MBAR	15.14	4.27	3.40	2.57	2.21	1.36	1.67	0.88
	NAUR	13.15	3.34	3.06	2.60	2.22	1.83	1.87	1.36
	NTUS	13.52	3.45	2.98	3.00	2.00	1.49	1.47	1.03
	KIRI	22.48	5.60	4.49	3.63	3.76	4.00	3.12	2.34
	BOAV	14.11	4.25	3.25	3.08	2.67	3.01	2.57	2.24
	KOUG	16.87	4.54	4.18	3.74	3.11	2.65	2.34	1.17
BJCO	16.49	4.89	3.59	2.74	2.57	1.96	1.52	1.12	
Middle Latitude Area	KERG	15.44	3.46	2.75	2.65	1.96	2.09	1.68	2.00
	BLUF	13.76	4.14	3.27	2.85	2.56	1.91	2.02	1.66
	DUND	27.76	9.55	6.90	6.14	5.54	4.67	4.23	1.25
	CHTI	16.22	4.28	2.91	3.29	2.32	2.06	1.15	0.52
	MQZG	11.54	3.58	2.78	2.52	2.04	2.08	1.81	1.07
	HOB2	12.22	3.40	3.11	2.85	2.54	2.39	2.02	1.85
	WGTV	15.08	4.17	3.53	3.35	2.44	1.75	1.84	1.22
	DNVK	18.70	5.69	3.57	2.98	2.44	2.08	1.45	1.41

Table C.4 Estimated RMS values of the denser accuracy model, for north (in mm)  
(cont'd)

Region	Site ID	Observing Session Duration (T)							
		1 h	2 h	3 h	4 h	6 h	8 h	12 h	24 h
Middle Latitude Area	BJNM	13.22	4.16	3.32	3.00	2.64	2.66	2.09	1.29
	CEBR	14.28	3.17	2.62	1.75	1.76	1.13	0.91	0.96
	SHIN	17.74	4.08	3.87	3.07	3.31	2.24	2.64	1.24
	EBRE	13.24	2.78	2.04	1.66	1.59	1.26	1.19	1.15
	ORID	20.18	6.40	4.25	4.23	3.81	3.91	3.46	3.09
	TASH	17.68	4.60	3.32	3.18	2.41	1.53	1.24	0.93
	UPTC	17.79	4.61	2.81	3.32	2.09	2.75	1.74	1.44
	GUAO	13.40	3.07	2.46	1.94	2.09	0.98	1.29	0.99
	ZECK	13.32	3.61	2.64	1.71	1.77	1.55	1.11	1.10
	CHAN	28.88	8.03	4.76	4.86	3.09	3.38	3.00	1.98
	MEDI	17.73	5.03	3.37	2.51	2.49	1.65	1.94	1.45
	HLFX	13.26	3.22	2.73	2.14	2.37	1.58	1.37	0.97
	MAWY	12.65	3.50	2.77	2.74	2.41	2.25	1.86	1.44
	SUP2	15.12	3.65	2.79	2.84	2.18	1.85	1.59	0.57
	BSMK	11.91	2.73	2.16	1.89	1.71	1.29	1.22	1.00
	MIKL	13.91	3.71	2.90	2.70	2.32	1.99	1.29	1.18
	YSSK	13.96	4.84	4.74	3.66	3.86	3.48	3.70	3.14
	LPOC	11.53	2.69	2.06	2.07	1.67	1.49	1.43	0.93
	STJO	18.17	3.68	3.45	2.74	2.24	2.11	0.95	1.01
	ULAB	15.12	2.41	2.02	1.44	1.53	1.33	0.88	1.11
ELIZ	13.30	4.75	3.33	2.63	2.10	2.11	1.79	1.04	

Table C.4 Estimated RMS values of the denser accuracy model, for north (in mm)  
(cont'd)

Region	Site ID	Observing Session Duration (T)							
		1 h	2 h	3 h	4 h	6 h	8 h	12 h	24 h
High Latitude Area	MCM4	14.95	3.41	2.88	2.61	2.14	2.27	1.89	1.69
	SYOG	12.72	3.48	3.08	2.73	2.55	2.44	1.95	1.44
	DAV1	15.53	5.99	4.72	3.97	3.71	2.66	2.02	1.89
	MAW1	15.68	4.77	3.72	2.46	2.45	2.19	1.73	0.90
	DUM1	12.17	3.39	2.36	2.12	1.50	1.81	1.42	1.06
	CAS1	13.24	4.15	3.19	2.98	2.22	2.01	1.91	0.70
	VNAD	20.39	3.73	3.02	2.75	2.20	1.83	1.65	0.73
	OHI3	13.99	2.65	2.37	1.99	1.42	1.48	1.49	1.29
	YAKT	14.33	4.41	3.51	3.45	2.27	2.13	2.30	1.75
	TLKA	12.75	2.98	2.12	2.60	1.81	1.35	1.28	0.79
	TRDS	16.96	3.18	2.71	2.22	1.74	1.51	1.20	0.93
	BAKE	11.64	2.31	1.55	1.61	1.11	0.95	0.65	0.58
	AB11	13.49	3.38	2.61	2.04	1.59	1.25	0.80	0.58
	SKE0	14.30	3.52	2.44	2.29	1.74	1.87	1.46	1.22
	KULU	10.23	2.47	1.99	1.81	1.06	1.29	1.15	0.86
	KELY	12.74	3.20	2.55	2.33	1.77	1.97	1.53	0.89
	BILB	9.10	2.31	2.36	1.96	1.88	1.75	0.97	1.17
	NRIL	10.10	2.55	2.17	1.75	1.19	0.88	0.86	0.67
	TUKT	43.57	14.12	8.65	6.51	6.54	4.98	2.78	2.47
	VARS	12.80	4.41	4.41	3.44	2.96	3.11	2.20	1.04
SCOR	11.23	3.48	2.60	2.46	2.03	1.70	1.61	1.02	
HOLM	14.19	3.27	2.38	1.84	1.92	1.71	1.15	1.17	
THU3	39.17	21.56	13.94	5.16	4.93	1.97	1.36	1.05	



Table C.5 Estimated RMS values of the denser accuracy model, for east (in mm)

Region	Site ID	Observing Session Duration (T)							
		1 h	2 h	3 h	4 h	6 h	8 h	12 h	24 h
Equatorial Area	RIOB	57.83	6.96	5.18	3.57	3.47	2.61	1.93	2.15
	RECF	39.33	3.76	2.97	2.11	2.15	1.59	1.41	1.11
	DGAR	49.07	4.40	3.69	4.12	2.44	2.96	2.02	1.26
	MAL2	56.33	6.72	4.10	3.71	2.52	2.82	1.88	1.51
	SALU	43.44	5.62	3.50	3.28	2.34	1.68	1.61	1.05
	PNGM	46.85	5.73	4.51	3.85	2.93	2.57	1.67	1.72
	RIOP	49.25	4.54	3.20	3.58	2.30	1.93	1.39	1.19
	GLPS	35.87	5.69	3.53	3.85	2.63	2.84	2.63	1.86
	MBAR	46.99	4.19	3.45	2.97	2.61	2.06	1.88	1.66
	NAUR	44.77	4.61	3.32	2.89	2.24	2.16	1.47	1.26
	NTUS	36.30	4.28	3.22	3.36	2.62	2.69	1.44	1.04
	KIRI	61.44	10.26	6.45	5.35	4.68	3.14	3.58	0.89
	BOAV	33.97	4.12	3.45	2.58	2.65	1.96	1.40	1.58
	KOUG	49.36	4.56	3.36	3.13	2.17	2.18	1.89	1.17
BJCO	45.61	5.74	5.28	3.76	3.35	2.76	2.46	2.21	
Middle Latitude Area	KERG	36.88	3.11	2.88	2.33	2.15	1.25	1.70	1.25
	BLUF	30.80	3.37	2.98	2.55	2.33	2.35	1.86	1.44
	DUND	61.94	6.79	4.97	4.88	3.45	4.19	2.90	1.48
	CHTI	43.31	3.98	2.64	2.39	2.16	2.00	1.85	1.59
	MQZG	28.57	2.88	2.38	2.14	2.01	1.67	1.69	1.07
	HOB2	34.68	3.86	3.14	2.56	1.94	1.65	1.55	0.92
	WGTV	38.63	3.51	3.02	2.64	2.53	1.80	2.05	1.20
	DNVK	39.52	4.29	3.05	3.29	2.57	1.73	1.61	1.05

Table C.5 Estimated RMS values of the denser accuracy model, for east (in mm)  
(cont'd)

Region	Site ID	Observing Session Duration (T)							
		1 h	2 h	3 h	4 h	6 h	8 h	12 h	24 h
Middle Latitude Area	BJNM	26.35	2.97	2.79	2.31	1.75	1.60	1.43	0.51
	CEBR	27.30	2.80	2.49	2.07	1.95	1.89	1.79	1.24
	SHIN	37.40	3.59	3.27	2.92	2.74	2.44	1.76	1.46
	EBRE	20.89	1.92	1.87	1.49	1.59	1.26	1.13	0.92
	ORID	39.33	6.31	5.57	4.38	3.47	3.05	1.81	1.48
	TASH	33.68	3.96	2.79	2.37	1.65	1.45	1.19	1.00
	UPTC	34.00	3.78	2.47	2.06	1.84	1.57	0.96	0.77
	GUAO	27.24	2.88	2.22	1.93	1.90	1.75	1.66	1.50
	ZECK	28.74	2.66	1.99	1.93	1.31	0.72	1.03	0.93
	CHAN	63.74	6.02	4.65	3.07	2.53	1.97	1.63	0.51
	MEDI	31.65	5.23	4.12	3.86	3.80	3.55	3.22	2.74
	HLFX	25.43	2.27	1.87	1.81	1.53	1.37	1.32	0.98
	MAWY	34.38	3.10	2.23	1.94	1.81	1.25	1.35	1.53
	SUP2	26.77	3.48	2.59	2.17	2.00	1.70	1.63	1.19
	BSMK	22.72	2.34	2.27	1.94	1.98	1.91	1.67	1.60
	MIKL	30.06	2.92	2.67	2.55	2.35	1.90	1.65	1.97
	YSSK	33.10	2.99	2.39	2.12	1.96	2.05	0.89	1.16
	LPOC	20.39	2.09	1.75	1.46	1.22	1.18	0.94	0.79
	STJO	50.01	3.56	3.19	3.27	1.99	1.96	1.40	1.18
	ULAB	22.82	2.66	2.14	2.20	1.95	2.14	1.47	1.44
ELIZ	28.78	3.61	2.52	2.37	1.56	2.09	1.26	1.12	

Table C.5 Estimated RMS values of the denser accuracy model, for east (in mm)  
(cont'd)

Region	Site ID	Observing Session Duration (T)							
		1 h	2 h	3 h	4 h	6 h	8 h	12 h	24 h
High Latitude Area	MCM4	18.25	2.50	2.16	2.28	1.81	1.88	1.38	1.32
	SYOG	15.35	2.29	2.21	1.82	1.59	1.16	1.20	1.05
	DAV1	26.78	5.16	4.27	3.46	3.59	2.75	2.47	2.02
	MAW1	21.58	4.54	3.21	3.27	2.72	2.67	2.31	2.46
	DUM1	16.40	2.78	2.51	2.32	1.90	1.83	1.38	1.20
	CAS1	21.85	3.15	2.32	1.99	1.61	1.30	0.74	0.55
	VNAD	21.36	4.26	3.13	2.54	2.55	2.12	1.23	0.80
	OHI3	21.09	2.16	1.80	1.39	1.24	1.06	1.07	0.77
	YAKT	15.18	3.32	2.75	2.49	2.32	2.30	2.14	1.93
	TLKA	22.04	3.15	2.31	1.83	1.94	1.45	1.36	1.18
	TRDS	24.64	2.59	2.14	2.04	1.75	1.37	1.30	0.79
	BAKE	17.83	2.16	1.75	1.69	1.35	1.28	1.19	1.14
	AB11	18.90	2.02	1.91	1.48	1.52	1.15	0.98	0.91
	SKE0	18.83	3.08	2.76	2.83	2.15	1.73	1.66	1.36
	KULU	16.22	2.16	1.73	1.00	0.91	0.82	0.93	0.70
	KELY	17.15	2.25	1.92	1.36	1.32	1.29	1.26	0.92
	BILB	12.64	1.60	1.16	1.16	0.95	1.00	0.72	0.55
	NRIL	14.02	2.31	1.97	1.61	1.62	1.51	1.22	1.11
	TUKT	67.09	21.53	10.21	12.08	11.66	7.64	5.46	4.44
	VAR5	20.06	2.68	2.47	2.13	2.06	1.89	1.56	1.17
SCOR	18.90	3.05	2.03	2.01	1.76	1.51	1.41	1.37	
HOLM	15.99	2.04	1.61	1.32	1.21	1.01	0.77	0.27	
THU3	58.22	38.27	8.16	2.76	12.84	2.12	0.65	0.43	

Table C.6 Estimated RMS values of the denser accuracy model, for vertical (in mm)

Region	Site ID	Observing Session Duration (T)							
		1 h	2 h	3 h	4 h	6 h	8 h	12 h	24 h
Equatorial Area	RIOB	73.27	28.60	15.82	12.56	11.63	7.38	7.62	4.12
	RECF	39.96	15.00	9.91	11.54	8.24	6.64	5.66	4.43
	DGAR	48.67	18.21	14.06	13.62	13.52	12.14	10.15	8.50
	MAL2	53.98	28.18	19.26	14.36	15.40	12.14	11.15	9.62
	SALU	44.86	17.97	15.52	11.52	12.24	10.26	7.60	5.73
	PNGM	50.56	25.68	17.01	17.66	15.38	12.62	5.48	3.29
	RIOP	55.11	21.98	13.59	10.81	8.45	6.76	7.05	4.14
	GLPS	51.89	18.75	14.49	11.90	11.06	7.12	6.03	6.56
	MBAR	42.52	20.08	13.36	10.12	8.99	5.75	6.37	4.87
	NAUR	37.08	18.26	11.71	9.90	8.96	7.82	5.90	4.21
	NTUS	37.97	16.52	13.25	11.23	8.72	6.89	6.31	4.28
	KIRI	87.07	25.64	20.11	16.41	12.72	16.07	10.52	5.09
	BOAV	35.09	19.41	13.45	11.67	8.04	7.56	4.08	5.60
	KOUG	53.82	23.49	17.45	14.62	11.47	10.38	8.48	3.81
BJCO	66.33	19.13	15.02	13.56	8.23	8.69	7.10	4.45	
Middle Latitude Area	KERG	36.25	12.06	12.16	10.77	9.01	9.94	7.51	5.87
	BLUF	34.61	11.20	9.66	8.76	6.16	6.92	5.66	4.55
	DUND	81.50	27.86	19.84	17.09	11.74	8.92	7.33	5.12
	CHTI	43.84	14.81	12.22	9.98	8.73	6.98	7.77	3.57
	MQZG	29.64	9.97	8.77	7.87	6.99	6.69	5.38	4.48
	HOB2	39.16	12.70	11.63	9.05	7.09	5.77	5.73	3.89
	WGTN	37.55	14.61	13.12	11.20	9.34	7.48	6.97	4.42
	DNVK	46.42	14.51	11.62	9.54	7.70	7.56	4.80	3.98

Table C.6 Estimated RMS values of the denser accuracy model, for vertical (in mm)  
(cont'd)

Region	Site ID	Observing Session Duration (T)							
		1 h	2 h	3 h	4 h	6 h	8 h	12 h	24 h
Middle Latitude Area	BJNM	31.48	10.15	9.06	7.49	7.15	6.30	6.16	5.28
	CEBR	31.38	11.42	8.65	7.61	5.99	5.83	4.42	4.02
	SHIN	44.69	13.88	10.49	9.85	5.64	6.04	3.83	3.60
	EBRE	28.56	9.27	7.78	6.83	6.28	5.87	4.64	4.28
	ORID	55.81	27.44	17.68	13.39	11.70	9.29	7.91	6.93
	TASH	40.55	14.82	9.59	9.43	5.45	5.51	4.33	4.07
	UPTC	42.10	10.02	9.60	6.98	6.86	6.07	5.20	4.54
	GUAO	28.83	9.22	8.06	5.69	5.37	4.83	2.55	2.22
	ZECK	33.62	12.37	10.19	8.11	8.84	6.92	5.76	3.74
	CHAN	87.73	26.34	17.16	14.45	7.72	6.65	6.44	4.39
	MEDI	42.36	13.74	10.08	8.58	6.53	4.07	3.33	3.33
	HLFX	23.50	8.57	7.44	6.30	6.33	5.28	4.86	4.11
	MAWY	34.40	9.64	6.83	5.45	5.93	4.25	6.00	4.59
	SUP2	42.03	13.74	9.04	9.29	8.61	6.10	5.64	3.64
	BSMK	28.36	9.30	7.24	5.95	5.62	5.67	4.58	3.46
	MIKL	27.65	8.70	8.09	7.56	6.42	5.13	5.10	4.15
	YSSK	33.31	14.92	12.95	9.89	7.89	8.14	8.14	9.45
	LPOC	26.48	10.98	8.75	7.31	6.27	5.13	4.40	3.79
	STJO	52.97	16.01	12.38	12.90	8.98	9.48	4.60	3.48
	ULAB	27.39	10.83	9.20	8.54	7.61	6.75	5.00	4.87
ELIZ	32.04	13.84	9.71	7.62	7.44	5.15	4.74	4.30	

Table C.6 Estimated RMS values of the denser accuracy model, for vertical (in mm)  
(cont'd)

Region	Site ID	Observing Session Duration (T)							
		1 h	2 h	3 h	4 h	6 h	8 h	12 h	24 h
High Latitude Area	MCM4	27.32	11.31	8.72	7.62	4.70	6.13	4.29	3.69
	SYOG	29.26	13.16	8.69	8.70	7.07	7.04	4.49	2.66
	DAV1	32.89	20.62	16.71	16.02	14.11	11.36	12.60	7.89
	MAW1	39.93	20.48	14.93	10.22	10.45	10.97	5.73	7.15
	DUM1	24.05	9.51	6.87	7.00	5.37	5.72	4.26	2.32
	CAS1	32.01	15.33	10.37	8.23	5.12	5.54	4.82	2.82
	VNAD	33.07	13.38	10.76	9.64	5.53	5.66	4.28	2.24
	OHI3	24.30	11.43	9.40	6.12	5.83	5.84	4.61	3.56
	YAKT	22.54	12.00	10.59	9.49	9.27	8.31	8.42	7.50
	TLKA	34.59	14.09	7.86	7.25	5.53	5.39	4.62	3.24
	TRDS	32.95	10.51	11.89	9.80	7.64	7.62	6.21	5.79
	BAKE	32.40	12.58	9.29	7.97	7.65	5.73	3.96	3.45
	AB11	29.55	11.65	9.66	7.60	5.90	4.54	3.60	3.28
	SKE0	27.90	12.37	8.08	6.71	6.55	4.81	4.79	4.20
	KULU	24.11	7.53	6.67	6.23	5.04	3.23	3.15	2.28
	KELY	26.28	12.78	11.00	9.47	8.40	7.73	7.53	6.55
	BILB	15.81	8.33	6.76	6.99	6.15	6.01	4.40	2.35
	NRIL	29.97	11.12	10.25	8.48	6.54	6.71	5.46	3.28
	TUKT	118.63	45.64	26.89	27.09	20.48	16.43	8.82	10.28
	VAR5	31.32	12.71	12.47	12.27	10.72	10.48	9.66	8.55
SCOR	31.31	14.55	10.46	10.23	8.63	7.43	6.24	5.22	
HOLM	28.99	11.76	8.31	8.75	6.08	6.60	4.15	3.15	
THU3	52.96	40.80	22.76	12.84	7.38	6.63	3.21	2.70	

Table C.7 Estimated coefficients, their 1-sigma uncertainties and ratio values of the denser accuracy model, for position components north, east and vertical

<b>Coefficient</b>	<b>Estimate</b>	<b>Uncertainty</b>	<b>Ratio</b>
$a_n(\text{mm}^2 \cdot h)$	33.85	6.63	5.11
$a_e(\text{mm}^2 \cdot h)$	29.00	18.58	1.56
$a_v(\text{mm}^2 \cdot h)$	507.89	76.87	6.61
$b_n(\text{mm}^2 \cdot h/\text{degree}^2)$	7.47E-04	2.21E-03	0.34
$b_e(\text{mm}^2 \cdot h/\text{degree}^2)$	4.73E-03	6.19E-03	0.76
$b_v(\text{mm}^2 \cdot h/\text{degree}^2)$	-2.74E-02	2.56E-02	-1.07
$c_n$	1.13	1.00	1.13
$c_e$	0.30	2.81	0.11
$c_v$	6.04	11.64	0.52
$d_n(\text{mm}^2/\text{degree}^2)$	-2.27E-04	3.34E-04	-0.68
$d_e(\text{mm}^2/\text{degree}^2)$	5.66E-05	9.37E-04	0.06
$d_v(\text{mm}^2/\text{degree}^2)$	-5.08E-04	3.88E-03	-0.13

PPP ACCURACY MODEL FIT FIGURES

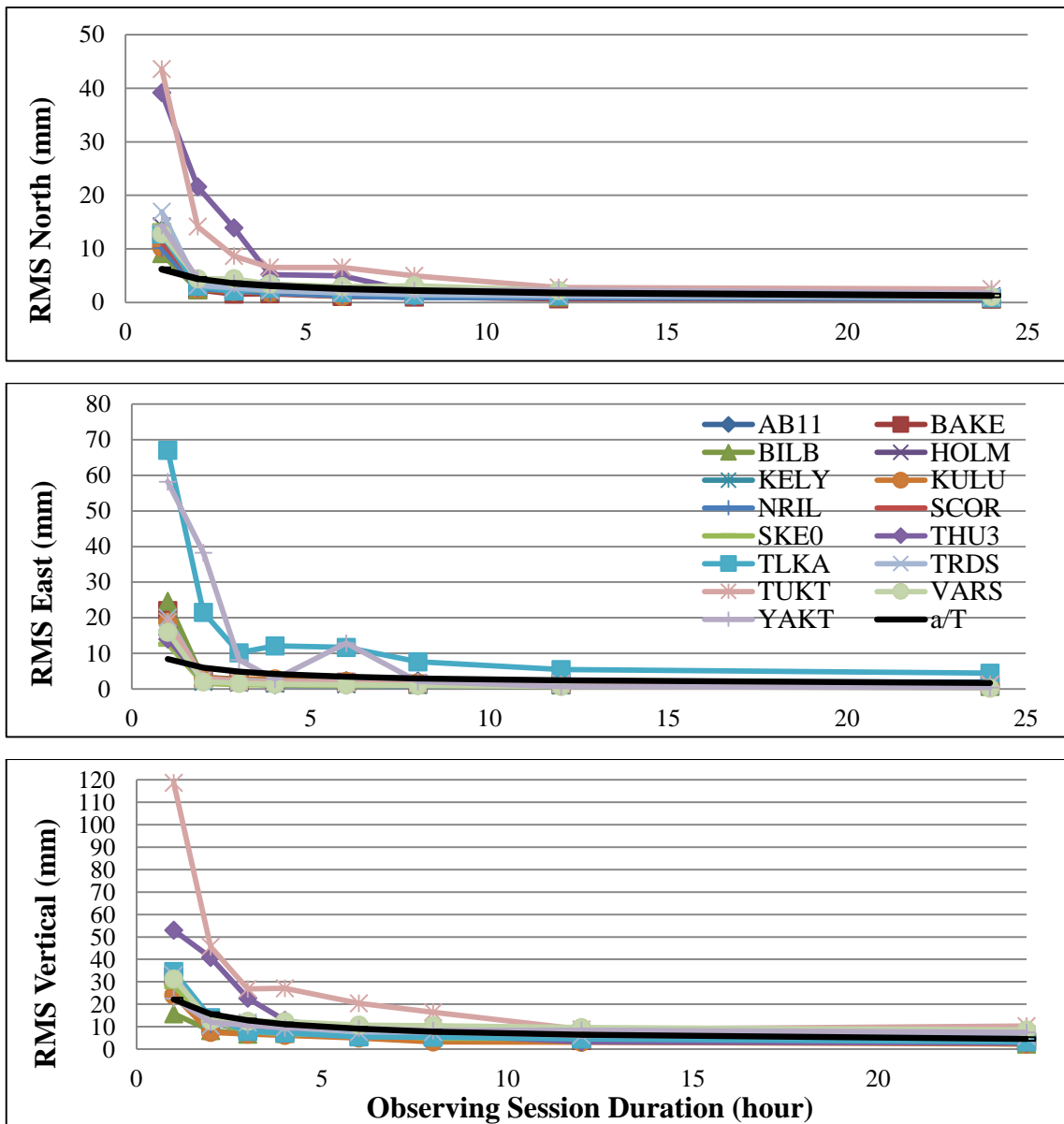


Figure D.1 Prediction/model fit of the regional accuracy models to the RMS values of this study, from observing session durations of 1 through 24 h (high latitude northern hemisphere)



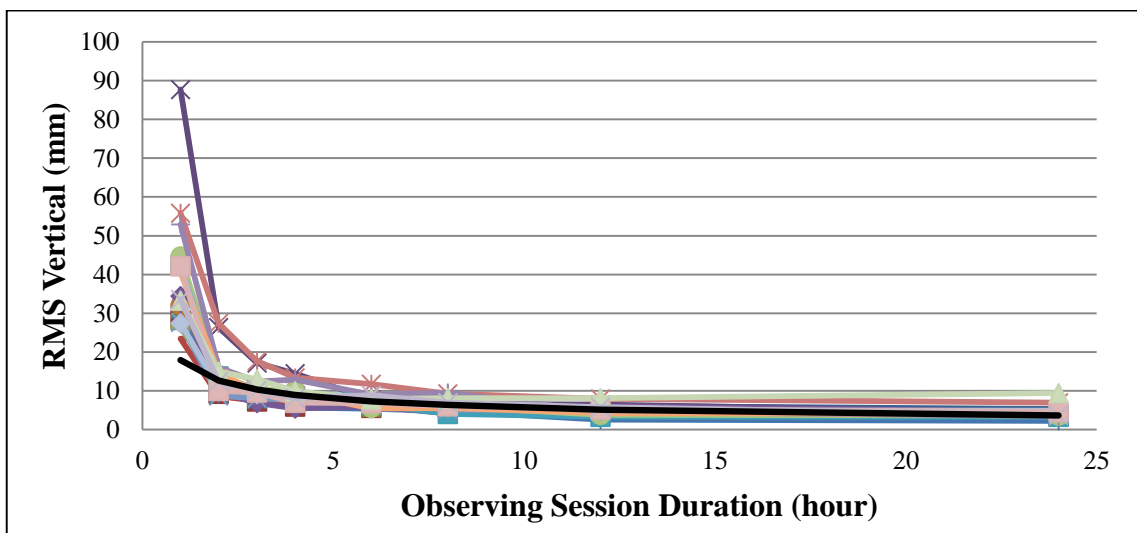
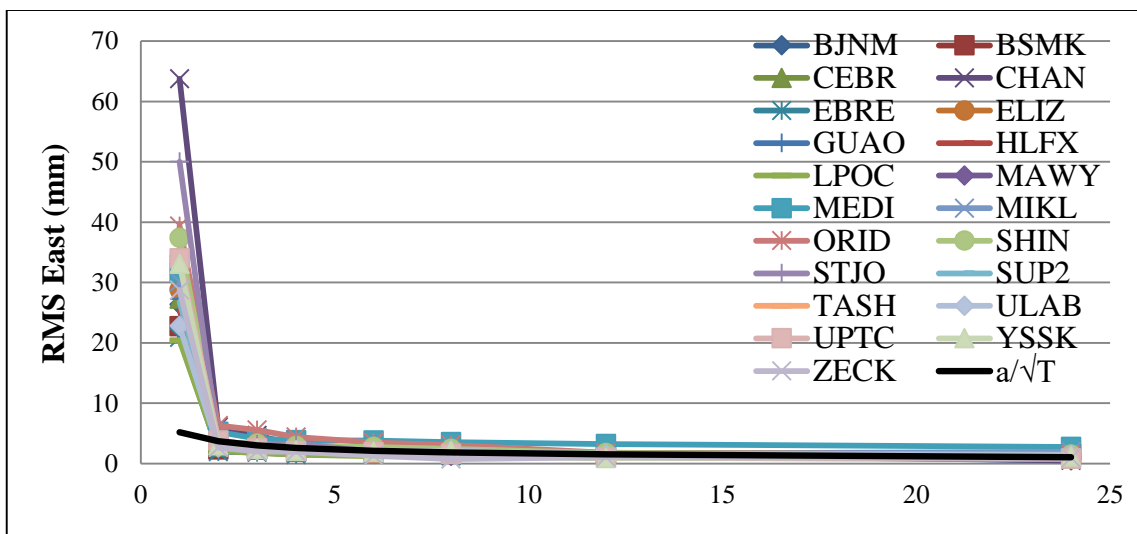
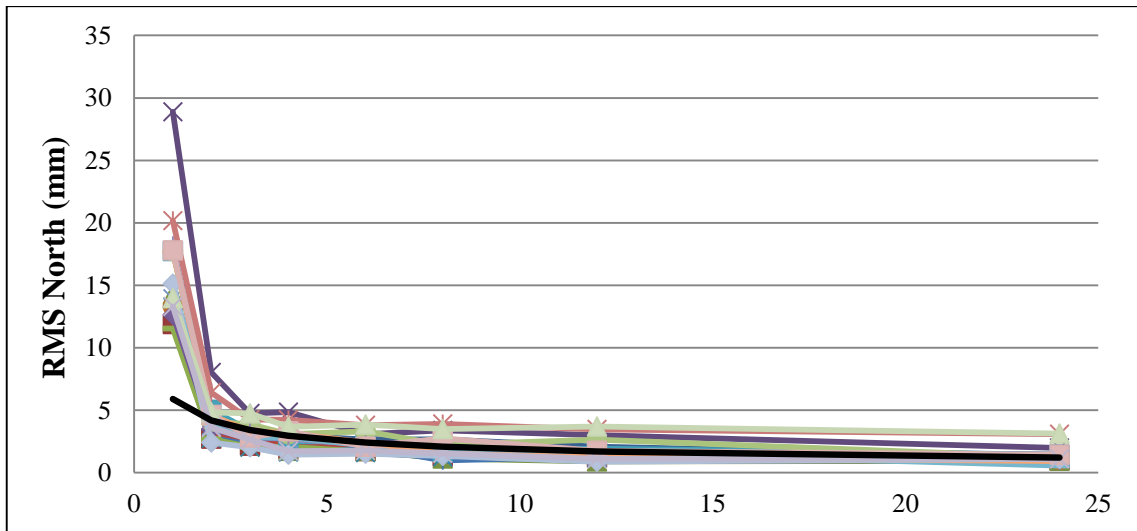


Figure D.2 Prediction/model fit of the regional accuracy models to the RMS values of this study, from observing session durations of 1 through 24 h (middle latitude northern hemisphere)

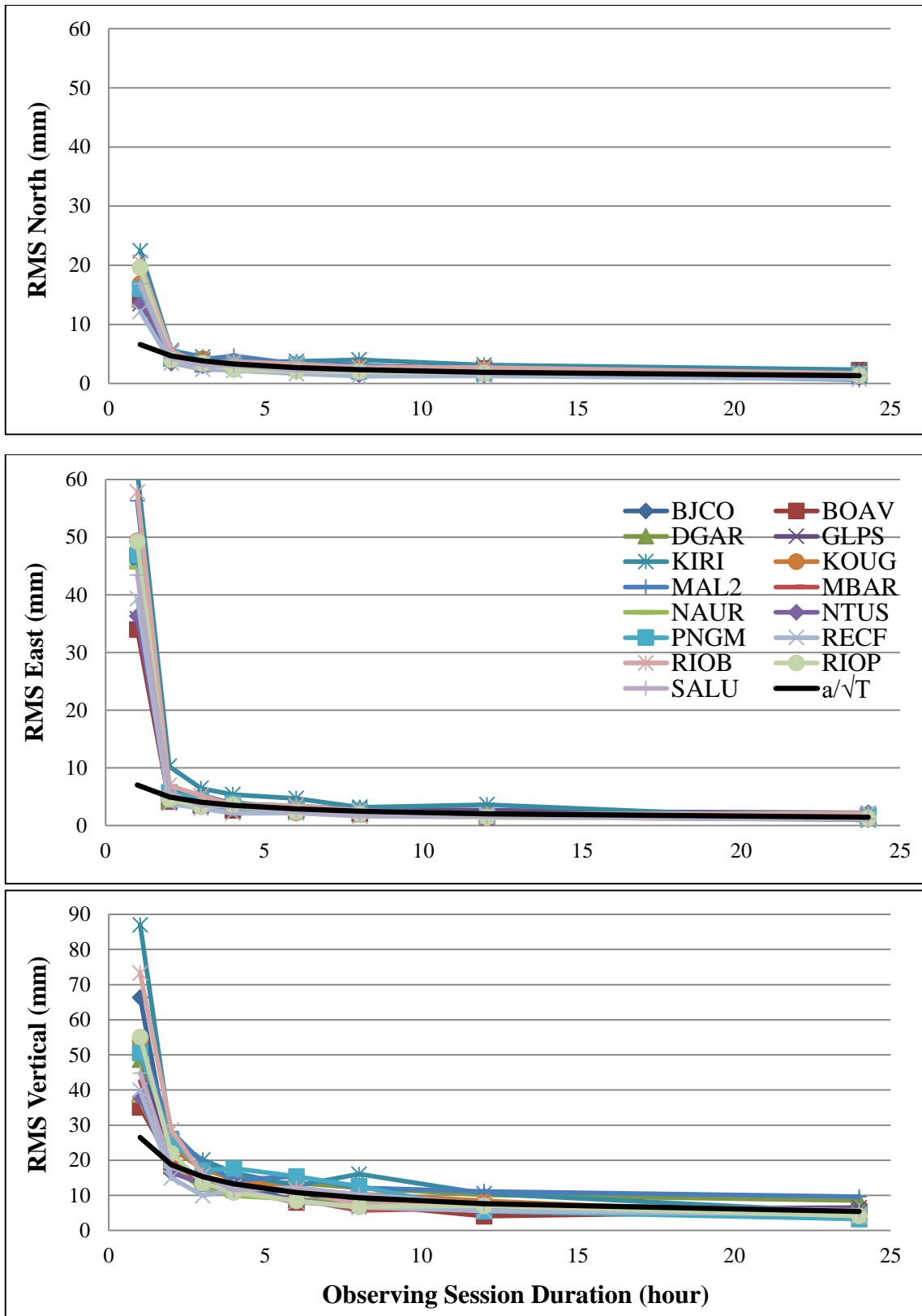


Figure D.3 Prediction/model fit of the regional accuracy models to the RMS values of this study, from observing session durations of 1 through 24 h (equatorial)

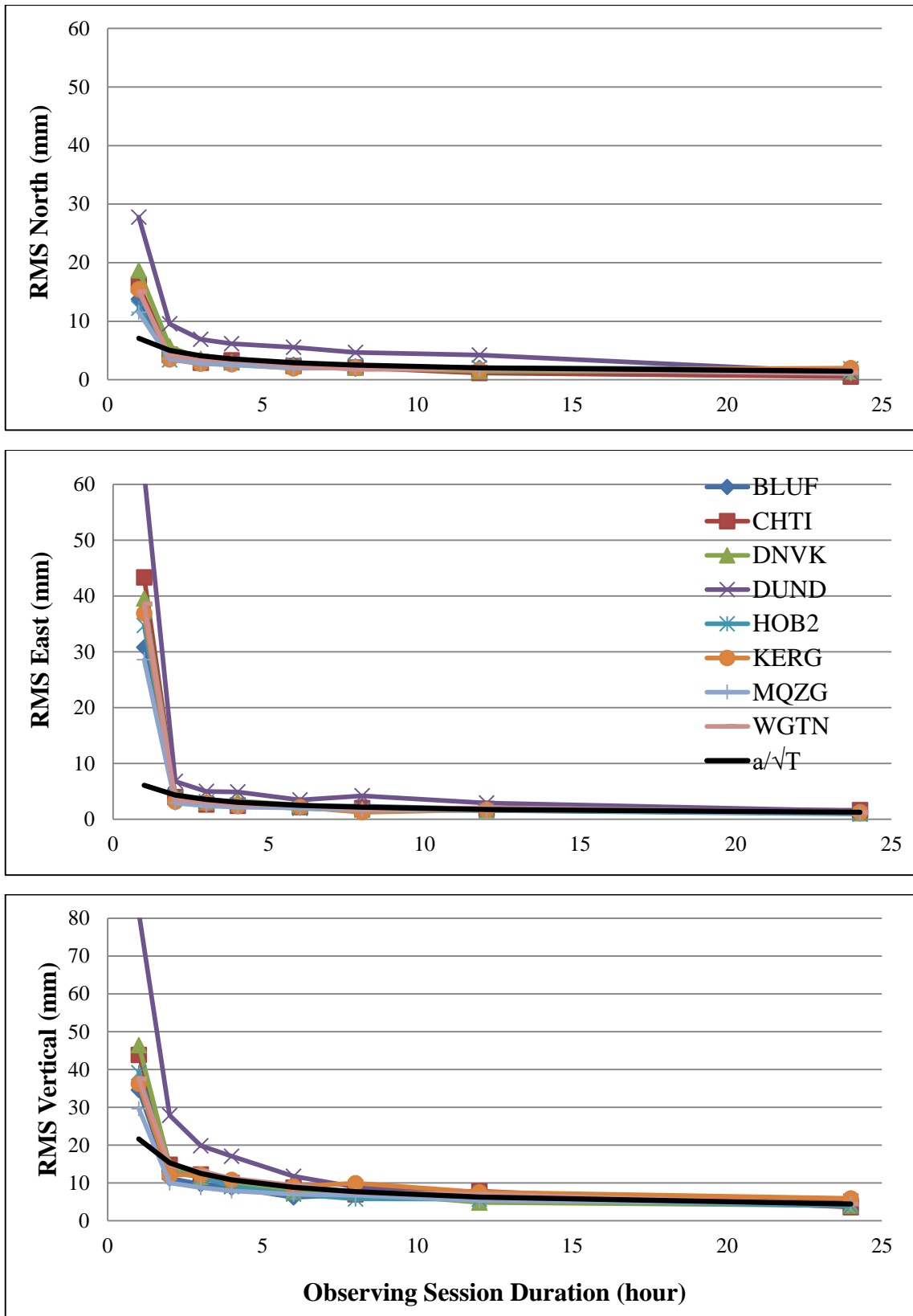


Figure D.4 Prediction/model fit of the regional accuracy models to the RMS values of this study, from observing session durations of 1 through 24 h (middle latitude southern hemisphere)

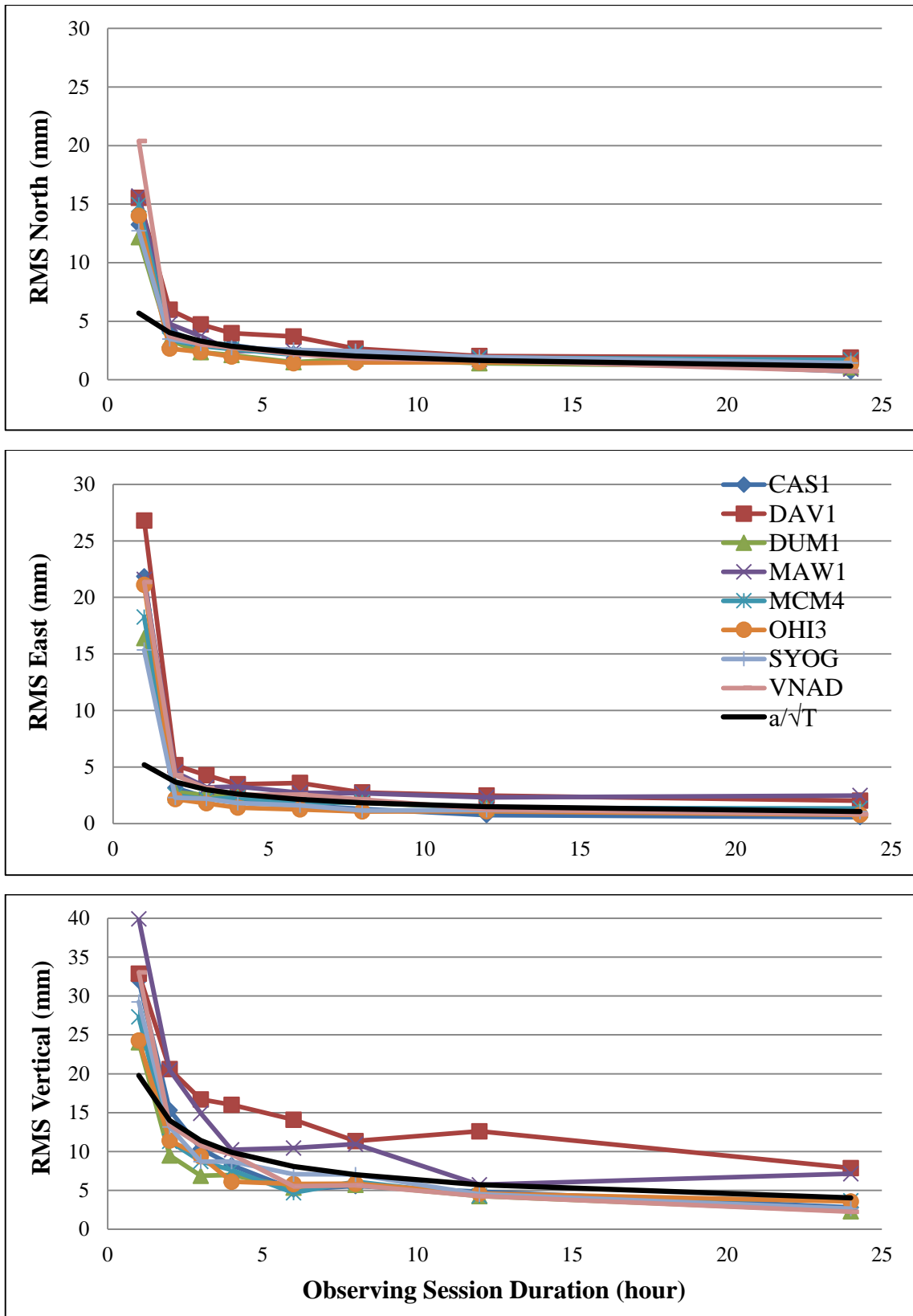


Figure D.5 Prediction/model fit of the regional accuracy models to the RMS values of this study, from observing session durations of 1 through 24 h (high latitude southern hemisphere)

## CURRICULUM VITAE

---

### PERSONAL INFORMATION

**Name Surname** : Adem Gökhan HAYAL  
**Date of birth and place** : 1980 / Trabzon  
**Foreign Languages** : English  
**E-mail** : ademhayal@nevsehir.edu.tr

### EDUCATION

<b>Degree</b>	<b>Department</b>	<b>University</b>	<b>Date of Graduation</b>
Master	Geodetic Science	Ohio State University	2010
Undergraduate	Geomatic Engineering	Karadeniz Technical Univ.	2005
High School	Math-Science Class	Trabzon Ataturk Hihg Sc.	1998

### WORK EXPERIENCE

<b>Year</b>	<b>Corporation/Institute</b>	<b>Enrollment</b>
2015 - Continues	Nevsehir H. B. V. University	Research Assistant
2012-2015	Yildiz Technical University	Research Assistant
2011-2012	Nevsehir University	Research Assistant

2010-2011	Ministry of National Education, Uskudar County Department	IT Officer
2008-2010	Ohio State University	Research Associate
2005-2007	Karadeniz Technical University	Research Assistant
2005-2005	Hapa Engineering Company	Surveying Engineer

## **PUBLISHERMENTS**

### **Papers**

1. Hayal, A. G. and Sanli, D. U. (2016): Revisiting The Role of Observation Session Duration on Precise Point Positioning Accuracy Using GIPSY/OASIS II Software, *Boletim de Ciências Geodésicas*, vol:22, iss:2, 2016 (in press)

### **Conference Papers**

1. Hayal, A. G. and Sanli, D. U. (2015): Accuracy of GIPSY PPP From a Denser Network, EGU General Assembly 2015, Vienna, Austria, April 12 – 17, 2015. (Poster)
2. Hayal, A. G. and Sanli, D. U. (2014): Accuracy of GIPSY From Version 6.2: A Robust Method to Remove Outliers, EGU General Assembly 2014, Vienna, Austria, April 27 – May 2, 2014. (Poster)
3. Hayal, A. G. and Sanli, D. U. (2013): Accuracy of GIPSY From Version 6, GNSS Precise Point Positioning Workshop: Reaching Full Potential, Ottawa, Canada, June 12-14, 2013. (Poster)
4. Lee, J. K., Hayal, A.G. and Jekeli, C. (2009): Handheld Geolocation System (HGS) for UXO Detection and Discrimination Using Low-Cost Inertial Measurement Unit (IMU), Partners in Environmental Technology Technical Symposium & Workshop, Washington D.C., US, December 1-3, 2009. (Poster)
5. Lee, J. K., Jekeli, C. and Hayal, A. G. (2008): Nonlinear Filter Based Smoothing Methods for MEC Detection and Characterization Using Free Inertial Navigation System, Partners in Environmental Technology Technical Symposium & Workshop, Washington D.C., US, December 2-4, 2008. (Poster)

### **Projects**

1. A project for developing the prototype of an imaging system (MUTOMOPRO) based on the use the cosmic muons principle, Researcher, SANTEZ, January 2014 - Continues